

Electronic Supplementary Information

Iron complexes supported by silyl–NHC chelate ligands: synthesis and use for double hydroboration of nitriles

Takashi Komuro,* Kohei Hayasaka, Kasumi Takahashi, Nozomu Ishiwata,

Kota Yamauchi, Hiromi Tobita and Hisako Hashimoto*

*Department of Chemistry, Graduate School of Science, Tohoku University, Sendai 980-8578,
Japan.*

E-mail: takashi.komuro.c5@tohoku.ac.jp (T.K.); hisako.hashimoto.b7@tohoku.ac.jp (H.H.)

Contents

1. Experimental procedures and characterisation data	S2
● Synthesis of ligand precursors and silyl–NHC chelate complexes	S4
● Fig. S1: Methods for the synthesis of silyl–NHC chelate complexes	S14
● Catalytic double hydroboration of nitriles with HBpin	S15
● Fig. S3: Time course of the double hydroboration using 0.5 mol% of 1 and 2	S18
● Synthesis of <i>N</i> -silylimine complexes 5,6 by stoichiometric reaction of 1 with nitriles and double hydroboration of nitriles catalysed by 6	S24
2. X-ray crystal structure analysis	S28
● Table S5: Crystallographic data for 1 , 3 and 5	S29
● Fig. S4: Crystal structure of 3	S30
3. DFT calculations of complex 1	S31
4. References	S36
5. Spectra of newly-synthesised organosilicon compounds, ligand precursors and silyl–NHC chelate complexes (Figs. S7–S33)	S38
6. NMR spectra of <i>N,N</i> -bis(boryl)amines in reaction mixtures of catalytic double hydroboration of nitriles (Figs. S34–S65)	S52
7. NMR and IR spectra of <i>N</i> -silylimine complexes 5 and 6 (Figs. S66–S75)	S76

1. Experimental procedures and characterisation data

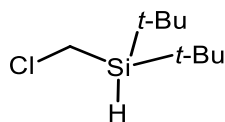
General considerations. All manipulations, except purification of organosilicon compounds and ligand precursors, were performed under dry argon or nitrogen in a glovebox or using a high-vacuum line and standard Schlenk techniques. Glassware was dried under vacuum prior to use. Purification of organosilicon compounds and ligand precursors was performed in the air.

Materials. Benzene- d_6 (C_6D_6), toluene, diethyl ether (Et_2O), hexamethyldisiloxane, benzonitrile, acetonitrile and pivalonitrile were dried over CaH_2 , vacuum-transferred and then stored under argon over 4 Å molecular sieves in a glovebox. Pinacolborane and *p*-tolnitrile were dried and degassed by the same manner but stored without the 4 Å molecular sieves in a glovebox. THF and hexane were dried using a Glass Contour alumina column (Nikko Hansen & Co., Ltd), degassed by three freeze-pump-thaw cycles and then stored under argon over 4 Å molecular sieves in a glovebox. 4-Fluorobenzonitrile, 4-methoxybenzonitrile and 4-trifluoromethylbenzonitrile were degassed under reduced pressure and stored in a glovebox. $KN(SiMe_3)_2$, $Fe_3(CO)_{12}$ and $Ru_3(CO)_{12}$ were purchased from Aldrich, stored in a glovebox and used as received. Bromochloromethane was dried over CaH_2 and distilled before use. $CDCl_3$ for NMR spectroscopy of organic compounds was dehydrated with 4 Å molecular sieves. NaI was dried under vacuum for 2.5 days. Acetone (FUJIFILM Wako Chemicals, dehydrated), *t*-BuOK (TCI Chemicals) and MeI (TCI Chemicals) were purchased and used as received. 1-(2',6'-Diisopropylphenyl)-4,5-dimethylimidzaol,^{S1} 4,5-dimethyl-1*H*-imizazol^{S2} and $ClSi(t-Bu)_2H$ ^{S3} were prepared according to the previously reported methods, and among them 1-(2',6'-diisopropylphenyl)-4,5-dimethylimidzaol was purified by Kugelrohr distillation. 4,5-Dimethyl-1*H*-imizazol contained trace pale brown impurities but was used without further purification. Silica gel 60N (40–50 μm, spherical, neutral; Kanto Chemical) and glass TLC plates (silica gel 60F₂₅₄, layer thickness 250 μm; Merck) were used for flash chromatography. Ethyl acetate (EtOAc) and hexane for flash chromatography were used as received.

Spectroscopic measurements. ^1H , $^{11}\text{B}\{^1\text{H}\}$, $^{13}\text{C}\{^1\text{H}\}$, $^{19}\text{F}\{^1\text{H}\}$ and $^{29}\text{Si}\{^1\text{H}\}$ NMR spectra were recorded on a Bruker AVANCE III 400 Fourier transform spectrometer. Chemical shifts are reported in parts per million (ppm), and coupling constants (J) and line widths at half-height ($\Delta\nu_{1/2}$) are given in Hz. For $^{29}\text{Si}\{^1\text{H}\}$ NMR, DEPT or inverse gate decoupling (IG) pulse sequence was used. The residual proton ($\text{C}_6\text{D}_5\text{H}$, 7.15 ppm; CHCl_3 , 7.24 ppm) and the carbon (C_6D_6 , 128.0 ppm; CDCl_3 , 77.0 ppm) resonances of deuterated solvents were used as internal references for ^1H and ^{13}C resonances, respectively. For the assignments of NMR signals, the following abbreviations were used: ArH, aromatic proton; ArC, aromatic carbon; ImH, imidazole proton; ImC, imidazole carbon and Im-Me, methyl proton/carbon at the 4,5-positions of an imidazole group. $^{11}\text{B}\{^1\text{H}\}$, $^{19}\text{F}\{^1\text{H}\}$ and $^{29}\text{Si}\{^1\text{H}\}$ NMR chemical shifts were referenced to $\text{BF}_3\cdot\text{Et}_2\text{O}$ (0 ppm), $\text{C}_6\text{H}_5\text{CF}_3$ (-63.7 ppm) and SiMe_4 (0 ppm), respectively, as external standards. NMR data were collected at room temperature unless otherwise indicated. Infrared spectra were recorded for a solid sample in a KBr pellet, for a neat sample placed between KBr plates or for a solution sample a liquid cell assembled with KBr plates using a Horiba FT-720 spectrometer. High-resolution mass spectra (HRMS) and mass spectra were recorded on a JEOL JMS-T100GCV spectrometer operating in field desorption (FD) mode. Elemental analyses were performed using a J-Science Lab JM11 microanalyzer. Mass spectroscopic measurements and elemental analyses were performed at the Research and Analytical Center for Giant Molecules, Tohoku University.

Light source for photoreaction. For all photoreactions, a 450 W medium-pressure mercury lamp manufactured by USHIO Inc. was used. A sample solution was placed in a Pyrex glass reaction tube and irradiated at ca. 7 °C. The reaction tube was placed in close contact with a quartz glass jacket (for cooling the mercury lamp). The distance from the light source to the reaction tube was approximately 4 cm.

1.1 Synthesis of di-*tert*-butyl(chloromethyl)silane.^{S4a}

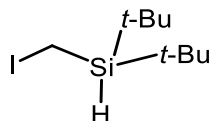


In a 300 mL three necked round-bottomed flask equipped with a reflux condenser and a 100 mL dropping funnel, bromochloromethane (14.0 g, 108 mmol) and di-*tert*-butylchlorosilane (12.2 g, 68.1 mmol) were dissolved in THF (75 mL). The solution was cooled at ca. $-90\text{ }^{\circ}\text{C}$ using an EtOH/liq. N_2 bath. To the solution was added dropwise *n*-BuLi (1.56 M, 69 mL, 0.11 mol) from the dropping funnel for 50 min. The resulting white suspended solution was treated with a saturated NH_4Cl aq. (50 mL) while cooling to quench the reaction. The mixture was allowed to warm to room temperature, and water (50 mL) was added. After the mixture was transferred to a separating funnel, the organic phase was collected, and the aqueous phase was extracted four times with Et_2O (400 mL total). The organic phase was combined and dried over anhydrous MgSO_4 . After filtration, the filtrate was evaporated under vacuum to give a pale-yellow oil (13.9 g). The ^1H NMR analysis of this oil showed that it contained the target compound, di-*tert*-butylsilanol and *n*-BuBr. The oil was then purified by flash chromatography [eluent: hexane, silica gel (140 g)]. The eluate involving the target compound [confirmed by TLC ($R_f = 0.65$)] was collected. Evaporation of the solution under vacuum to give a colourless liquid (10.4 g). The liquid was further distilled under reduced pressure (14 mmHg, b.p. $80\text{--}81\text{ }^{\circ}\text{C}$). Di-*tert*-butyl(chloromethyl)silane was obtained as a colourless liquid (9.66 g, 53.1 mmol; 74%).

^1H NMR (400 MHz, CDCl_3): δ 1.08 (s with satellites, 18H, $^3J_{\text{SiH}} = 6.0\text{ Hz}$, *t*-Bu), 2.98 (d with satellites, 2H, $^3J_{\text{HH}} = \text{ca. } 2\text{ Hz}$, $^2J_{\text{SiH}} = \text{ca. } 5\text{ Hz}$, SiCH_2Cl), 3.52 (br t with satellites, 1H, $^3J_{\text{HH}} = \text{ca. } 2\text{ Hz}$, $^1J_{\text{SiH}} = 187\text{ Hz}$, SiH). $^{13}\text{C}\{^1\text{H}\}$ NMR (101 MHz, CDCl_3): δ 19.0 (SiCMe_3), 25.1 (SiCH_2Cl), 28.7 (SiCMe_3).^{S5} $^{29}\text{Si}\{^1\text{H}\}$ NMR (79.5 MHz, DEPT, CDCl_3): δ 9.1. IR (neat, cm^{-1}): 2121 (m, ν_{SiH}), 2096 (m, ν_{SiH}). Two absorption peaks of Si–H stretching were observed, which is possibly due to the presence of two rotational isomers (conformers) and their slow

interconversion on the IR timescale. HRMS (FD): m/z calcd for $[^{12}\text{C}_9^1\text{H}_{21}^{28}\text{Si}_1^{35}\text{Cl}_1]^+$ ($[\text{M}]^+$) 192.1096, found 192.1103. Anal. Calcd for $\text{C}_9\text{H}_{21}\text{SiCl}$: C, 56.06; H, 10.98. Found: C, 56.05; H, 10.95.

1.2 Synthesis of di-*tert*-butyl(iodomethyl)silane^{S4b}

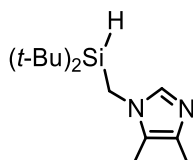


In a two-necked round bottomed flask (100 mL) equipped with a reflux condenser, NaI (4.68 g, 31.2 mmol) was dissolved in acetone (35 mL). To the solution was added di-*tert*-butyl(chloromethyl)silane (1.99 g, 10.3 mmol), giving a pale-yellow suspension. The mixture was refluxed using an oil bath for 6 h, and the reaction was monitored by GC. The resulting yellow-white suspension was evaporated using a diaphragm pump to remove a most of the solvent. The residue (an orange solid) was mixed with saturated aqueous $\text{Na}_2\text{S}_2\text{O}_3$ (20 mL) and extracted three times with Et_2O (60 mL total). The organic phase was combined and dried over anhydrous MgSO_4 . After filtration through a cotton plug, the solvent was removed under reduced pressure using an evaporator to give a pale-yellow liquid (2.50 g). Purification by Kugelrohr distillation (0.28 mmHg, 55–60 °C) afforded di-*tert*-butyl(iodomethyl)silane as a colourless liquid (2.32 g, 8.16 mmol; 79%).

^1H NMR (400 MHz, CDCl_3): δ 1.07 (s with satellites, 18H, $^3J_{\text{SiH}} = 6.0$ Hz, *t*-Bu), 2.03 (d with satellites, 2H, $^3J_{\text{HH}} = 2.3$ Hz, $^2J_{\text{SiH}} = \text{ca. } 5$ Hz, SiCH_2I), 3.93 (t with satellites, 1H, $^3J_{\text{HH}} = 2.3$ Hz, $^1J_{\text{SiH}} = 190$ Hz, SiH). $^{13}\text{C}\{^1\text{H}\}$ NMR (101 MHz, CDCl_3): δ -25.4 (SiCH_2I), 20.0 (SiCMe_3), 28.8 (SiCMe_3).^{S5} $^{29}\text{Si}\{^1\text{H}\}$ NMR (79.5 MHz, DEPT, CDCl_3): δ 14.9. IR (neat, cm^{-1}): 2117 (m, ν_{SiH}), 2087 (m, ν_{SiH}). Two absorption peaks of Si–H stretching were observed, which is possibly due to the presence of two rotational isomers (conformers) and their slow interconversion on the IR timescale. HRMS (FD): m/z calcd for $[^{12}\text{C}_9^1\text{H}_{21}^{28}\text{Si}_1^{127}\text{I}_1]^+$ ($[\text{M}]^+$)

284.0455, found 284.0452. Anal. Calcd for C₉H₂₁SiI: C, 38.03; H, 7.45. Found: C, 37.96; H, 7.39.

1.3 Synthesis of 1-[(di-*tert*-butylsilyl)methyl]-4,5-dimethylimidazole^{S4c}

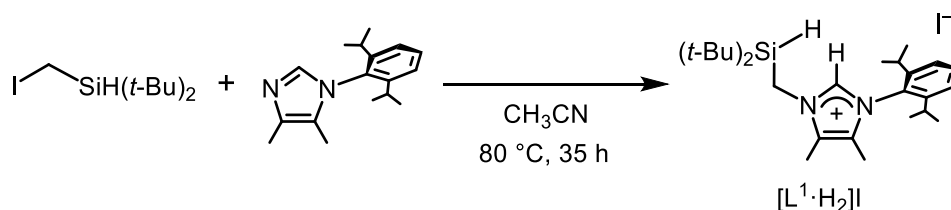


In a 100 mL two-necked round-bottomed flask, *t*-BuOK (845 mg, 7.53 mmol) and 4,5-dimethyl-1*H*-imidazole (724 mg, 7.53 mmol; containing trace pale-brown impurities) were dissolved in acetonitrile (15 mL). The pale-brown solution was refluxed by an oil bath (85 °C) for 5 h. Di-*tert*-butyl(chloromethyl)silane (1.48 g, 7.65 mmol) was added dropwise to the resulting brown suspension, and then the mixture was refluxed for further 1.5 h. The reaction was quenched by adding a saturated NaCl solution (20 mL) to the reaction mixture. The solution was extracted three times with Et₂O (75 mL total). The organic phase obtained was dried over anhydrous MgSO₄. After the solution was filtered through a cotton plug, the filtrate was evaporated under vacuum to give a pale red oil (2.22 g). This oil was dissolved in a minimum amount of AcOEt and purified by flash chromatography [eluent: EtOAc, silica gel (118 g)]. A fraction involving the target compound [confirmed by TLC (R_f = 0.35)] was collected and evaporated under vacuum to remove the solvent completely. 1-[(Di-*tert*-butylsilyl)methyl]-4,5-dimethyl-imidazole was obtained as a pale red liquid (1.29 g, 5.12 mmol; ca. 68%). Although the product contained red-coloured impurities, the NMR spectra of the pale red liquid obtained showed no noticeable signals originate from the impurities (Figs. S13–S15). Therefore, the product was used without further purification for the synthesis of imidazolium salt [L²·H₂I] (see section 1.5).

¹H NMR (400 MHz, r.t., CDCl₃): δ 0.95 (s, 18H, Si(*t*-Bu)₂), 2.08, 2.09 (s, 3H×2, Im-Me), 3.41 (d, ³J_{HH} = 3.2 Hz, 2H, SiCH₂), 3.74 (t with satellites, ³J_{HH} = 3.2 Hz, ¹J_{HH} = 187 Hz, 1H,

SiH), 7.33 (s, 1H, 2-ImH). $^{13}\text{C}\{^1\text{H}\}$ NMR (101 MHz, r.t., CDCl_3): δ 9.0, 13.0 (Im-Me \times 2), 18.7 ($\text{SiC}(\text{CH}_3)_3$), 28.5 ($\text{SiC}(\text{CH}_3)_3$), 29.2 (SiCH_2Im), 122.7, 133.5 (4,5-ImC \times 2), 135.4 (2-ImC).^{S5} $^{29}\text{Si}\{^1\text{H}\}$ NMR (79.5 MHz, DEPT, r.t., CDCl_3): δ 5.5. IR (KBr plate, neat, cm^{-1}): 2012 (m, ν_{SiH}). HRMS (FD): m/z calcd for $[\text{C}_{14}\text{H}_{28}\text{N}_2\text{Si}]^+$ ($[\text{M}]^+$) 252.2022, found 252.2021.

1.4 Synthesis of 1-[(di-*tert*-butylsilyl)methyl]-3-(2',6'-diisopropylphenyl)-4,5-dimethylimidazolium iodide ($[\text{L}^1\cdot\text{H}_2]\text{I}$)

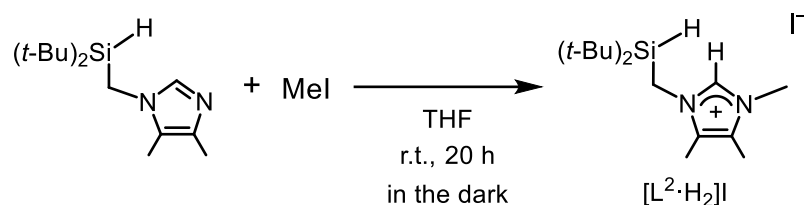


In a 30 mL round bottomed flask with a reflux condenser and a stirring bar, 1-(2,6-diisopropylphenyl)-4,5-dimethyl-1*H*-imidazole (0.570 g, 2.23 mmol) was dissolved in CH_3CN (10 mL). Di-*tert*-butyl(iodomethyl)silane (1.06 g, 3.72 mmol) was added to the solution dropwise with a syringe while stirring. The mixture was refluxed for 35 h using an oil bath (85 $^\circ\text{C}$). The reaction mixture was evaporated under vacuum to give a mixture of a colourless solid and a yellow oil. Hexane was added to the mixture, and then the suspension was filtered through a membrane filter. The solid on the filter was washed with hexane and then dried under vacuum. The title imidazolium salt $[\text{L}^1\cdot\text{H}_2]\text{I}$ was obtained as a colourless solid (0.996 g, 1.84 mmol) in 83% yield.

^1H NMR (400 MHz, r.t., CDCl_3): δ 1.08 (s, 18H, $\text{Si}(\text{t-Bu})_2$), 1.11, 1.19 (d, $^3J_{\text{HH}} = 6.8$ Hz, 6H \times 2, $\text{CH}(\text{CH}_3)_2$), 1.93, 2.43 (s, 3H \times 2, Im-Me), 2.19 (sept, $^3J_{\text{HH}} = 6.8$ Hz, 2H, $\text{CH}(\text{CH}_3)_2$), 3.78 (t with satellites, $^3J_{\text{HH}} = 3.4$ Hz, $^1J_{\text{SiH}} = 184$ Hz, 1H, Si-H), 4.62 (d, $^3J_{\text{HH}} = 3.4$ Hz, 2H, SiCH_2), 7.28 (d, $^3J_{\text{HH}} = 7.8$ Hz, 2H, *m*-ArH), 7.50 (t, $^3J_{\text{HH}} = 7.8$ Hz, 1H, *p*-ArH), 9.85 (s, 1H, 2-ImH). $^{13}\text{C}\{^1\text{H}\}$ NMR (101 MHz, r.t., CDCl_3): δ 8.7, 10.0 (Im-Me \times 2), 19.2 ($\text{SiC}(\text{CH}_3)_3$),

23.4, 25.4 ($\text{CH}(\underline{\text{C}}\text{H}_3)_2 \times 2$), 28.5 ($\underline{\text{C}}\text{H}(\text{CH}_3)_2$), 28.6 ($\text{SiC}(\underline{\text{C}}\text{H}_3)_3$), 34.8 (SiCH_2Im), 122.3, 122.4 ($4,5\text{-ImC} \times 2$),[†] 124.9 (*m*-ArC), 128.0 (*ipso*-ArC), 131.8 (*p*-ArC), 135.2 (2-ImC), 145.8 (*o*-ArC).^{S5} † The ^{13}C signals for the 4,5-carbons of the imidazolium ring were not observed in the $^{13}\text{C}\{^1\text{H}\}$ NMR spectrum. Therefore, instead, the chemical shifts of these signals were determined based on the $^1\text{H}\text{-}^{13}\text{C}$ HMBC spectrum. $^{29}\text{Si}\{^1\text{H}\}$ NMR (79.5 MHz, DEPT, r.t., CDCl_3): δ 5.3. IR (KBr-pellet, cm^{-1}): 2146 (m, ν_{SiH}), 2123 (w, ν_{SiH}). HRMS (FD, positive): m/z calcd for $[\text{}^{12}\text{C}_{26}\text{}^1\text{H}_{45}\text{}^{14}\text{N}_2\text{}^{28}\text{Si}]^+$ (the cation part of $[\text{L}^1 \cdot \text{H}_2]\text{I}$) 413.3352, found 413.3351. Anal. Calcd for $\text{C}_{26}\text{H}_{45}\text{N}_2\text{SiI}$: C, 57.76; H, 8.39; N, 5.18. Found: C, 57.52; H, 8.42; N, 5.20.

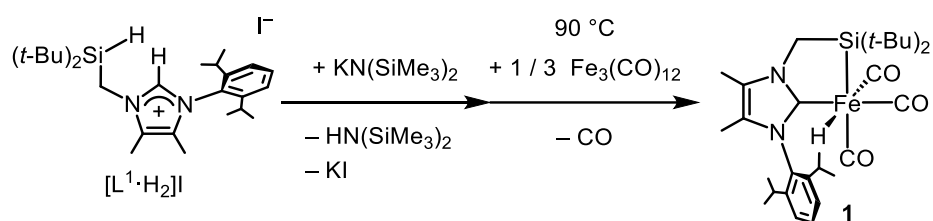
1.5 Synthesis of 1-[(di-*tert*-butylsilyl)methyl]-3,4,5-trimethylimidazolium iodide ($[\text{L}^2 \cdot \text{H}_2]\text{I}$)



In a 15 mL Schlenk tube with a stirring bar, [(hydrosilyl)methyl]imidazole [523 mg, ca. 2.07 mmol (a pale red liquid)] was dissolved in THF (6 mL). To the pale red solution was added iodomethane (1.37 g, 9.84 mmol; 4.8 equiv.) dropwise via a syringe with stirring. The Schlenk tube was covered with aluminium foil, and the mixture was stirred at room temperature for 20 h in the dark. A white solid was precipitated from the reaction mixture. The resulting mixture was evaporated under vacuum, and the pale red residue was suspended in Et_2O . The suspension was filtered through a membrane filter (Omnipore membrane, pore size: 0.2 μm , diameter: 25 mm). A white solid on the filter was washed with Et_2O and then dried under vacuum. The title compound $[\text{L}^2 \cdot \text{H}_2]\text{I}$ was obtained as a colourless solid (680 mg, 1.72 mmol) in 83% yield.

^1H NMR (400 MHz, r.t., CDCl_3): δ 1.34 (s, 18H, $\text{Si}(t\text{-Bu})_2$), 2.23, 2.26 (s, 3H \times 2, Im-Me), 3.80 (t with satellites, $^3J_{\text{HH}} = 3.2$ Hz, $^1J_{\text{SiH}} = 188$ Hz, 1H, SiH), 3.89 (d, $^3J_{\text{HH}} = 3.2$ Hz, 2H, SiCH_2), 3.90 (s, 3H, NMe), 9.93 (s, 1H, 2-ImH). $^{13}\text{C}\{^1\text{H}\}$ NMR (101 MHz, r.t., CDCl_3): δ 8.6, 9.3 (Im-Me \times 2), 19.0 ($\text{Si}\underline{\text{C}}(\text{CH}_3)_3$), 28.5 ($\text{Si}\underline{\text{C}}(\underline{\text{C}}\text{H}_3)_3$), 33.0 (SiCH_2Im), 34.3 (NMe), 127.00, 127.03 (4,5-ImC), 135.8 (2-ImC).^{S5} $^{29}\text{Si}\{^1\text{H}\}$ NMR (79.5 MHz, DEPT, r.t., CDCl_3): δ 6.0. IR (KBr-pellet, cm^{-1}): 2120 (m, ν_{SiH}). HRMS (FD, positive): m/z calcd for $[\text{C}_{15}\text{H}_{31}\text{N}_2\text{Si}]^+$ (the cation part of $[\text{L}^1\cdot\text{H}_2]\text{I}$) 267.2256, found 267.2255. Anal. Calcd for $\text{C}_{15}\text{H}_{31}\text{N}_2\text{Si}$: C, 45.68; H, 7.92; N, 7.10. Found: C, 45.64; H, 7.86; N, 7.07.

1.6 Synthesis of $\text{Fe}(\text{L}^1)(\text{H})(\text{CO})_3$ (**1**).



In a reaction tube with a Teflon needle valve (20 mmf), $[\text{L}^1\cdot\text{H}_2]\text{I}$ (420 mg, 0.776 mmol), $\text{KN}(\text{SiMe}_3)_2$ (169 mg, 0.847 mmol) and toluene (16 mL) were mixed to give a white suspension. To the suspension was then immediately (< 5 min) added $\text{Fe}_3(\text{CO})_{12}$ (164 mg, 0.326 mmol; 0.42 equiv.), and the resulting reddish-brown suspension was heated and stirred under flow of nitrogen at $90\text{ }^\circ\text{C}$ for 37 h using an oil bath. The reaction mixture (a deep brown solution and a gray solid) was filtered through a membrane filter to remove an insoluble solid involving KI. The filtrate was evaporated under vacuum to give a brown-orange solid (436 mg). The solid was purified by flash chromatography using silica gel (14.1 g) and a 2 : 1 mixture of hexane/toluene as eluent. A pale-yellow fraction involving **1** was collected and evaporated under vacuum to give a colourless solid (302 mg). The solid was suspended in Et_2O and stored in a freezer ($-35\text{ }^\circ\text{C}$). The mother liquid was removed by a Paster pipet, and

the solid was dried under vacuum to give the title iron complex $\text{Fe}(\text{L}^1)(\text{H})(\text{CO})_3$ (**1**) as a colourless solid (256 mg, 0.463 mmol) in 60% yield.

^1H NMR (400 MHz, r.t., C_6D_6): δ -8.92 (s, 1H, Fe-H), 0.96 (d, $^3J_{\text{HH}} = 6.8$ Hz, 6H, $\text{CH}(\underline{\text{CH}_3})_2$), 1.11–1.48 (br, 18H, $\text{Si}(t\text{-Bu})_2$), 1.41, 1.57 (s, 3H \times 2, Im-Me), 1.45 (d, $^3J_{\text{HH}} = 6.8$ Hz, 6H, $\text{CH}(\underline{\text{CH}_3})_2$), 2.39–2.54 (m, 2H, $\underline{\text{CH}}(\text{CH}_3)_2$), 3.13 (br, $\Delta\nu_{1/2} = 62$ Hz, 2H, SiCH_2), 7.10 (d, $^3J_{\text{HH}} = 7.8$ Hz, 2H, *m*-ArH), 7.51 (t, $^3J_{\text{HH}} = 7.8$ Hz, 1H, *p*-ArH). $^{13}\text{C}\{^1\text{H}\}$ NMR (101 MHz, r.t., C_6D_6): δ 10.0, 10.2 (Im-Me), 24.1 ($\text{CH}(\underline{\text{CH}_3})_2$), 24.3–25.1 (br, $\text{SiC}(\underline{\text{CH}_3})_3 + \text{CH}(\underline{\text{CH}_3})_2$), 28.2 ($\underline{\text{CH}}(\text{CH}_3)_2$), 29.4, 31.2 (br, $\text{SiC}(\underline{\text{CH}_3})_3$), 38.0 (SiCH_2Im), 124.8 (*m*-ArC), 125.9, 127.4 (4,5-ImC), 130.8 (*p*-ArC), 135.1 (*ipso*-ArC), 147.1 (*o*-ArC), 186.8 (2-ImC), 210.5, 214.6, 215.6 (CO).^{S5} $^{29}\text{Si}\{^1\text{H}\}$ NMR (79.5 MHz, r.t., IG, C_6D_6): δ 75.9. IR (a toluene solution in a KBr liquid cell, cm^{-1}): 2028 (s, ν_{CO}), 1967 (s, ν_{CO}), 1954 (s, ν_{CO}). UV-Vis (1.4×10^{-4} M, THF) 275 (sh, $\epsilon = 3.7 \times 10^3 \text{ M}^{-1} \text{ cm}^{-1}$), 291 (sh, $\epsilon = 2.5 \times 10^3 \text{ M}^{-1} \text{ cm}^{-1}$). HRMS (FD, positive): *m/z* calcd for $[\text{C}_{29}\text{H}_{44}\text{N}_2\text{O}_3\text{Si}^{56}\text{Fe}]^+$ ($[\text{M}]^+$) 552.2471, found 552.2468. Anal. Calcd for $\text{C}_{29}\text{H}_{44}\text{N}_2\text{O}_3\text{SiFe}$: C, 63.03; H, 8.03; N, 5.07. Found: C, 63.10; H, 8.01; N, 5.14.

1.7 Variable-temperature ^1H NMR spectroscopy of complex **1**.

To a Pyrex NMR tube with J Young Teflon valve was added a solution of **1** in toluene-*d*₈. The solution was frozen and degassed under vacuum, and then the NMR tube was sealed under vacuum. ^1H NMR spectra of the solution was collected at temperatures in the range of 250–300 K. This observation indicates that **1** shows dynamic behaviour via exchange of two *t*-Bu groups on Si and two methylene protons of the SiCH_2 moiety. A possible mechanism for the behaviour is depicted in Scheme S1.

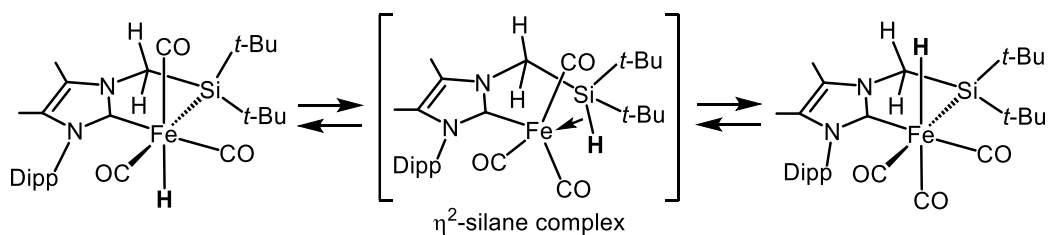
*^1H NMR data for complex **1** at selected temperatures:*

250 K: ^1H NMR (400 MHz, toluene-*d*₈): δ -8.94 (s, 1H, Fe-H), 0.97, 0.99 (d, $^3J_{\text{HH}} = 6.8$ Hz, 3H \times 2, $\text{CH}(\underline{\text{CH}_3})_2$), 1.16, 1.43 (s, 9H \times 2, $\text{Si}(t\text{-Bu})_2$), 1.39, 1.50 (s, 3H \times 2, Im-Me), 1.42, 1.47 (d, $^3J_{\text{HH}} = 6.8$ Hz, 3H \times 2, $\text{CH}(\underline{\text{CH}_3})_2$), 2.40, 2.48 (sept, $^3J_{\text{HH}} = 6.8$ Hz, 1H \times 2, $\underline{\text{CH}}(\text{CH}_3)_2$), 2.97,

3.17 (AB quartet, 2H, $^2J_{\text{HH}} = 13.7$ Hz, SiCH₂Im), 7.03, 7.07 (d, $^3J_{\text{HH}} = 7.8$ Hz, 1H×2, *m*-ArH), 7.25 (t, $^3J_{\text{HH}} = 7.8$ Hz, 1H, *p*-ArH).

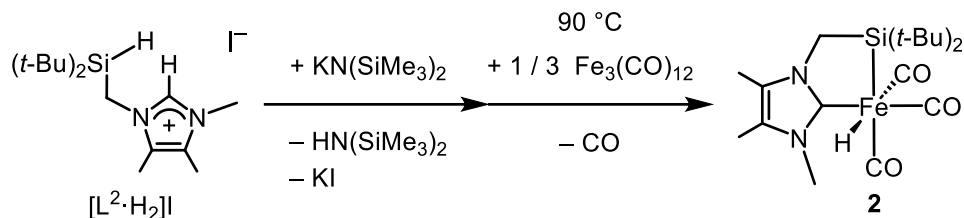
270 K: ¹H NMR (400 MHz, toluene-*d*₃): δ -8.97 (s, 1H, Fe-H), 0.98, 1.42 (br, 6H×2, CH(CH₃)₂), 1.14, 1.41 (br s, 9H×2, Si(*t*-Bu)₂), 1.42, 1.57 (s, 3H×2, Im-Me), 2.34–2.53 (m, 2H, CH(CH₃)₂), 3.00, 3.20 (br AB quartet, 2H, $^2J_{\text{HH}} = 13.6$ Hz, SiCH₂Im), 7.08 (d, $^3J_{\text{HH}} = 7.8$ Hz, 2H, *m*-ArH), 7.25 (t, $^3J_{\text{HH}} = 7.8$ Hz, 1H, *p*-ArH).

300 K: ¹H NMR (400 MHz, toluene-*d*₃): δ -9.00 (s, 1H, Fe-H), 0.98 (d, $^3J_{\text{HH}} = 6.8$ Hz, 6H, CH(CH₃)₂), 1.10–1.43 (br, 18H, Si(*t*-Bu)₂), 1.39 (d, $^3J_{\text{HH}} = 6.8$ Hz, 6H, CH(CH₃)₂), 1.46, 1.65 (s, 3H×2, Im-Me), 2.38–2.50 (m, 2H, CH(CH₃)₂), 3.14 (br, 2H, SiCH₂Im), 7.08 (d, $^3J_{\text{HH}} = 7.8$ Hz, 2H, *m*-ArH), 7.25 (t, $^3J_{\text{HH}} = 7.8$ Hz, 1H, *p*-ArH).



Scheme S1 A possible mechanism for the dynamic behaviour of complex **1** in solution.

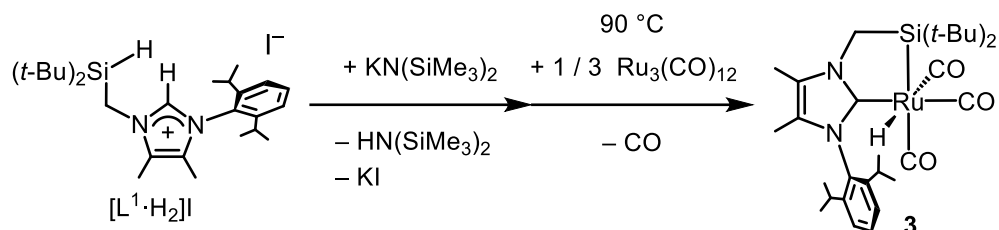
1.8 Synthesis of Fe(L²)(H)(CO)₃ (**2**).



By a procedure similar to that for the synthesis of **1**, the title complex was synthesised by use of [L²·H₂]I (182 mg, 0.463 mmol), KN(SiMe₃)₂ (104 mg, 0.521 mmol) and Fe₃(CO)₁₂ (85 mg, 0.17 mmol; 0.37 equiv.) in toluene (11 mL). After heating of the reaction mixture at 90 °C for 24 h under nitrogen flow, the resulting mixture (a deep brown solution and a gray solid) was filtered. The filtrate was evaporated under vacuum to give a red solid (180 mg). The solid was purified by flash chromatography [eluent: hexane : toluene = 5 : 1, silica gel (12.6 g)]. A pale-yellow solution involving **2** was collected and evaporated under vacuum to give a colourless solid with a trace amount of a yellow solid (157 mg). The residual solid was washed with hexamethyldisiloxane and dried under vacuum to give the title complex Fe(L²)(H)(CO)₃ (**2**) as a colourless solid (102 mg, 0.250 mmol) in 54% yield.

¹H NMR (400 MHz, r.t., C₆D₆): δ -8.88 (s, 1H, Fe-H), 1.19, 1.46 (s, 3H×2, Im-Me), 1.24 (s, 18H, Si(*t*-Bu)₂), 2.91 (s, 2H, SiCH₂), 3.06 (s, 3H, NMe). ¹³C{¹H} NMR (101 MHz, r.t., C₆D₆): δ 9.0, 9.5 (Im-Me×2), 24.3 (SiC(CH₃)₃), 30.3 (SiC(CH₃)₃), 34.3 (NMe), 38.6 (SiCH₂Im), 125.1, 125.6 (4,5-ImC), 182.7 (2-ImC), 214.7, 216.8 (CO).^{S5} ²⁹Si{¹H} NMR (79.5 MHz, r.t., IG, C₆D₆): δ 76.2. IR (a toluene solution in a KBr liquid cell, cm⁻¹): 2025 (s, ν_{CO}), 1961 (s (sh), ν_{CO}), 1952 (s, ν_{CO}). UV-Vis (7.4 × 10⁻⁵ M, THF) 268 (sh, ε = 4.9 × 10³ M⁻¹ cm⁻¹), 288 (sh, ε = 2.6 × 10³ M⁻¹ cm⁻¹). HRMS (FD; positive): *m/z* calcd for [¹²C₁₈¹H₃₀¹⁴N₂¹⁶O₃²⁸Si⁵⁶Fe]⁺ ([M]⁺) 406.1375, found 406.1374. Anal. Calcd for C₁₈H₃₀N₂O₃SiFe: C, 53.20; H, 7.44; N, 6.89. Found: C, 53.24; H, 7.55; N, 6.82.

1.9 Synthesis of Ru(L¹)(H)(CO)₃ (**3**).

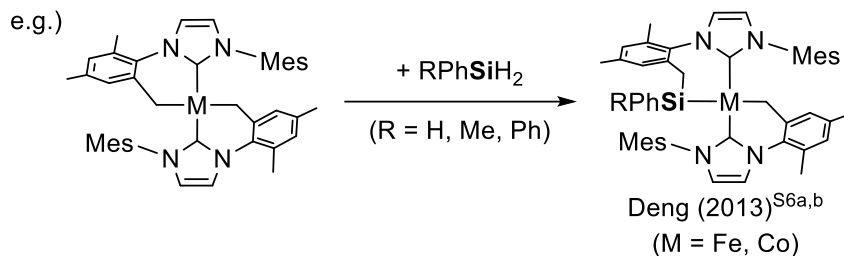


The title ruthenium complex was synthesised and isolated by a procedure similar to that for iron complex **1** (see section 1.6): A mixture of [L¹·H₂]I (121 mg, 0.224 mmol), KN(SiMe₃)₂ (49 mg, 0.25 mmol) and Ru₃(CO)₁₂ (49 mg, 0.076 mmol; 0.34 equiv.) in toluene (7 mL) was heated at 80 °C for 24 h. The reaction mixture was filtered, and the filtrate was evaporated under vacuum. Purification of the residue by flash chromatography [eluent: hexane : toluene = 3 : 1, under argon, silica gel (6.8 g)] afforded a colourless solid of crude **3** (68 mg). The solid was suspended in Et₂O, and then the suspension was cooled at -35 °C in a freezer. Ru(L¹)(H)(CO)₃ (**3**) was obtained as a colourless solid (63 mg, 99 μmol) in 46% yield.

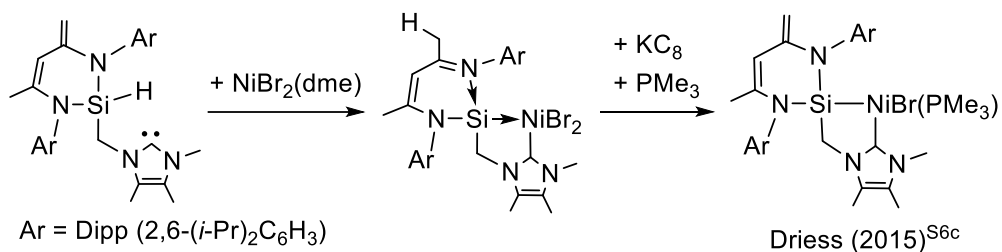
¹H NMR (400 MHz, r.t., C₆D₆): δ -7.21 (s, 1H, Ru-H), 0.92, 0.95 (d, ³J_{HH} = 6.8 Hz, 3H×2, CH(CH₃)₂), 1.20, 1.39 (s, 9H×2, Si(t-Bu)₂), 1.36, 1.42 (d, ³J_{HH} = 6.8 Hz, 3H×2, CH(CH₃)₂), 1.43, 1.60 (s, 3H×2, Im-Me), 2.43, 2.44 (sept, ³J_{HH} = 6.8 Hz, 1H×2, CH(CH₃)₂), 2.99, 3.31 (d, 1H×2, ²J_{HH} = 13.7 Hz, SiCH₂Im), 7.09 (d, ³J_{HH} = 7.8 Hz, 2H, *m*-ArH), 7.26 (t, ³J_{HH} = 7.8 Hz, 1H, *p*-ArH). ¹³C{¹H} NMR (101 MHz, r.t., C₆D₆): δ 10.2, 10.3 (Im-Me), 23.4, 23.9 (SiC(CH₃)₃), 23.9, 24.0, 24.4, 24.6 (CH(CH₃)₂), 28.1, 28.2 (CH(CH₃)₂), 29.4, 31.5 (SiC(CH₃)₃), 39.6 (SiCH₂Im), 124.6, 125.0 (*m*-ArC), 125.6, 126.4 (4,5-ImC), 130.8 (*p*-ArC), 135.5 (*ipso*-ArC), 146.6, 147.4 (*o*-ArC), 179.6 (2-ImC), 194.9, 200.1, 202.4 (CO). ²⁹Si{¹H} NMR (79.5 MHz, r.t., IG, C₆D₆): δ 64.8. IR (KBr liquid cell, a toluene solution, cm⁻¹): 2052 (s, ν_{CO}), 2000 (s, ν_{CO}), 1979 (s, ν_{CO}). UV-Vis (1.3 × 10⁻⁴ M, THF, λ / nm) ca. 2.6 × 10² (sh, ε = 6 × 10³ M⁻¹ cm⁻¹), ca. 2.7 × 10² (sh, ε = 2 × 10³ M⁻¹ cm⁻¹). HRMS (FD; positive): *m/z*

calcd for $[^{12}\text{C}_{29}^{1}\text{H}_{44}^{14}\text{N}_2^{16}\text{O}_3^{28}\text{Si}^{102}\text{Ru}]^+$ ($[\text{M}]^+$) 598.2165, found 598.2161. Anal. Calcd for $\text{C}_{29}\text{H}_{44}\text{N}_2\text{O}_3\text{SiRu}$: C, 58.26; H, 7.42; N, 4.69. Found: C, 58.15; H, 7.48; N, 4.83.

(a) Si–C coupling of cyclometalated NHC complexes with hydrosilanes



(b) Complexation with *N*-(hydrosilyl)methyl NHC followed by reduction



(c) **This work** Use of *N*-(hydrosilyl)methyl imidazolium salts

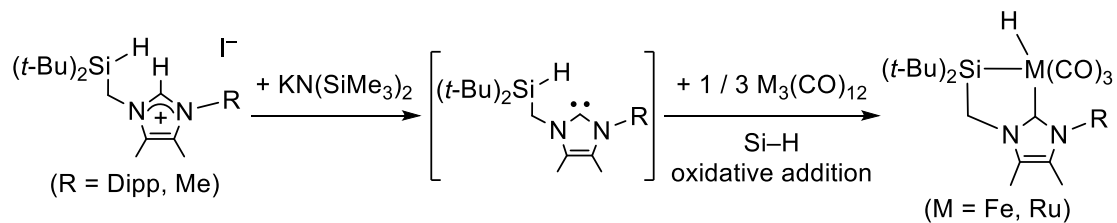


Fig. S1 Methods for the synthesis of silyl–NHC chelate complexes.^{S6}

1.10 NMR monitoring of the double hydroboration of nitriles with pinacolborane (HBpin) using silyl–NHC iron/ruthenium complexes.

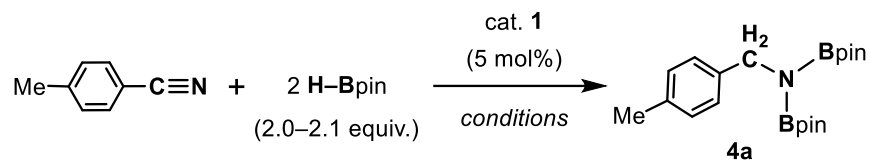
General considerations

The NMR yields (%) of double hydroboration products **4** and time to reaction completion were calculated from the average of two experiments performed on each. These yields were determined by ^1H NMR based on the molar amount of nitrile before reaction. Products **4** were identified by comparing ^1H , $^{13}\text{C}\{^1\text{H}\}$ and ^{11}B NMR data with literature values.^{S7}

1.10.1 Optimisation of catalytic conditions: general procedure

These reactions were all carried out by nearly the same procedures except the conditions shown in Table S1, and a general procedure for them is as follows. In a 5 mL vial, $\text{Fe}(\text{L}^1)(\text{H})(\text{CO})_3$ (**1**) (10 mg, 18 μmol ; 5 mol% based on nitrile), *p*-tolunitrile (43 mg, 0.37 mmol; 1.0 equiv.), HBpin (96–97 mg, 0.75–0.76 mmol; 2.0–2.1 equiv.) and C_6Me_6 (ca. 2–3 mg, internal standard) were dissolved in C_6D_6 (1.0 mL). The colourless solution obtained was evenly distributed and transferred to two J Young NMR tubes to perform the same monitoring experiment twice. ^1H NMR spectra of each solution was recorded to confirm the integration ratio of the signals between *p*-tolunitrile and the internal standard. Each solution was treated under conditions shown in Table S1, and the reaction was monitored by ^1H NMR spectroscopy. For example, under the conditions of entry 1, the solution was photoirradiated for 2 h using a medium pressure Hg lamp and then was heated using an oil bath at 60 °C for 3.5 h. The NMR yield of hydroboration product **4a** as the average of the two experiments was determined by comparison of the integration ratio of the ^1H NMR signals between **4a** and the internal standard. The conditions and results are summarised in Table S1. The time course of the yield of **4a** for entries 1–3 in Table S1 is depicted in Fig. S2.

Table S1 Optimization of conditions for hydroboration of *p*-tolunitrile with HBpin using complex **1**



entry	equiv. of HBPin	conditions	NMR yield of 4a / %
1	2.0	$h\nu$ ($\lambda > 300$ nm), ca. 7 °C, 11 h ^a	95
2	2.0	$h\nu$ ($\lambda > 300$ nm), ca. 7 °C, 2 h; ^a then ca. 24 °C (r.t.), 22 h	41
3	2.0	$h\nu$ ($\lambda > 300$ nm), ca. 7 °C, 2 h; ^a then 60 °C, 3.5 h (optimised conditions)	89
4	2.1	60 °C, 16 h	~0

^aAfter UV irradiation for 2 h, colour of a reaction solution was changed to deep brown, and complex **1** was consumed completely. At this point, double hydroboration product **4a** was formed in ca. 20~30% NMR yield.

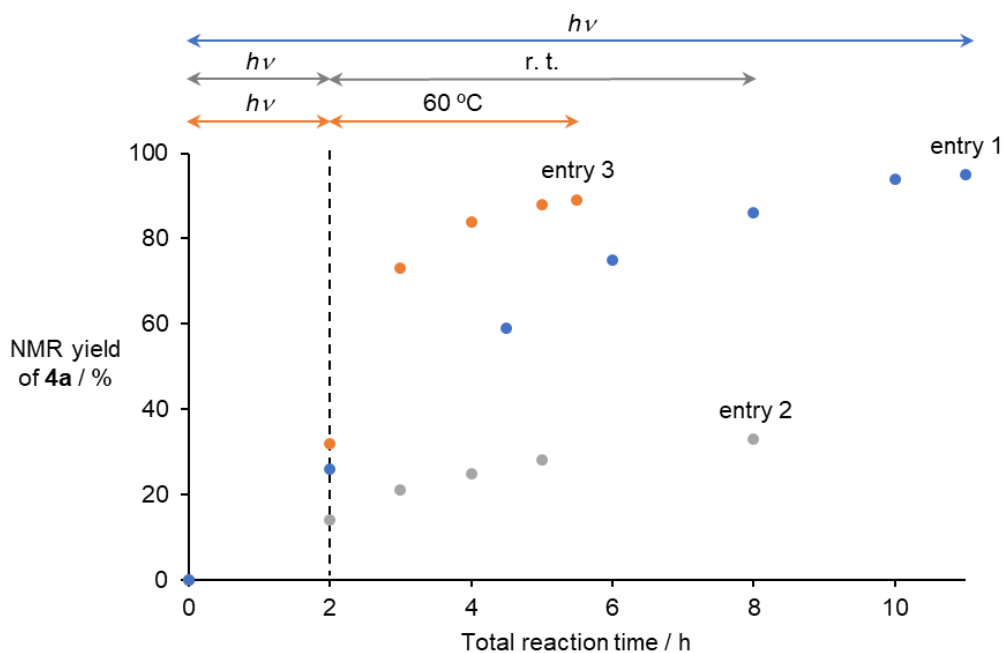


Fig. S2 Time course of catalytic double hydroboration of *p*-tolunitrile with HBpin using 5 mol% of complex **1** for entries 1–3 in Table S1.

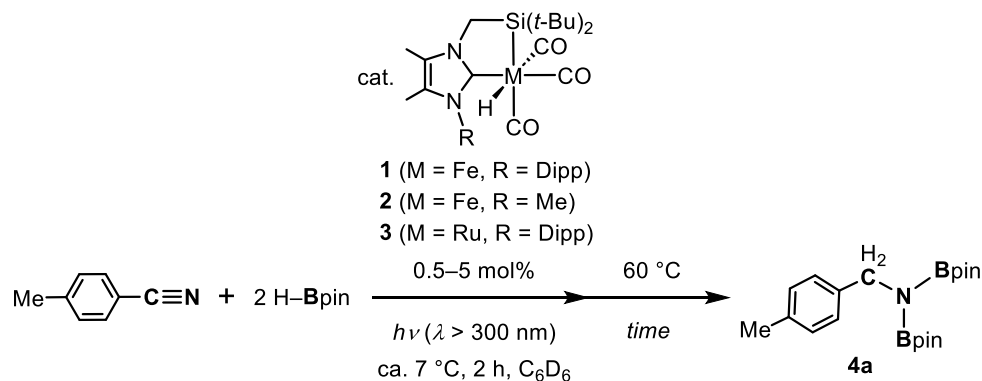
1.10.2 Comparison of catalytic activity between complexes **1**, **2** and **3**.

According to the optimised conditions using complex **1** described in Section 1.10.1, the double hydroboration of *p*-tolunitrile with HBpin in the presence of a catalytic amount of Fe(L²)(H)(CO)₃ (**2**) and Ru(L¹)(H)(CO)₃ (**3**) were carried out for the comparison of their catalytic activity with that of **1**. A solution of *p*-tolunitrile (43 mg, 0.37 mmol), HBpin (97 mg, 0.76 mmol; 2.0 equiv.), internal standard (C₆Me₆) and catalyst **2** or **3** (7 mg, 0.02 mmol; 5 mol%) in C₆D₆ (1.0 mL) was used for the reaction. The reaction was monitored by ¹H NMR. The reaction catalysed by **2** and **3** afforded the hydroboration product **4a** in 88 and 11% NMR yields, respectively (time of heating at 60 °C: 3.0 h for **2** and 3.5 h for **3**).

The same catalytic reaction was also carried out using 0.5 mol% of **1** or **2**. *p*-Tolunitrile (44 mg, 0.37 mmol; 1.0 equiv.), H-Bpin (98 mg, 0.76 mmol; 2.1 equiv.) and C₆Me₆ (ca. 2–3 mg, internal standard) were added to a C₆D₆ solution of **1** or **2** (2 mmol L⁻¹, 1.0 mL, 2 μmol; 0.5 mol%). The solution was evenly distributed into two NMR tubes with Teflon needle valves. These solutions were irradiated with a medium-pressure mercury lamp (λ > 300 nm) at ca. 7 °C for 2 h. The resulting reaction solutions were then heated at 60 °C. The reaction catalysed by **1** afforded product **4a** in 92% NMR yield after 17 h of heating accompanied by complete consumption of *p*-tolunitrile. On the other hand, when 0.5 mol% of **2** was used, **4a** was formed in 29% NMR yield after 17 h of heating, and this yield was nearly the same as that (28%) for the reaction mixture after 6 h of heating. At the end of the reaction, ca. 70% of the nitrile remained unreacted in the reaction mixture. The time course of the yield of **4a** for the reactions using 0.5 mol% of **1** and **2** is depicted in Fig. S3.

The NMR yields of the hydroboration product **4a** and reaction conditions in this section are summarised in Table S2.

Table S2 Comparison of catalytic performance in the double hydroboration of *p*-tolunitrile between complexes **1**, **2** and **3**.



entry	cat.	loading / mol%	time / h	NMR yield of 4a / %
1	1 (M = Fe, R = Dipp)	5	3.5	89
2	1	0.5	17	92
3	2 (M = Fe, R = Me)	5	3.0	88
4	2	0.5	17	29
5	3 (M = Ru, R = Dipp)	5	3.5	11

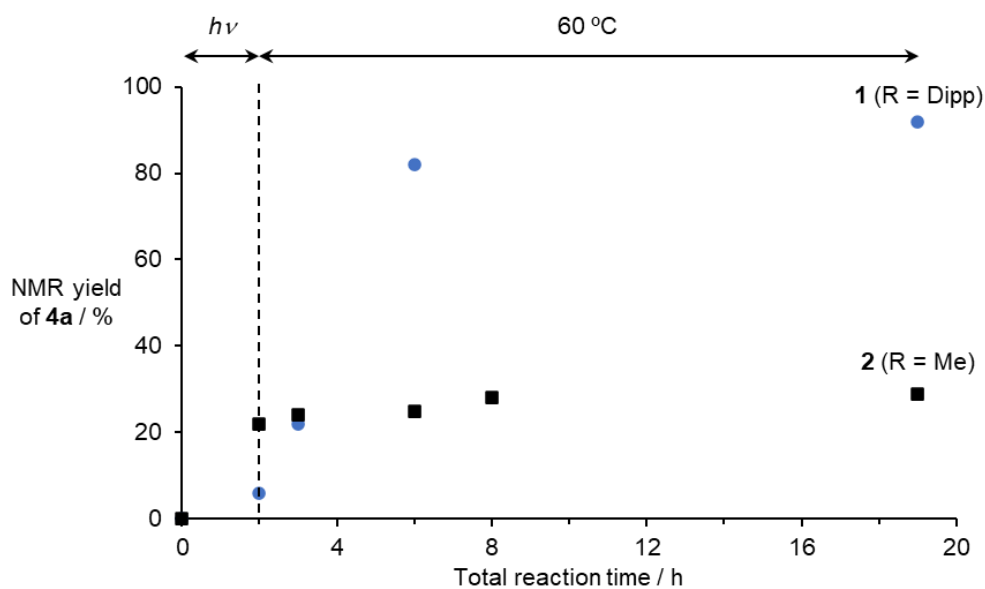


Fig. S3 Time course of catalytic double hydroboration of *p*-tolunitrile with HBpin using 0.5 mol% of complexes **1** and **2** (entries 2 and 4 in Table S2).

1.10.3 Scope of nitriles in the double hydroboration using complex **1**

General procedure

The procedure was carried out according to the method optimised by the experiment described in section 1.10.1 using a solution of $\text{Fe}(\text{L}^1)(\text{H})(\text{CO})_3$ (**1**) (18 μmol , 5 mol%), aryl/alkylnitriles (0.36–0.38 mmol, 1.0 equiv.), HBpin (0.76–0.78 mmol, 2.0–2.1 equiv.) and C_6Me_6 or $\text{Si}(\text{SiMe}_3)_4$ (a minimum amount, internal standard) in C_6D_6 (1.0 mL) (equally divided in two samples). After 2 h of UV irradiation followed by heating of the solution at 60 °C for 1–30 h, nitrile was consumed completely, and double hydroboration product **4** was formed in 85–95% NMR yield (average of two runs). The results and conditions are summarised in Table S3.

*Double hydroboration of benzonitrile using **1** at a low catalyst loading of 0.5 mol%*

A reaction by a procedure similar to the above general procedure was also performed with benzonitrile (40 mg, 0.39 mmol; 1.0 equiv.), HBpin (98 mg, 0.77 mmol; 2.0 equiv.), C_6Me_6 (ca. 2–3 mg, internal standard) and a C_6D_6 solution of **1** (2 mmol L^{-1} , 1.0 mL, 2 μmol ; 0.5 mol%). After 42 h of heating, the double hydroboration product **4e** was formed in 92% NMR yield.

*Isolation of double hydroboration product **4f***

This procedure was carried out in a glovebox under argon atmosphere. A reaction mixture of *m*-tolunitrile with HBpin using 5 mol% **1** (entry 6 in Table S3) involving bis(boryl)amine **4f** as the main product was evaporated under vacuum. The residue was extracted with hexane, and the extract was then filtered through a syringe filter. After the filtrate was evaporated under vacuum, the residue was recrystallized from pentane at –35 °C in a freezer, leading to the precipitation of a colorless solid. Removal of the mother liquid, washing with a minimum amount of cold pentane, followed by evaporation afforded **4f** as a colorless powder in 33% yield (23 mg). A second crop of the product was obtained from the combined solution of the mother liquid and the pentane washing solution in a similar manner

in 29% yield (20 mg). Total yield of **4f**: 62% (43 mg). The ^1H , $^{13}\text{C}\{^1\text{H}\}$ and $^{11}\text{B}\{^1\text{H}\}$ NMR spectra of isolated **4f** were depicted in Figs. S54, S55 and S56, respectively.

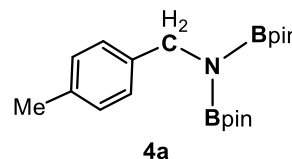
Table S3 Scope of nitrile for the double hydroboration with HBpin using complex **1**

entry	R	heating time / h	product	NMR yield / %
1	<i>p</i> -MeC ₆ H ₄	3.5	4a	89
2	<i>p</i> -MeOC ₆ H ₄	2.0	4b	89
3	<i>p</i> -CF ₃ C ₆ H ₄	6.0	4c	88
4	<i>p</i> -FC ₆ H ₄	11.0	4d	85
5	C ₆ H ₅	17.5	4e	86
6	<i>m</i> -MeC ₆ H ₄	3.5	4f	92 (62) ^a
7	Me	1.0	4g	95
8	Et	1.5	4h	92
9	<i>t</i> -Bu	30.0	4i	92

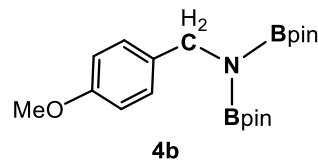
^aIsolated yield.

NMR spectroscopic data for bis(boryl)amines **4**:

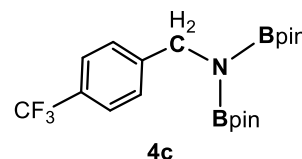
(*p*-MeC₆H₄)CH₂N(Bpin)₂ (4a**):** ^1H NMR (400 MHz, C₆D₆): δ 1.03 (s, 24H, Bpin-Me), 2.14 (s, 3H, *p*-Me), 4.57 (s, 2H, NCH₂), 7.06 (d, $^3J_{\text{HH}} = 7.9$ Hz, 2H, ArH), 7.50 (d, $^3J_{\text{HH}} = 7.9$ Hz, 2H, ArH). $^{13}\text{C}\{^1\text{H}\}$ NMR (101 MHz, C₆D₆): δ 21.1 (*p*-Me), 24.7 (Bpin-Me), 47.6 (NCH₂), 82.5 (OCMe), 128.1, 129.0, 135.7, 140.8 (ArC). $^{11}\text{B}\{^1\text{H}\}$ NMR (128 MHz, C₆D₆): δ 26.6 (br, $\Delta\nu_{1/2} = 417$ Hz).



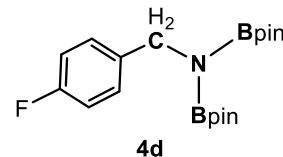
(*p*-OMeC₆H₄)CH₂N(Bpin)₂ (4b): ¹H NMR (400 MHz, C₆D₆): δ 1.03 (s, 24H, Bpin-Me), 3.35 (s, 3H, *p*-OMe), 4.54 (s, 2H, NCH₂), 6.85 (d, ³J_{HH} = 8.6 Hz, 2H, ArH), 7.53 (d, ³J_{HH} = 8.6 Hz, 2H, ArH). ¹³C{¹H} NMR (101 MHz, C₆D₆): δ 24.7 (Bpin-Me), 47.2 (NCH₂), 54.7 (*p*-OMe), 82.5 (OCMe₂), 113.8, 129.4, 136.0, 158.9 (ArC). ¹¹B{¹H} NMR (128 MHz, C₆D₆): δ 26.3 (br, Δν_{1/2} = 504 Hz).



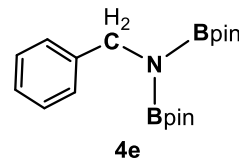
(*p*-CF₃C₆H₄)CH₂N(Bpin)₂ (4c): ¹H NMR (400 MHz, C₆D₆): δ 1.00 (s, 24H, Bpin-Me), 4.45 (s, 2H, NCH₂), 7.40 (s, 4H, ArH). ¹³C{¹H} NMR (101 MHz, C₆D₆): δ 24.6 (Bpin-Me), 47.4 (NCH₂), 82.7 (OCMe₂), 125.20 (q, ¹J_{CF} = 272 Hz, CF₃), 125.21 (q, ³J_{CF} = 3.7 Hz, *m*-ArC), 128.1 (*o*-ArC), 128.9 (q, ²J_{CF} = 32 Hz, *p*-ArC), 147.7 (*ipso*-ArC). ¹¹B{¹H} NMR (128 MHz, C₆D₆): δ 26.1 (br, Δν_{1/2} = 437 Hz). ¹⁹F{¹H} NMR (376 MHz, C₆D₆): δ -62.0.



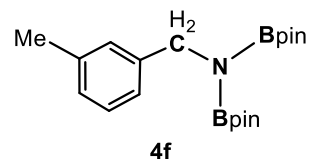
(*p*-FC₆H₄)CH₂N(Bpin)₂ (4d): ¹H NMR (400 MHz, C₆D₆): δ 1.01 (s, 24H, Bpin-Me), 4.45 (s, 2H, NCH₂), 6.84–6.91 (m, 2H, ArH), 7.37–7.43 (m, 2H, ArH). ¹³C{¹H} NMR (101 MHz, C₆D₆): δ 24.6 (Bpin-Me), 47.1 (NCH₂), 82.6 (OCMe₂), 114.9 (d, ²J_{CF} = 21 Hz, *m*-ArC), 129.8 (d, ³J_{CF} = 9 Hz, *o*-ArC), 139.5 (d, ⁴J_{CF} = 3 Hz, *ipso*-ArC), 162.2 (d, ¹J_{CF} = 243 Hz, *p*-ArC). ¹¹B{¹H} NMR (128 MHz, C₆D₆): δ 26.3 (br, Δν_{1/2} = 350 Hz). ¹⁹F{¹H} NMR (376 MHz, C₆D₆): δ -116.9.



PhCH₂N(Bpin)₂ (4e): ¹H NMR (400 MHz, C₆D₆): δ 1.02 (s, 24H, Bpin-Me), 4.58 (s, 2H, NCH₂), 7.07–7.13 (m, 1H, ArH), 7.20–7.26 (m, 2H, ArH), 7.54–7.58 (m, 2H, ArH). ¹³C{¹H} NMR (101 MHz, C₆D₆): δ 24.7 (Bpin-Me), 47.9 (NCH₂), 82.5 (OCMe₂), 126.6, 128.0, 128.3, 143.7 (ArC). ¹¹B{¹H} NMR (128 MHz, C₆D₆): δ 26.4 (br, Δν_{1/2} = 312 Hz).

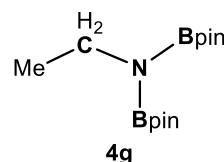


(*m*-MeC₆H₄)CH₂N(Bpin)₂ (4f): ¹H NMR (400 MHz, C₆D₆): δ 1.03 (s, 24H, Bpin-Me), 2.18 (s, 3H, *m*-Me), 4.58 (s, 2H, NCH₂), 6.95 (d, ³J_{HH} = 7.5 Hz, 1H, ArH), 7.19 (t, ³J_{HH} = 7.5 Hz, 2H, ArH), 7.37 (s, 1H, ArH), 7.41 (d, ³J_{HH} = 7.5 Hz, 1H, ArH). ¹³C{¹H} NMR (101 MHz, C₆D₆): δ 21.5 (*m*-Me), 24.7 (Bpin-Me), 47.8 (NCH₂), 82.5 (OCMe), 125.0, 127.3, 128.9, 137.4, 143.6 (ArC). An ArC signal (δ ca. 128) was not observed due to the overlap with that of C₆D₆.

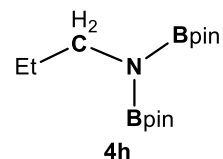


¹¹B{¹H} NMR (128 MHz, C₆D₆): δ 26.4 (br, Δν_{1/2} = 320 Hz).

MeCH₂N(Bpin)₂ (4g): ¹H NMR (400 MHz, C₆D₆): δ 1.05 (s, 24H, Bpin-Me), 1.31 (t, ³J_{HH} = 7.0 Hz, 3H, Me), 3.46 (q, ³J_{HH} = 7.0 Hz, 2H, NCH₂). ¹³C{¹H} NMR (101 MHz, C₆D₆): δ 19.2 (NCH₂Me), 24.7 (Bpin-Me), 39.1 (NCH₂), 82.2 (OCMe₂). ¹¹B{¹H} NMR (128 MHz, C₆D₆): δ 26.1 (br, Δν_{1/2} = 206 Hz).



EtCH₂N(Bpin)₂ (4h): ¹H NMR (400 MHz, C₆D₆): δ 0.94 (t, ³J_{HH} = 7.5 Hz, 2H, NCH₂CH₂CH₃), 1.05 (s, 24H, Bpin-Me), 1.68–1.79 (m, 2H, NCH₂CH₂CH₃), 3.39 (t, ³J_{HH} = 7.2 Hz, 2H, NCH₂). ¹³C{¹H} NMR (101 MHz, C₆D₆): δ 11.5 (NCH₂CH₂CH₃), 24.7 (Bpin-Me), 26.8 (NCH₂CH₂CH₃), 46.0 (NCH₂), 82.2 (OCMe₂). ¹¹B{¹H} NMR (128 MHz, C₆D₆): δ 26.2 (br, Δν_{1/2} = 271 Hz).



(*t*-Bu)CH₂N(Bpin)₂ (4i): ¹H NMR (400 MHz, C₆D₆): δ 1.01 (s, 9H, *t*-Bu), 1.07 (s, 24H, Bpin-Me), 3.29 (s, 2H, NCH₂). ¹³C{¹H} NMR (101 MHz, C₆D₆): δ 24.7 (Bpin-Me), 28.0 (C(CH₃)₃), 33.6 (C(CH₃)₃), 54.9 (NCH₂), 82.2 (OCMe₂). ¹¹B{¹H} NMR (128 MHz, C₆D₆): δ 26.2 (br, Δν_{1/2} = 274 Hz).

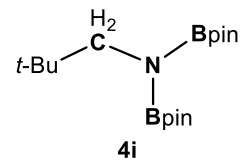
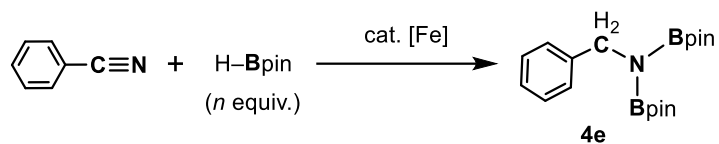
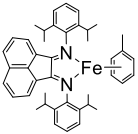
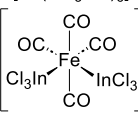


Table S4 Comparison of catalytic performance of complex **1** and previously-reported iron complexes^{S8} in the double hydroboration of benzonitrile.



entry	cat. [Fe]	loading / mol%	equiv. of HBpin (<i>n</i>)	conditions (solvent, temp., time)	yield / %
1	1	5	2.0	C ₆ D ₆ , <i>hν</i> ($\lambda > 300$ nm), 7 °C, 2 h; then 60 °C, 17.5 h	86 (NMR)
2	1	0.5	2.0	C ₆ D ₆ , <i>hν</i> ($\lambda > 300$ nm), 7 °C, 2 h; then 60 °C, 42 h	92 (NMR)
3		1	2.5	neat, r.t., 3.5 h	98 (NMR) ^{S8a}
	(Findlater et al.)				
4	Fe(OTf) ₂ (CH ₃ CN) ₂ with KO ^t Bu (additive, 9 mol%) (de Ruiter et al.)	3	3.0	C ₆ D ₆ , r.t., 3 h,	73 (NMR) ^{S8b}
5	[Fe(CH ₃ CN) ₆] 	5 (vs. HBpin)	0.2	neat, 80 °C, 24 h	65 (isolated) ^{S8c}
	(Nakazawa et al.)				

1.11 Synthesis of *N*-silylimine complexes **5** and **6** by stoichiometric reactions of silyl-NHC complex **1** with aryl nitriles and hydroboration of nitriles catalysed by **6**

1.11.1 Stoichiometric reactions of Fe(L¹)(H)(CO)₃ (**1**) with *p*-tolunitrile and *p*-(trifluoromethyl)benzotrile

(a) NMR scale reactions

Reaction with p-tolunitrile: In an NMR tube with a Teflon needle valve, Fe(L¹)(H)(CO)₃ (**1**) (11 mg, 20 μmol), *p*-tolunitrile (3 mg, 0.03 mmol; ca. 1.4 equiv.) and C₆Me₆ (< 1 mg, internal standard) were dissolved in C₆D₆ (0.6 mL) to give a colourless solution. The solution was irradiated with a medium-pressure mercury lamp ($\lambda > 300$ nm) at ca. 7 °C, and the reaction progress was monitored by ¹H NMR. The colour of the solution changed from colourless to pale yellow upon UV irradiation. After 4 h of irradiation, complex **1** was consumed completely, and *N*-silylimine complex **5** was formed quantitatively.

Reaction with p-(trifluoromethyl)benzotrile: Similarly, a solution of complex **1** (10 mg, 19 μmol), *p*-(trifluoromethyl)benzotrile (4 mg, 0.02 mmol; ca. 1.2 equiv.) and C₆Me₆ (< 1 mg, internal standard) in C₆D₆ (0.6 mL) was irradiated for 5 h. The ¹H NMR spectrum of the reaction mixture showed that **1** was consumed completely, and *N*-silylimine complex **6** was formed quantitatively.

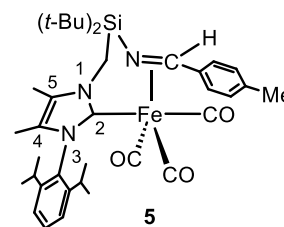
(b) Preparative scale reactions

Reaction with p-tolunitrile: To a 5 mL vial was added complex **1** (35 mg, 64 μmol), *p*-tolunitrile (9 mg, 0.08 mmol; ca. 1.3 equiv.) and toluene (1.0 mL) to give a colourless solution. The solution was transferred to a reaction tube with a Teflon needle valve (10 mmϕ). The vial was rinsed twice with toluene (2 mL total volume), and the solution obtained was also transferred to the reaction tube. The solution in the reaction tube was irradiated with a medium-pressure mercury lamp at ca. 7 °C for 6 h. The solution changed from colourless to deep yellow upon UV irradiation. The reaction solution was then transferred to a 5 mL vial, and the solvent was removed under reduced pressure to give a deep yellow powder. This

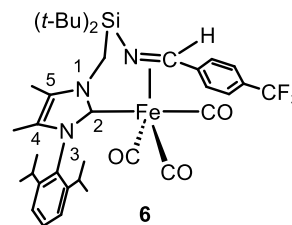
powder was washed with a small amount of hexane three times and then dried under reduced pressure to give *N*-silylimine complex **5** as a yellow powder (32 mg, 48 μmol , 75%).

Reaction with p-(trifluoromethyl)benzonitrile: By a procedure similar to that for the abovementioned synthesis of **5**, a solution of complex **1** (36 mg, 64 μmol) and *p*-(trifluoromethyl)benzonitrile (14 mg, 82 μmol ; 1.3 equiv.) in toluene (3 mL) was UV irradiated for 6 h. *N*-Silylimine complex **6** was isolated from the reaction mixture as a yellow powder (35 mg, 48 μmol ; 75%).

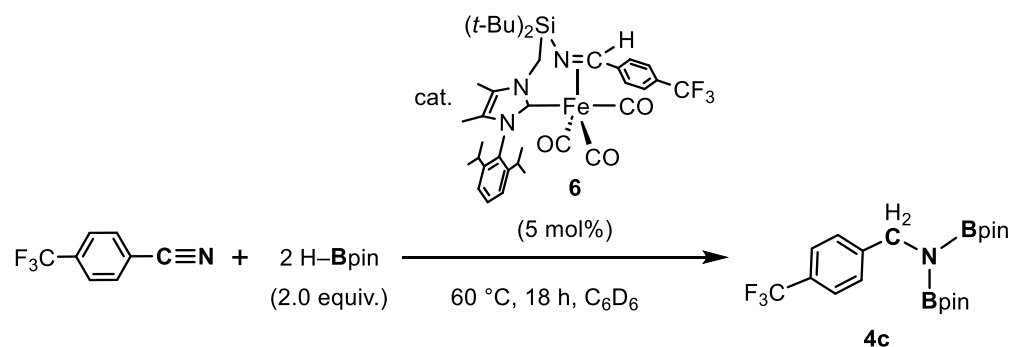
Data for *N*-silylimine complex **5.** ^1H NMR (400 MHz, C_6D_6): δ 0.90–0.95 (m, 6H, $\text{CH}(\underline{\text{C}}\text{H}_3)_2$), 0.93 (s, 9H, $\text{Si}(t\text{-Bu})$), 1.35 (s, 3H, Im-Me), 1.44 (d, $^3J_{\text{HH}} = 6.8$ Hz, 3H, $\text{CH}(\underline{\text{C}}\text{H}_3)$), 1.45 (s, 3H, Im-Me), 1.53 (s, 9H, $\text{Si}(t\text{-Bu})$), 1.70 (d, $^3J_{\text{HH}} = 6.8$ Hz, 3H, $\text{CH}(\underline{\text{C}}\text{H}_3)$), 2.05 (s, 3H, Me of the imine moiety), 2.32, 2.76 (sept, $^3J_{\text{HH}} = 6.8$ Hz, $1\text{H} \times 2$, $\underline{\text{C}}\text{H}(\text{C}\text{H}_3)_2$), 3.35, 3.60 (d, $^2J_{\text{HH}} = 15.0$ Hz, $1\text{H} \times 2$, SiCH_2Im), 6.08 (s, 1H, NCH of the imine moiety), 7.04 (d, $^3J_{\text{HH}} = 7.8$ Hz, 2H, ArH of the imine moiety), 7.11, 7.20 (d, $^3J_{\text{HH}} = 7.8$ Hz, $1\text{H} \times 2$, *m*-ArH of Dipp), 7.31 (t, $^3J_{\text{HH}} = 7.8$ Hz, 1H, *p*-ArH of Dipp), 7.82 (d, $^3J_{\text{HH}} = 7.8$ Hz, 2H, ArH of the imine moiety). $^{13}\text{C}\{^1\text{H}\}$ NMR (101 MHz, C_6D_6): δ 9.9, 10.5 (Im-Me), 21.1 (Me of the imine moiety), 22.66, 22.73 ($\underline{\text{C}}\text{H}(\text{C}\text{H}_3)_2$), 24.0 ($\text{CH}(\underline{\text{C}}\text{H}_3)_2$), 24.2, 24.8 ($\text{CH}(\underline{\text{C}}\text{H}_3)_2$), 28.26, 28.34 ($\text{Si}\underline{\text{C}}(\text{C}\text{H}_3)_3$), 28.7, 28.8 ($\text{SiC}(\underline{\text{C}}\text{H}_3)_3$), 34.4 (SiCH_2Im), 70.4 (NCH of the imine moiety), 124.6, 125.3 (*m*-ArC of Dipp), 125.6 (ArC of the imine moiety), 127.36, 127.41 (4,5-ImC), 129.2 (ArC of the imine moiety), 130.9 (*p*-ArC of Dipp), 134.9 (*p*-ArC of the imine moiety), 135.2 (*ipso*-ArC of Dipp), 146.2 (*ipso*-ArC of the imine moiety), 146.3, 147.7 (*o*-ArC of Dipp), 180.7 (2-ImC), 210.7, 212.9, 214.6 (CO). $^{29}\text{Si}\{^1\text{H}\}$ NMR (79.5 MHz, IG, C_6D_6): δ -2.6. IR (a toluene solution in a KBr cell, cm^{-1}): 2023 (s, ν_{CO}), 1959 (s, ν_{CO}), 1923 (s, ν_{CO}). HRMS (FD): m/z calcd for $[\text{C}_{37}\text{H}_{51}\text{N}_3\text{O}_3\text{Si}_1\text{Fe}_1]^+$ 669.3049, found 669.3049. Anal. Calcd for $\text{C}_{37}\text{H}_{51}\text{N}_3\text{O}_3\text{Si}_1\text{Fe}_1$: C, 66.35; H, 7.68; N, 6.27. Found: C, 66.48; H, 7.86; N, 6.08.



Data for *N*-silylimine complex **6.** ^1H NMR (400 MHz, C_6D_6): δ 0.87 (s, 9H, $\text{Si}(t\text{-Bu})$), 0.90, 0.91 (d, $^3J_{\text{HH}} = 6.8$ Hz, $3\text{H} \times 2$, $\text{CH}(\underline{\text{CH}}_3)_2$), 1.34 (s, 3H, Im-Me), 1.40 (d, $^3J_{\text{HH}} = 6.8$ Hz, 3H, $\text{CH}(\underline{\text{CH}}_3)$), 1.48 (s, 9H + 3H, $\text{Si}(t\text{-Bu})_2$ + Im-Me), 1.61 (d, $^3J_{\text{HH}} = 6.8$ Hz, 3H, $\text{CH}(\underline{\text{CH}}_3)$), 2.24, 2.70 (sept, $^3J_{\text{HH}} = 6.8$ Hz, $1\text{H} \times 2$, $\text{CH}(\underline{\text{CH}}_3)_2$), 3.32, 3.53 (d, $1\text{H} \times 2$, $^2J_{\text{HH}} = 15.2$ Hz, SiCH_2Im), 5.88 (s, 1H, NCH of the imine moiety), 7.09, 7.19 (d, $^3J_{\text{HH}} = 7.8$ Hz, $1\text{H} \times 2$, *m*-ArH of Dipp), 7.30 (t, $^3J_{\text{HH}} = 7.8$ Hz, 1H, *p*-ArH of Dipp), 7.36, 7.75 (d, $^3J_{\text{HH}} = 8.2$ Hz, $2\text{H} \times 2$, ArH of the imine moiety). $^{13}\text{C}\{^1\text{H}\}$ NMR (101 MHz, C_6D_6): δ 9.9, 10.4 (Im-Me), 22.5, 22.6 ($\underline{\text{C}}\text{H}(\underline{\text{CH}}_3)_2$), 24.0, 24.2, 24.65, 24.71 ($\text{CH}(\underline{\text{C}}\text{H}_3)_2$), 28.2, 28.3 ($\text{Si}\underline{\text{C}}(\underline{\text{C}}\text{H}_3)_3$), 28.6, 28.7 ($\text{SiC}(\underline{\text{C}}\text{H}_3)_3$), 34.3 (SiCH_2Im), 67.5 (NCH of the imine moiety), 124.6, 125.4 (*m*-ArC of Dipp), 125.5 (ArC of the imine moiety), 127.61, 127.63 (4,5-ImC), 131.0 (*p*-ArC of Dipp), 135.1 (*ipso*-ArC of Dipp), 146.2, 147.6 (*o*-ArC of Dipp), 153.5 (*ipso*-ArC of imine moiety), 179.5 (2-ImC), 209.8, 212.2, 213.8 (CO). The ^{13}C signals for CF_3 and *p*-ArC of the *N*-silylimine moiety could not be assigned because their intensities were very weak. $^{29}\text{Si}\{^1\text{H}\}$ NMR (79.5 MHz, IG, C_6D_6): δ -1.9. $^{19}\text{F}\{^1\text{H}\}$ NMR (376 MHz, C_6D_6): δ -61.7. IR (a toluene solution in a KBr cell, cm^{-1}): 2029 (s, ν_{CO}), 1965 (s, ν_{CO}), 1930 (s, ν_{CO}). HRMS (FD): m/z calcd for $[\text{C}_{37}\text{H}_{48}\text{N}_3\text{O}_3\text{F}_3\text{Si}_1\text{Fe}_1]^+$ 723.2766, found 723.2765. Anal. Calcd for $\text{C}_{37}\text{H}_{48}\text{N}_3\text{O}_3\text{F}_3\text{Si}_1\text{Fe}_1$: C, 61.40; H, 6.69; N, 5.81. Found: C, 61.45; H, 6.68; N, 5.86.



1.11.2 Double hydroboration of arynitrile with HBpin catalysed by *N*-silylimine complex **6**



In an NMR tube with a Teflon needle valve, *N*-silylimine complex **6** (5 mg, 7 μmol; 5 mol%), *p*-(trifluoromethyl)benzonitrile (24 mg, 0.14 mmol), HBpin (36 mg, 0.28 mmol; 2.0 equiv.) and C₆Me₆ (ca. 1 mg, internal standard) were dissolved into C₆D₆ (0.5 mL). The yellow solution obtained was then heated at 60 °C, and the reaction was monitored by NMR. After 18 h of heating, the nitrile was completely consumed, and the double hydroboration product **4c** was formed in 94% NMR yield.

2. X-ray crystal structure analysis

X-ray quality single crystals of **1**, **3** and **5**•THF were obtained as colourless plate crystals for **1** and **3** by being dissolved in a minimum amount of toluene at room temperature and then cooling at $-35\text{ }^{\circ}\text{C}$ or as pale-yellow plate crystals for **5**•THF from THF/hexane at room temperature. Intensity data for the analysis were collected on a Rigaku RAXIS-RAPID imaging plate diffractometer (for **1** and **3**) or on a Rigaku XtaLAB mini II diffractometer (for **5**•THF) with graphite monochromated Mo $K\alpha$ radiation ($\lambda = 0.71073\text{ \AA}$) under a cold nitrogen stream ($T = 150\text{ K}$). A numerical absorption correction was applied to the data. The structures were solved by the Patterson method using the DIRDIF-2008 program^{S9} and refined by full matrix least-squares techniques on all F^2 data with SHELXL-2018/1.^{S10} Anisotropic refinement was applied to all non-hydrogen atoms. The hydrido hydrogen atoms of **1** and **3** and the imine C–H hydrogen of **5** could be located on a difference Fourier map and refined isotropically. Other hydrogen atoms were put at calculated positions and refined using a riding model. Some reflections, i.e. $(h\ k\ l) = (0\ 1\ 0)$ and $(0\ -1\ 1)$ for **1**, $(0\ 0\ 1)$ and $(0\ -1\ 1)$ for **3** and $(-1\ 0\ 2)$ for **5**, were omitted from the final refinement because their intensities were significantly weakened by the beam stop. All calculations were carried out using Yadokari-XG.^{S11} Selected crystallographic data are given in Table S5. The crystal structure of **3** is depicted in Fig. S4. CCDC reference numbers: 2303857 (for **1**), 2303858 (for **3**) and 2303859 (for **5**•THF). Crystallographic data are available as a CIF file.

Table S5 Crystallographic data for M(L¹)(H)(CO)₃ [M = Fe (**1**) and Ru (**3**)] and Fe[L¹{N=C(H)(*p*-Tol)}](CO)₃ (**5**•THF).

compound	1	3	5 •THF
formula	C ₂₉ H ₄₄ N ₂ O ₃ SiFe	C ₂₉ H ₄₄ N ₂ O ₃ SiRu	C ₄₁ H ₅₉ N ₃ O ₄ SiFe
formula weight	552.60	597.82	741.85
crystal system	triclinic	triclinic	monoclinic
crystal size/mm ³	0.22 × 0.11 × 0.04	0.12 × 0.09 × 0.03	0.18 × 0.15 × 0.06
space group	<i>P</i> -1 (No. 2)	<i>P</i> -1 (No. 2)	<i>P</i> 2 ₁ / <i>c</i> (No. 14)
<i>a</i> /Å	8.5500(4)	8.8100(4)	13.5838(5)
<i>b</i> /Å	11.3730(6)	10.8356(3)	8.8169(4)
<i>c</i> /Å	16.0634(6)	16.6668(8)	33.9397(11)
α /°	105.0205(18)	105.883(2)	90
β /°	96.1600(10)	97.7180(12)	98.728(4)
γ /°	99.7320(10)	97.7921(9)	90
<i>V</i> /Å ³	1468.06(12)	1491.44(11)	4017.8(3)
<i>Z</i>	2	2	4
<i>D</i> _{calcd} /g·cm ⁻³	1.250	1.331	1.226
<i>F</i> (000)	592	628	1592
μ (Mo-K α)/mm ⁻¹	0.585	0.596	0.448
reflections collected	22916	23658	34543
unique reflections (<i>R</i> _{int})	6676 (0.1276)	6829 (0.0954)	9223 (0.0594)
refined parameters	341	341	468
<i>R</i> 1, <i>wR</i> 2 (all data) ^{<i>a,b</i>}	0.1012, 0.1236	0.0834, 0.1060	0.1027, 0.1312
<i>R</i> 1, <i>wR</i> 2 [<i>I</i> > 2 σ (<i>I</i>)] ^{<i>a,b</i>}	0.0688, 0.1151	0.0588, 0.1003	0.0599, 0.1176
GOF	1.125	1.115	1.011
largest residual peak, hole/e·Å ⁻³	0.433, -0.351	0.637, -1.377	0.839, -0.543

$$^a R1 = \sum ||F_o| - |F_c|| / \sum |F_o|, \quad ^b wR2 = \{ \sum [w (F_o^2 - F_c^2)^2] / \sum [w (F_o^2)^2] \}^{1/2}$$

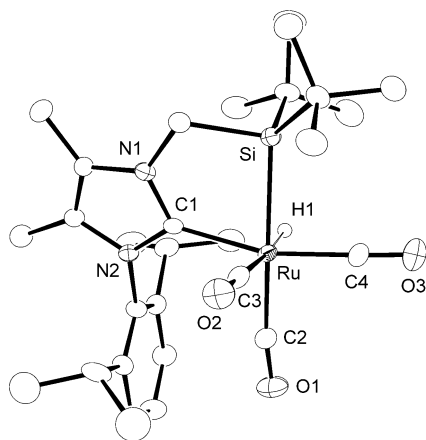
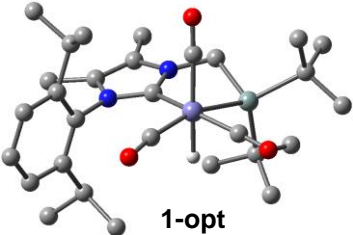
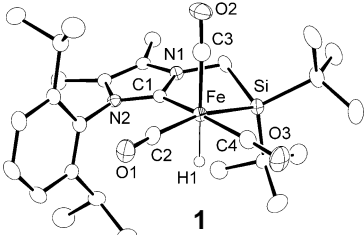


Fig. S4 Crystal structure of Ru(L¹)(H)(CO)₃ (**3**). Selected interatomic distances (Å) and angles (°): Ru–Si 2.4607(11), Ru–C1 2.119(4), Ru–C2 1.962(4), Ru–C3 1.948(4), Ru–C4 1.890(4), Ru–H1 1.64(4); Si–Ru–C1 78.00(10), Si–Ru–C2 168.02(12), Si–Ru–C3 95.38(12), Si–Ru–C4 87.99(13), Si–Ru–H1 81.1(15).

3. DFT calculations of complex **1**

The geometry of Fe(L¹)(H)(CO)₃ (**1**), i.e. **1-opt**, was optimized by the DFT method using the M06-L functional^{S12} and the def2-SVP basis set^{S13} for all atoms. Frequency calculations were performed to confirm that **1-opt** had no imaginary frequencies. For TD-DFT calculations of **1-opt**, the M06-L functional and the def2-TZVP^{S13} basis set were used for all atoms. The SMD model^{S14} was used to consider the solvent effect of THF for both the geometry optimization and the TD-DFT calculations. All calculations were carried out using the Gaussian 16 program package.^{S15} The selected bond distances and angles of **1-opt** with the corresponding values for the crystal structure of **1** are summarised in Table S6, showing that the geometry of **1-opt** is nearly identical with that of the crystal structure. HOMO–LUMO transition based on the TD-DFT calculations is illustrated in Fig. S5. Comparison of transitions to excited states based on the TD-DFT calculations and the UV-Vis spectrum of **1** in the range of 295–340 nm is shown in Fig. S6. Cartesian coordinates of all atoms in **1-opt** are listed in Table S7.

Table S6 Comparison of the geometric parameters of **1-opt** and the crystal structure of **1**

	Optimised structure (DFT)	Crystal structure (X-Ray)
		
Selected bond distances (Å)		
Fe–Si	2.374	2.3587(9)
Fe–C1 (carbene)	2.006	1.992(3)
Fe–C2 (CO)	1.792	1.804(3)
Fe–C3 (CO)	1.791	1.789(3)
Fe–C4 (CO)	1.760	1.758(3)
Fe–H1	1.532	1.43(4)

Selected bond angles (°)

Si-Fe-C1	80.0	80.49(8)
Si-Fe-C2	161.4	166.07(11)
C1-Fe-C4	160.7	162.68(13)
C2-Fe-C3	102.7	98.20(14)
C2-Fe-C4	94.4	93.02(14)
C3-Fe-C4	100.3	101.24(15)
Si-Fe-H1	76.6	79.7(15)
C3-Fe-H1	170.5	174.3(15)

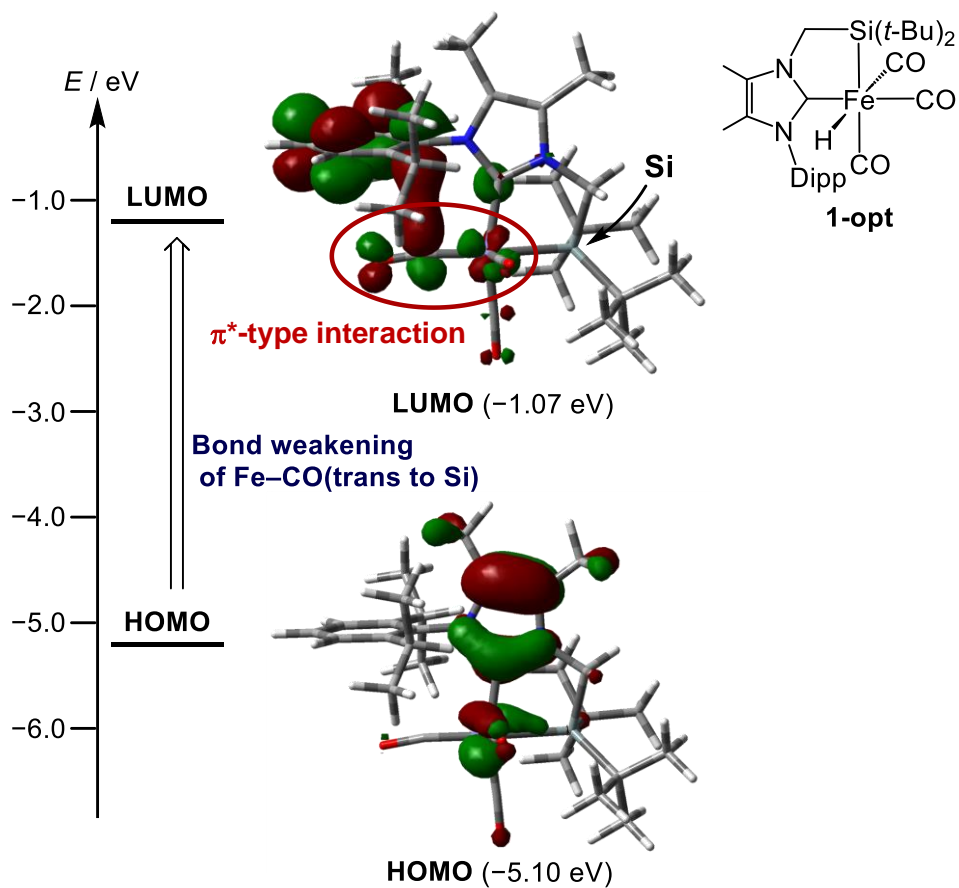


Fig. S5 HOMO-LUMO transition of **1-opt** based on the TD-DFT calculations

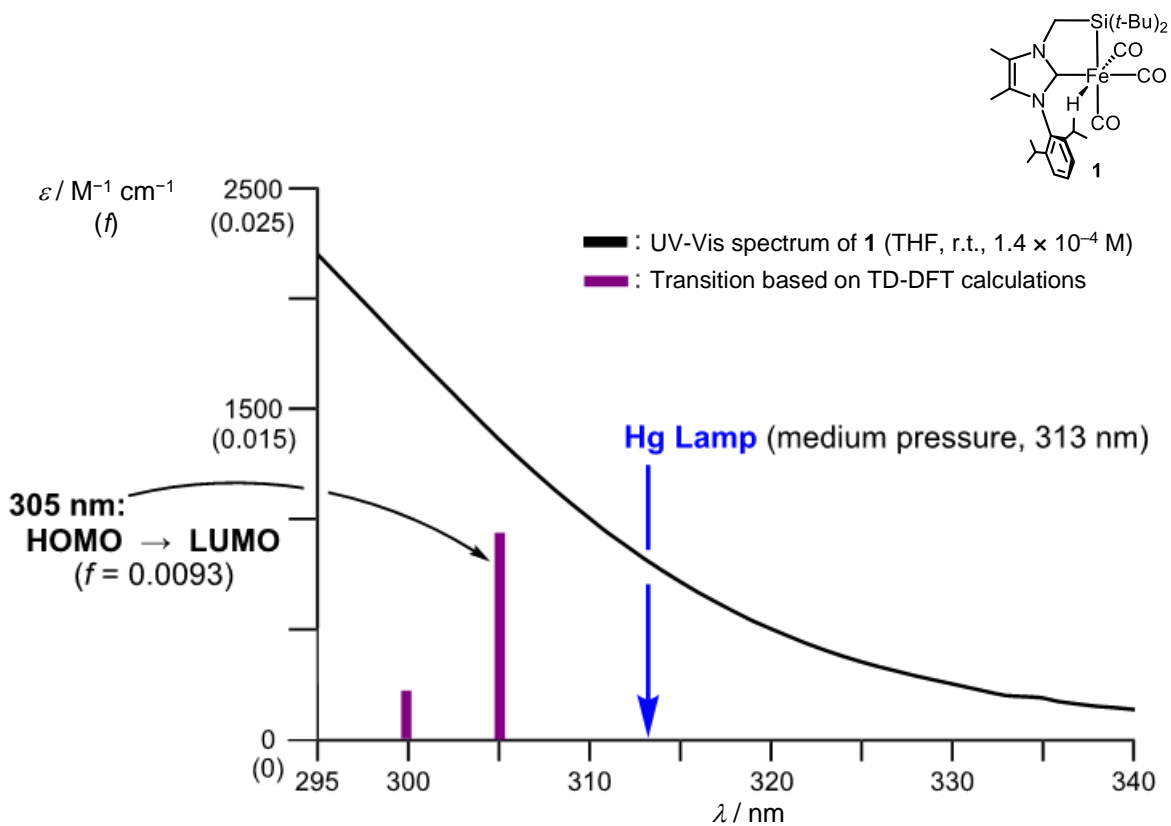


Fig. S6 UV-Vis spectrum of complex **1** and transitions based on TD-DFT calculations of **1-opt** in the range of 295–340 nm.

Table S7 Cartesian coordinates for **1-opt** (Total Energy = -3018.606555 a.u.)

Atomic type	Coordinates (Å)		
	x	y	z
Fe	0.001103	0.086532	-0.046437
Si	0.026163	0.049841	2.327433
C	1.979797	0.046263	0.281120
H	0.097111	-1.406127	0.285705
C	-0.025952	-0.458012	-1.753531
O	-0.227524	-0.861811	-2.819141
C	0.070176	1.869734	-0.202158
O	0.151963	3.019275	-0.321943
C	-1.727584	-0.141756	0.195083

O	-2.862878	-0.345751	0.325044
N	2.555854	0.433937	1.446271
N	3.032308	-0.303754	-0.509255
C	0.190195	-1.743818	3.073577
C	1.487221	-2.379622	2.566523
C	-0.982952	-2.627016	2.648113
C	0.262863	-1.712084	4.601776
C	-1.212675	1.165419	3.340607
C	-0.550501	1.630034	4.643082
C	-2.516154	0.443394	3.683481
C	-1.549506	2.414243	2.525595
C	1.753484	0.858469	2.577579
C	3.940856	0.330338	1.405736
C	4.249882	-0.143539	0.161027
C	4.795769	0.669747	2.562039
C	5.543922	-0.499075	-0.457545
C	2.963845	-0.719223	-1.878025
C	2.894183	0.268978	-2.880111
C	2.884442	-0.157801	-4.212214
C	2.933517	-1.510206	-4.534600
C	2.994340	-2.466578	-3.526158
C	3.019098	-2.094175	-2.177467
C	2.833808	1.751279	-2.565835
C	4.160606	2.433158	-2.885669
C	1.683546	2.438645	-3.292114
C	3.054921	-3.162026	-1.102283
C	1.702367	-3.862158	-1.001333
C	4.170761	-4.175129	-1.327594
H	1.540690	-2.411949	1.467634
H	2.384608	-1.852814	2.930141
H	1.567158	-3.422037	2.924294
H	-1.031383	-2.753865	1.554882
H	-0.885244	-3.637978	3.082535
H	-1.957034	-2.232216	2.975801
H	-0.671899	-1.371292	5.070013
H	0.459724	-2.725550	4.995277

H	1.076559	-1.068484	4.973508
H	-1.245282	2.272594	5.213433
H	-0.270235	0.801708	5.308690
H	0.353967	2.232003	4.465175
H	-3.050735	0.080937	2.793576
H	-2.362744	-0.418081	4.350089
H	-3.204731	1.128576	4.209779
H	-2.085911	2.182893	1.592116
H	-2.199871	3.089987	3.109184
H	-0.653032	2.993106	2.255038
H	1.696146	1.961586	2.599975
H	2.246902	0.547545	3.512631
H	4.610814	1.693040	2.922015
H	4.624242	-0.004677	3.415961
H	5.856878	0.597230	2.295770
H	5.697645	0.006137	-1.422907
H	6.375483	-0.222198	0.201499
H	5.622085	-1.580206	-0.653283
H	2.833828	0.586163	-5.011917
H	2.920393	-1.822096	-5.581946
H	3.021274	-3.527859	-3.788241
H	2.655761	1.865929	-1.484167
H	4.122830	3.503590	-2.634951
H	4.998193	1.992211	-2.326068
H	4.402417	2.355079	-3.957342
H	1.831459	2.442266	-4.382738
H	0.717455	1.952360	-3.091527
H	1.596909	3.488009	-2.975711
H	3.244438	-2.666018	-0.135737
H	1.461075	-4.397496	-1.933315
H	1.699776	-4.601903	-0.186345
H	0.886072	-3.149940	-0.808943
H	5.155244	-3.695978	-1.431577
H	4.231631	-4.878487	-0.484328
H	4.001630	-4.776875	-2.233487

4. References

- S1 M. Kuriyama, N. Hamaguchi, G. Yano, K. Tsukuda, K. Sato and O. Onomura, *J. Org. Chem.*, 2016, **81**, 8934–8946.
- S2 M. A. Bernd, F. Dyckhoff, B. J. Hofmann, A. D. Böth, J. F. Schlagintweit, J. Oberkofler, R. M. Reich and F. E. Kühn, *J. Catal.*, 2020, **391**, 548–561.
- S3 M. Weidenbruch, A. Schäfer and A. Lesch, in *Synthetic Methods of Organometallic and Inorganic Chemistry*, ed. W. A. Herrmann (vol. eds. N. Auner and U. Klingebiel), Georg Thieme Verlag, Stuttgart, New York, 1996, vol. 2, pp. 210–213.
- S4 For the synthesis of new organosilicon compounds, we referred to the synthetic procedures for the related compounds reported in the following literature. (a) T. Kobayashi and K. H. Pannell, *Organometallics*, 1991, **10**, 1960–1964; (b) M. Parasram, V. O. Iaroshenko and V. Gevorgyan, *J. Am. Chem. Soc.*, 2014, **136**, 17926–17929; (c) T. N. Komarova, L. I. Larina, E. V. Abramova and G. V. Dolgushin, *Russ. J. Gen. Chem.*, 2007, **77**, 1089–1092.
- S5 $^{13}\text{C}\{^1\text{H}\}$ NMR signals of organosilicon compounds, ligand precursors, complexes **1–3** were assigned based on $^1\text{H}\text{--}^{13}\text{C}$ HSQC and/or $^1\text{H}\text{--}^{13}\text{C}$ HMBC spectra.
- S6 (a) Z. Mo, Y. Liu and L. Deng, *Angew. Chem. Int. Ed.*, 2013, **52**, 10845–10849; (b) Z. Ouyang and L. Deng, *Organometallics*, 2013, **32**, 7268–7271; (c) G. Tan, S. Enthaler, S. Inoue, B. Blom and M. Driess, *Angew. Chem. Int. Ed.*, 2015, **54**, 2214–2218.
- S7 (a) P. Ghosh and A. J. von Wangelin, *Angew. Chem. Int. Ed.*, **2021**, *60*, 16035–16043; (b) N. Sarkar, S. Bera and S. Nembenna, *J. Org. Chem.* **2020**, *85*, 4999–5009.
- S8 (a) A. R. Bazkiaei, M. Wiseman and M. Findlater, *RSC Adv.*, 2021, **11**, 15284–15289; (b) R. Thenarukandiyil, V. Satheesh, L. J. W. Shimon and G. de Ruiter, *Chem. Asian J.*, 2021, **16**, 999–1006; (c) M. Ito, M. Itazaki and H. Nakazawa, *Inorg. Chem.*, 2017, **56**, 13709–13714.

- S9 P. T. Beurskens, G. Beurskens, R. de Gelder, S. Garcia-Granda, R. O. Gould and J. M. M. Smits, *The DIRDIF2008 program system*, Crystallography Laboratory, University of Nijmegen, The Netherlands, 2008.
- S10 (a) G. M. Sheldrick, *Acta Crystallogr., Sect. C: Struct. Chem.*, 2015, **71**, 3–8; (b) G. M. Sheldrick, *Acta Crystallogr., Sect. A: Found. Adv.*, 2008, **64**, 112–122.
- S11 (a) K. Wakita, *Yadokari-XG, Software for Crystal Structure Analyses*, 2001; (b) C. Kabuto, S. Akine, T. Nemoto and E. Kwon, Release of Software (Yadokari-XG 2009) for Crystal Structure Analyses, *J. Crystallogr. Soc. Jpn.*, 2009, **51**, 218–224.
- S12 Y. Zhao and D. G. Truhlar, *J. Chem. Phys.*, 2006, **125**, 194101.
- S13 (a) F. Weigend and R. Ahlrichs, *Phys. Chem. Chem. Phys.*, 2005, **7**, 3297–3305; (b) F. Weigend, *Phys. Chem. Chem. Phys.*, 2006, **8**, 1057–1065.
- S14 A. V. Marenich, C. J. Cramer and D. G. Truhlar, *J. Phys. Chem. B*, 2009, **113**, 6378–6396.
- S15 M. J. Frisch, G. W. Trucks, H. B. Schlegel, G. E. Scuseria, M. A. Robb, J. R. Cheeseman, G. Scalmani, V. Barone, G. A. Petersson, H. Nakatsuji, X. Li, M. Caricato, A. V. Marenich, J. Bloino, B. G. Janesko, R. Gomperts, B. Mennucci, H. P. Hratchian, J. V. Ortiz, A. F. Izmaylov, J. L. Sonnenberg, D. Williams-Young, F. Ding, F. Lipparini, F. Egidi, J. Goings, B. Peng, A. Petrone, T. Henderson, D. Ranasinghe, V. G. Zakrzewski, J. Gao, N. Rega, G. Zheng, W. Liang, M. Hada, M. Ehara, K. Toyota, R. Fukuda, J. Hasegawa, M. Ishida, T. Nakajima, Y. Honda, O. Kitao, H. Nakai, T. Vreven, K. Throssell, J. A. Montgomery, Jr., J. E. Peralta, F. Ogliaro, M. J. Bearpark, J. J. Heyd, E. N. Brothers, K. N. Kudin, V. N. Staroverov, T. A. Keith, R. Kobayashi, J. Normand, K. Raghavachari, A. P. Rendell, J. C. Burant, S. S. Iyengar, J. Tomasi, M. Cossi, J. M. Millam, M. Klene, C. Adamo, R. Cammi, J. W. Ochterski, R. L. Martin, K. Morokuma, O. Farkas, J. B. Foresman and D. J. Fox, *Gaussian 16, (Revision C.02)*, Gaussian, Inc., Wallingford CT, 2019.

5. Spectra of newly-synthesised organosilicon compounds, ligand precursors and silyl-NHC chelate complexes

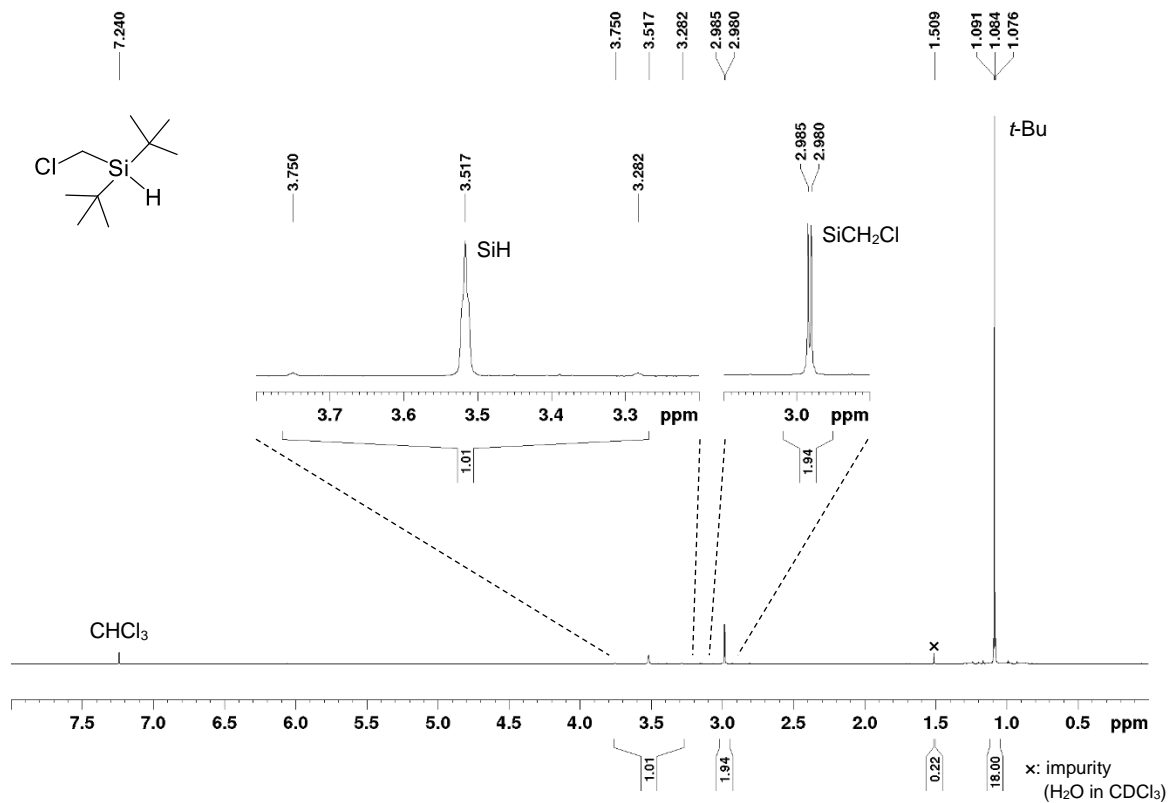


Fig. S7 ¹H NMR spectrum of di-*tert*-butyl(chloromethyl)silane (400 MHz, r.t., CDCl₃).

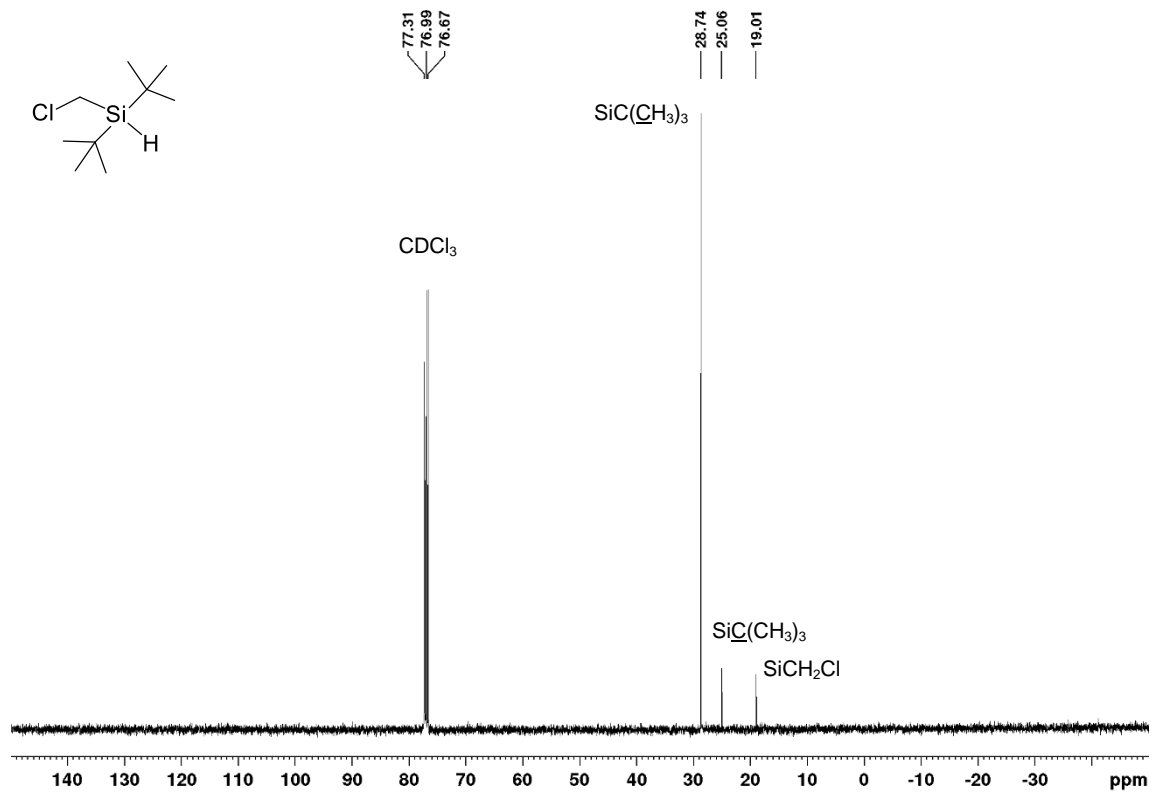


Fig. S8 $^{13}\text{C}\{^1\text{H}\}$ NMR spectrum of $(t\text{-Bu})_2\text{Si}(\text{H})\text{CH}_2\text{Cl}$ (101 MHz, r.t., CDCl_3).

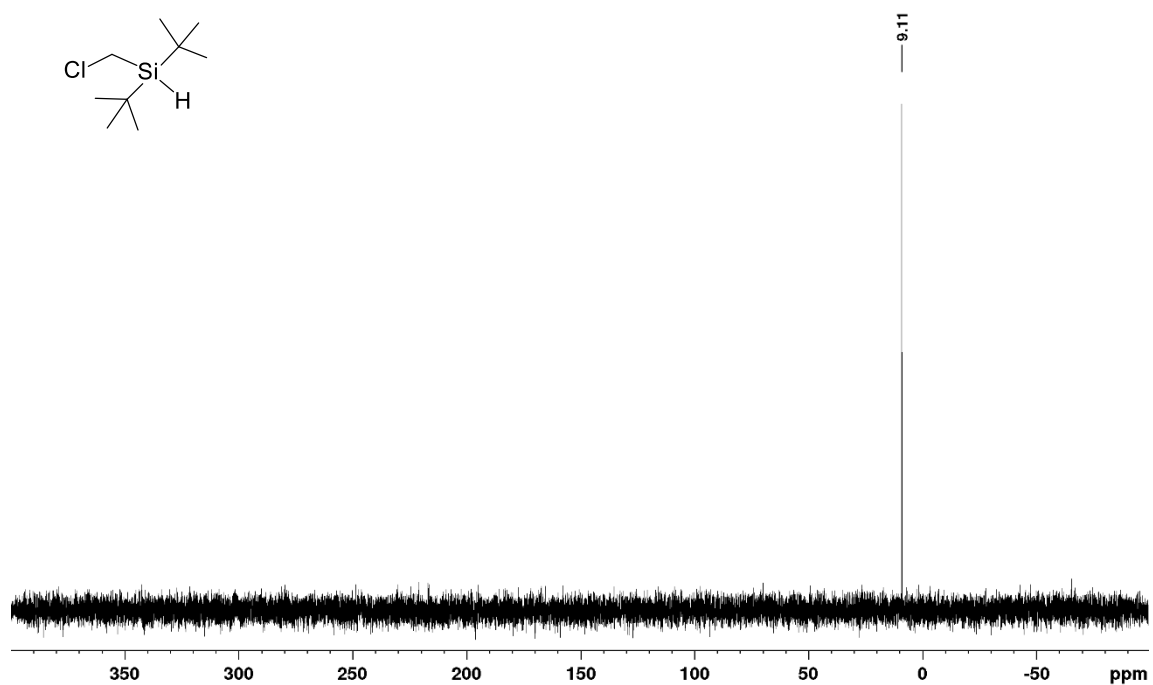


Fig. S9 $^{29}\text{Si}\{^1\text{H}\}$ NMR spectrum of $(t\text{-Bu})_2\text{Si}(\text{H})\text{CH}_2\text{Cl}$ (79.5 MHz, DEPT, r.t., CDCl_3).

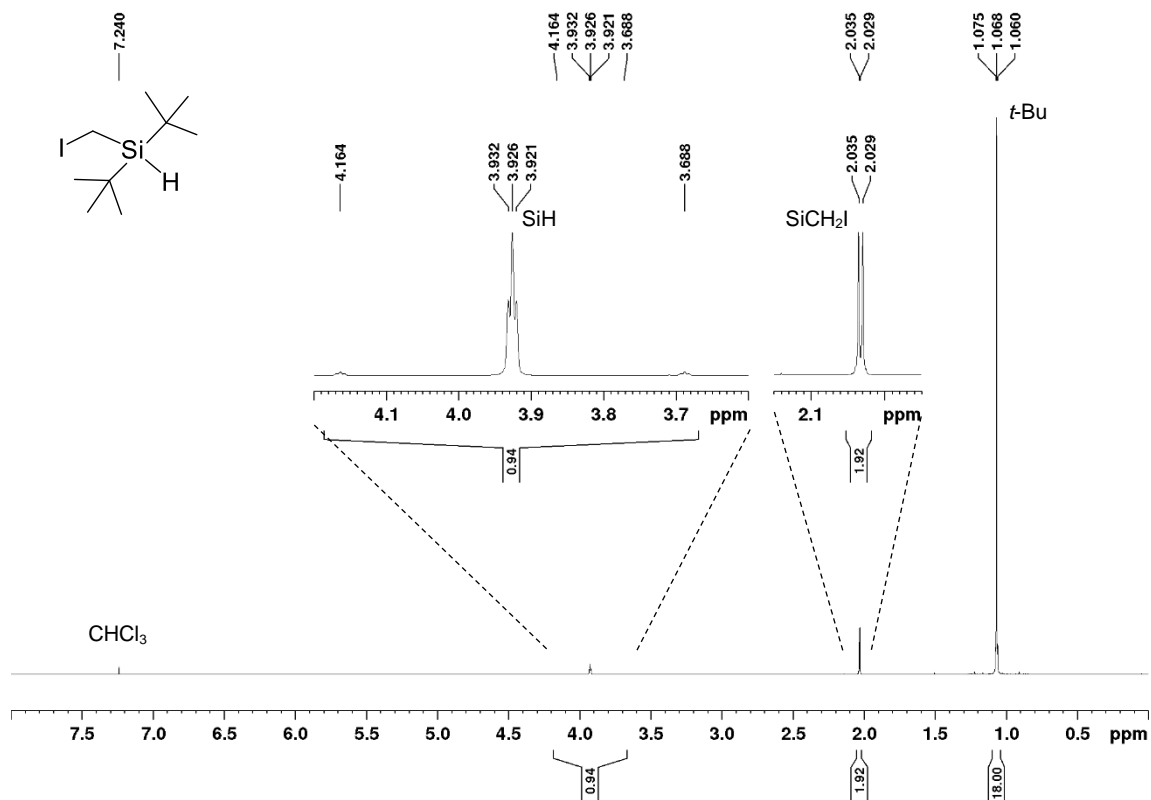


Fig. S10 ^1H NMR spectrum of di-*tert*-butyl(iodomethyl)silane (400 MHz, r.t., CDCl_3).

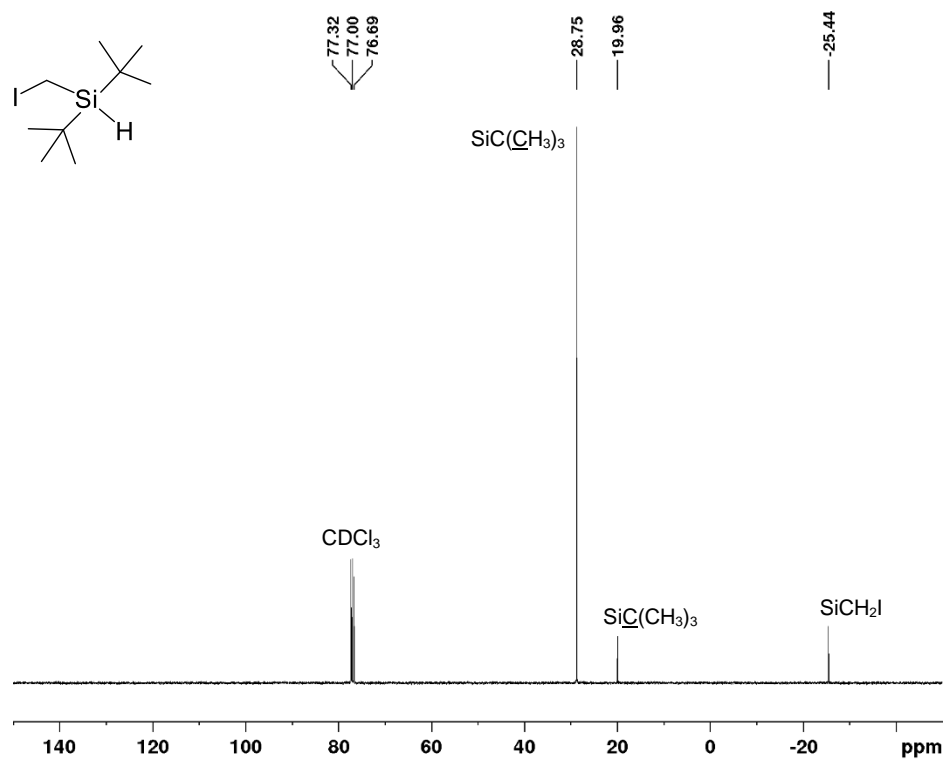


Fig. S11 $^{13}\text{C}\{^1\text{H}\}$ NMR spectrum of (*t*-Bu) $_2\text{Si}(\text{H})\text{CH}_2\text{I}$ (101 MHz, r.t., CDCl_3).

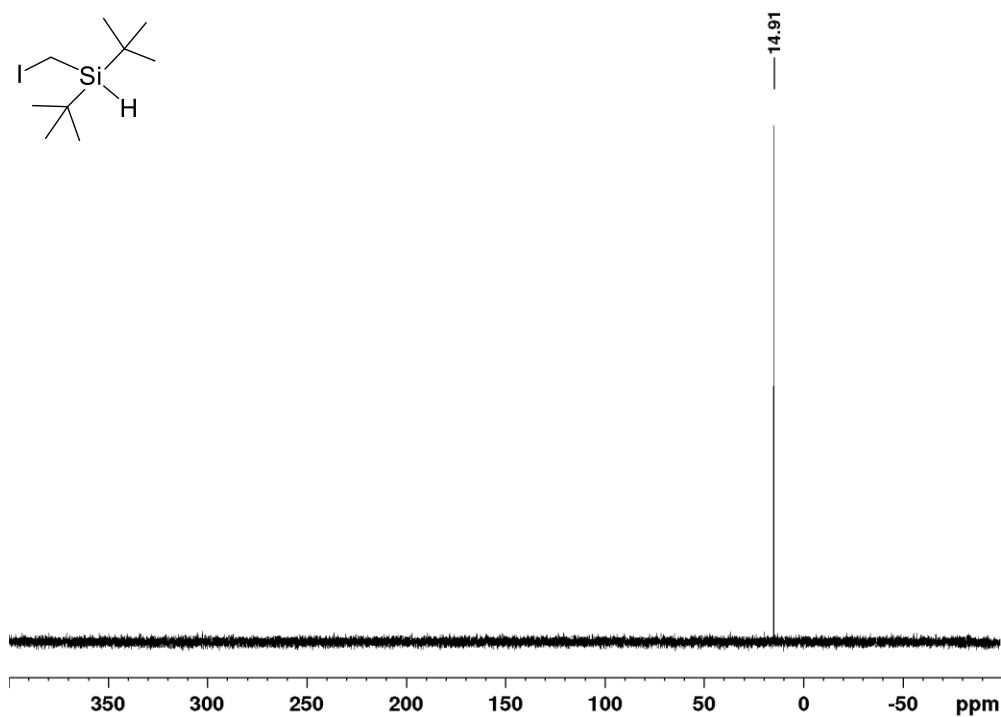


Fig. S12 $^{29}\text{Si}\{^1\text{H}\}$ NMR spectrum of $(t\text{-Bu})_2\text{Si}(\text{H})\text{CH}_2\text{I}$ (79.5 MHz, DEPT, r.t., CDCl_3).

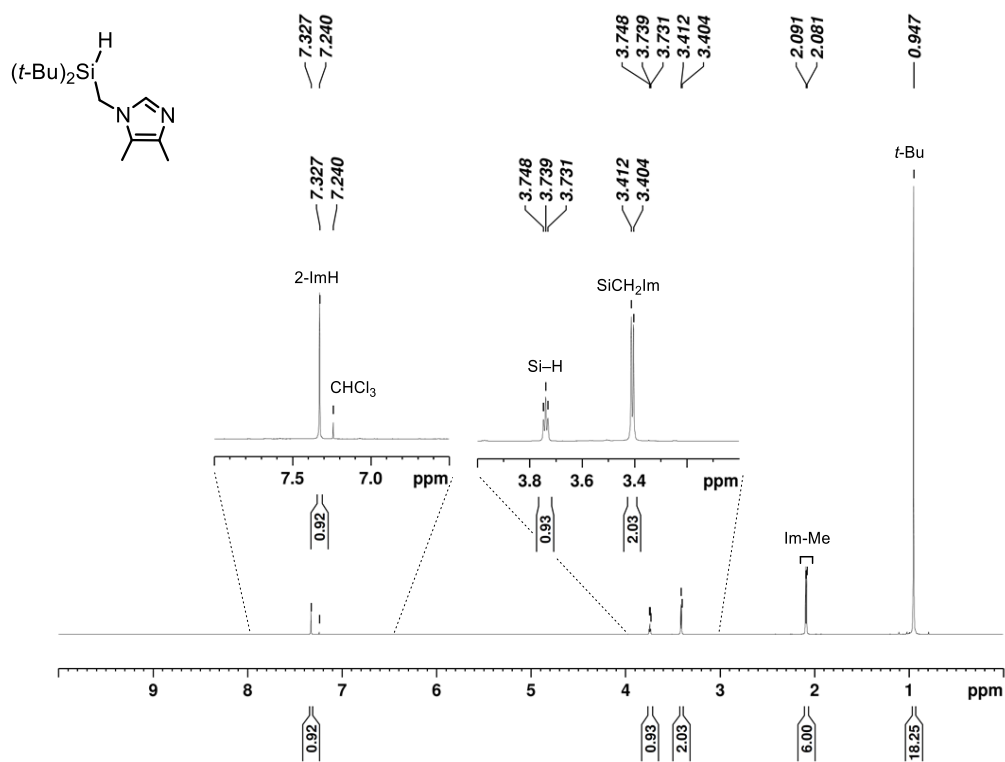


Fig. S13 ^1H NMR spectrum of 1-[(di-*tert*-butylsilyl)methyl]-4,5-dimethylimidazole (400 MHz, r.t., CDCl_3).

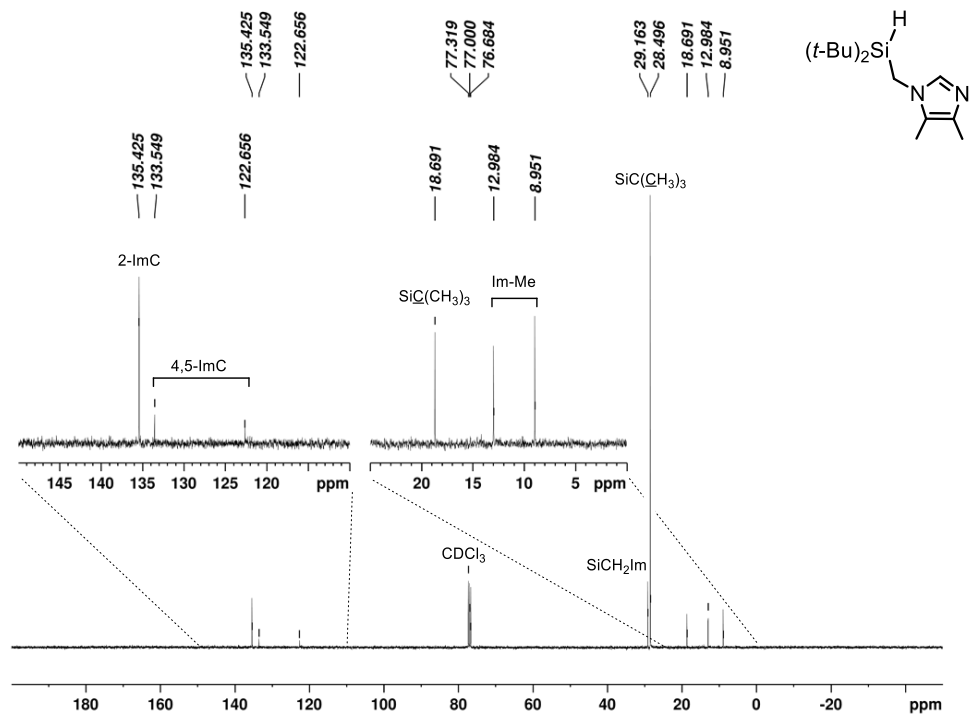


Fig. S14 $^{13}\text{C}\{^1\text{H}\}$ NMR spectrum of 1-[(di-*tert*-butylsilyl)methyl]-4,5-dimethylimidazole (101 MHz, r.t., CDCl_3).

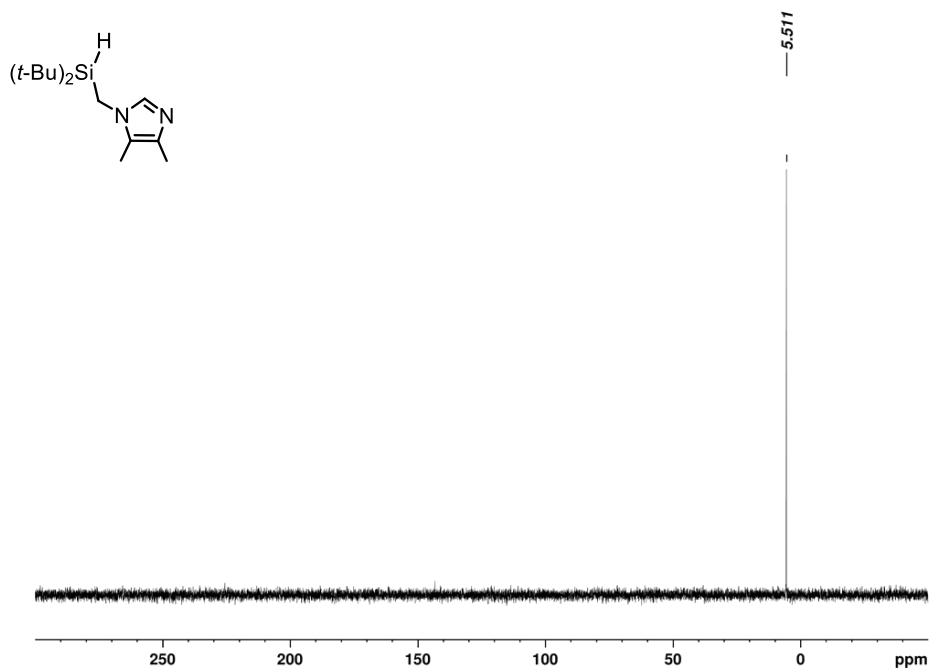
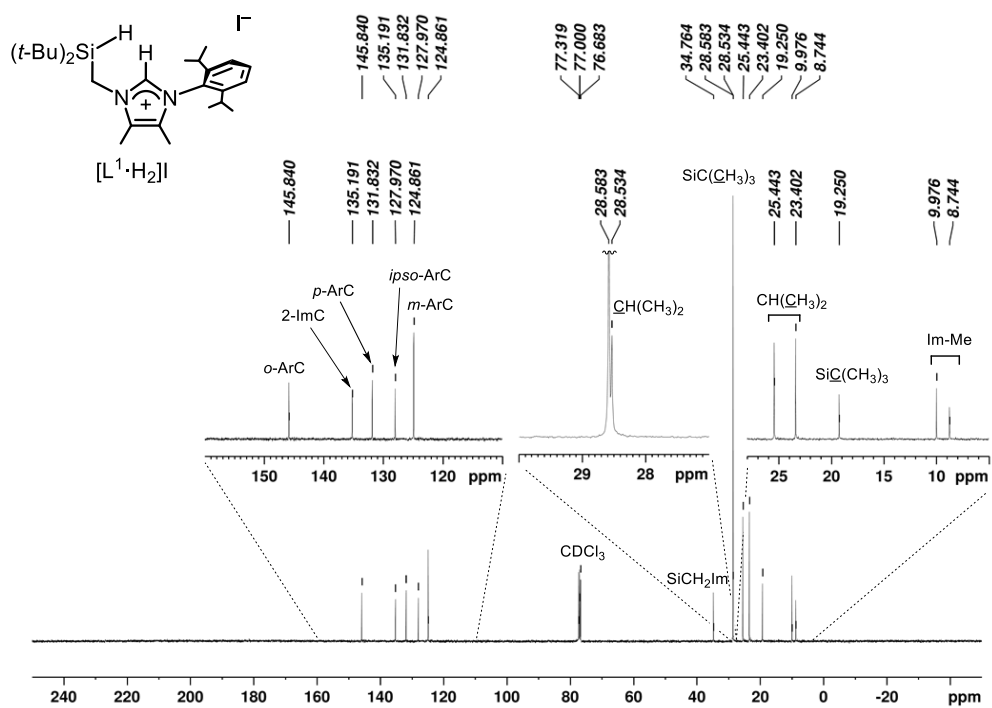
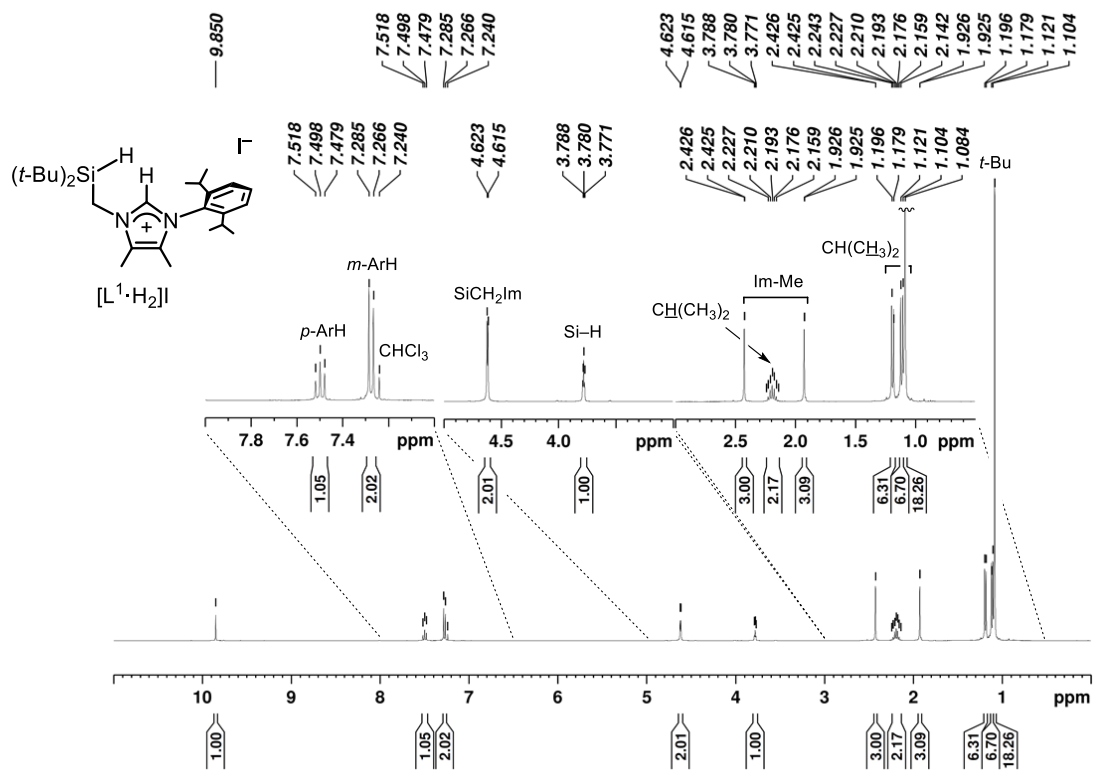


Fig. S15 $^{29}\text{Si}\{^1\text{H}\}$ NMR spectrum of 1-[(di-*tert*-butylsilyl)methyl]-4,5-dimethylimidazole (79.5 MHz, DEPT, r.t., CDCl_3).



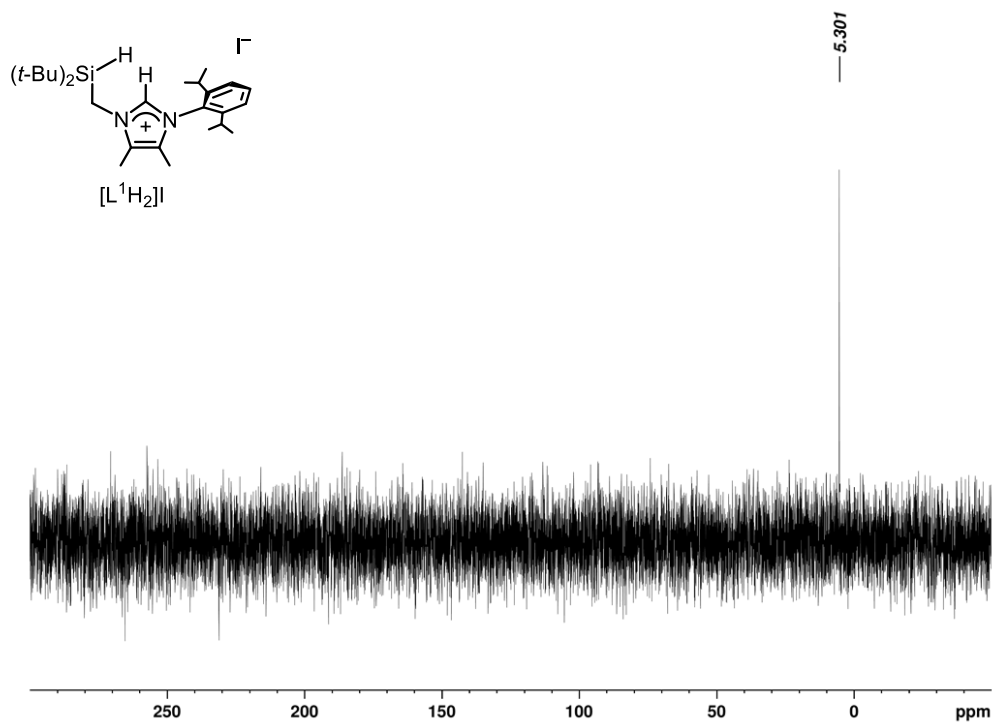


Fig. S18 $^{29}\text{Si}\{^1\text{H}\}$ NMR spectrum of $[L^1 \cdot H_2]I$ (79.5 MHz, DEPT, r.t., CDCl_3).

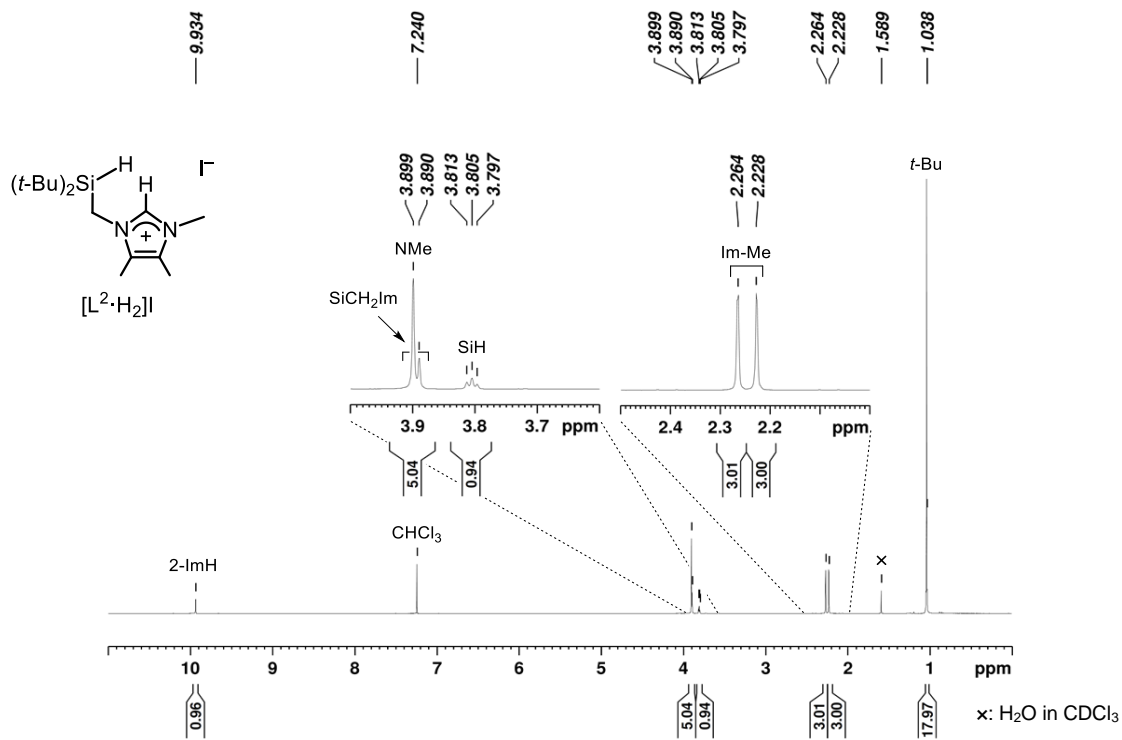


Fig. S19 ^1H NMR spectrum of $[L^2 \cdot H_2]I$ (400 MHz, r.t., CDCl_3).

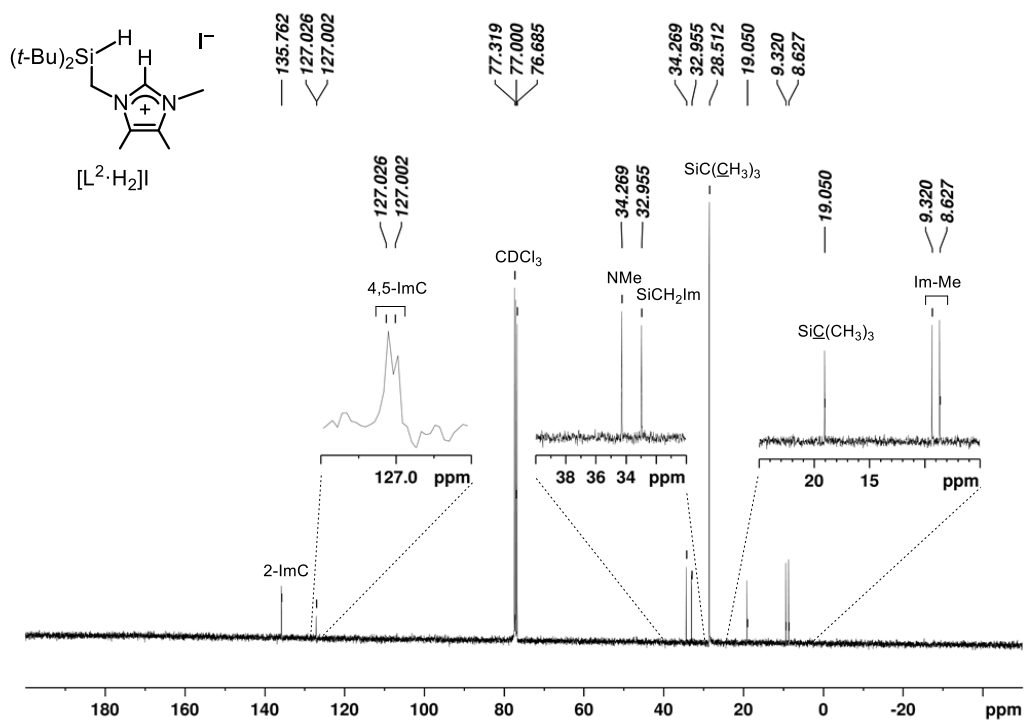


Fig. S20 ¹³C{¹H} NMR spectrum of [L²·H₂]I (101 MHz, r.t., CDCl₃).

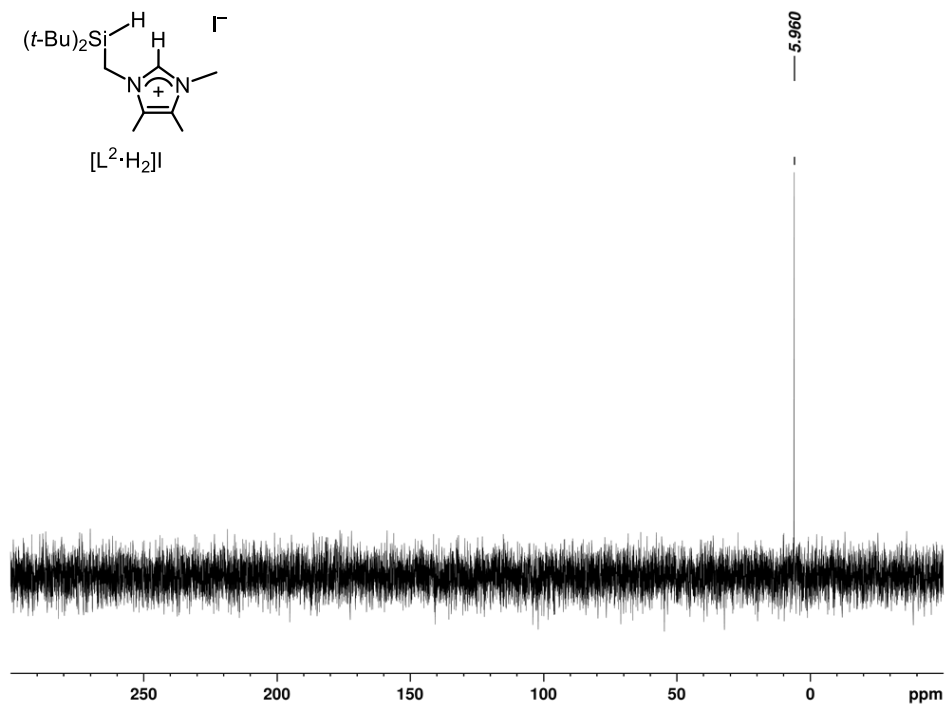
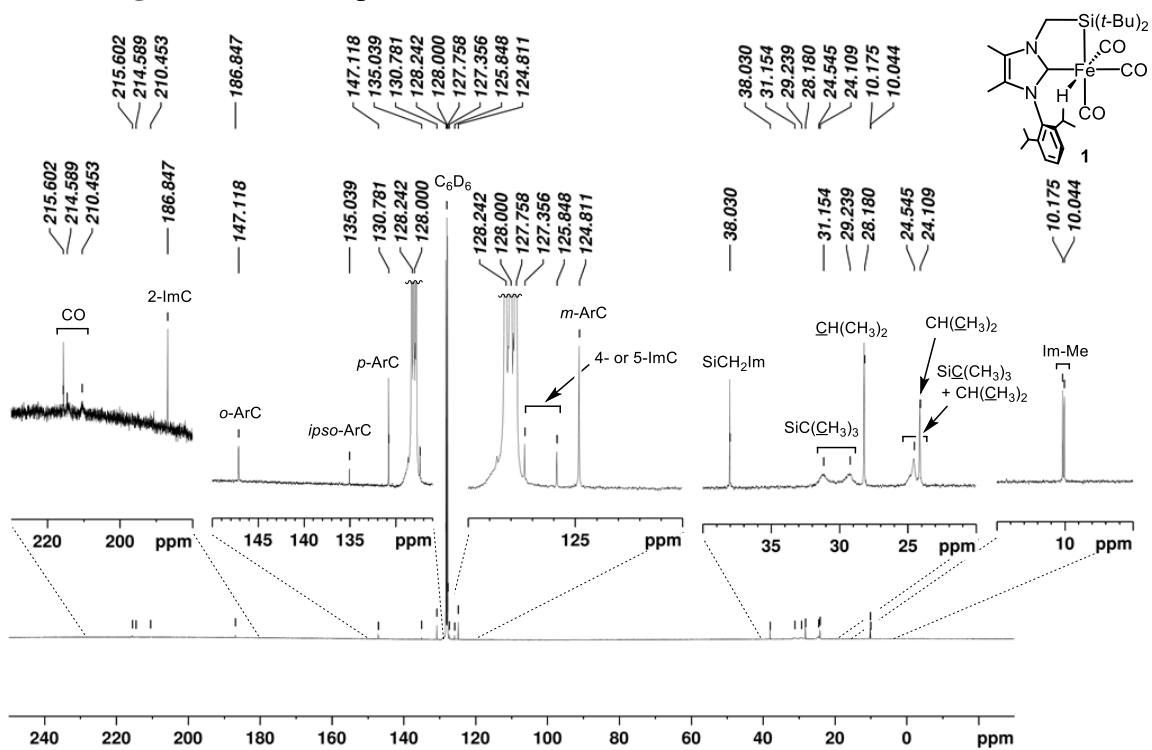
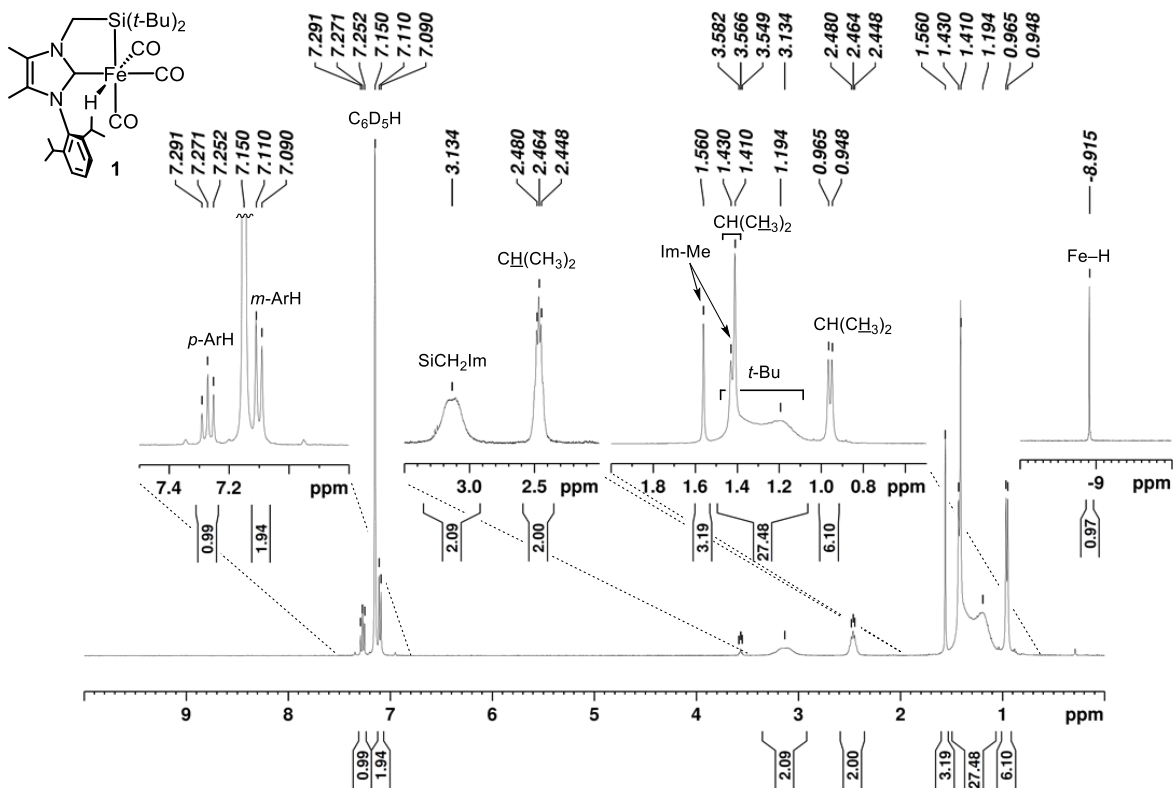


Fig. S21 ²⁹Si{¹H} NMR spectrum of [L²·H₂]I (79.5 MHz, DEPT, r.t., CDCl₃).



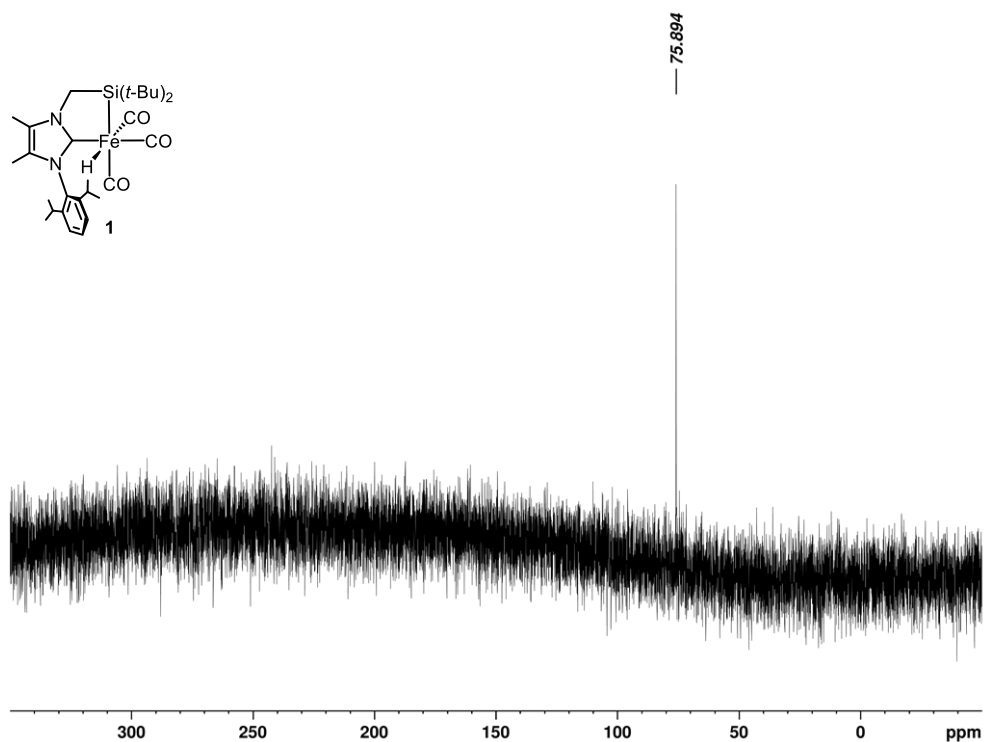


Fig. S24 $^{29}\text{Si}\{^1\text{H}\}$ NMR spectrum of **1** (79.5 MHz, IG, r.t., C_6D_6).

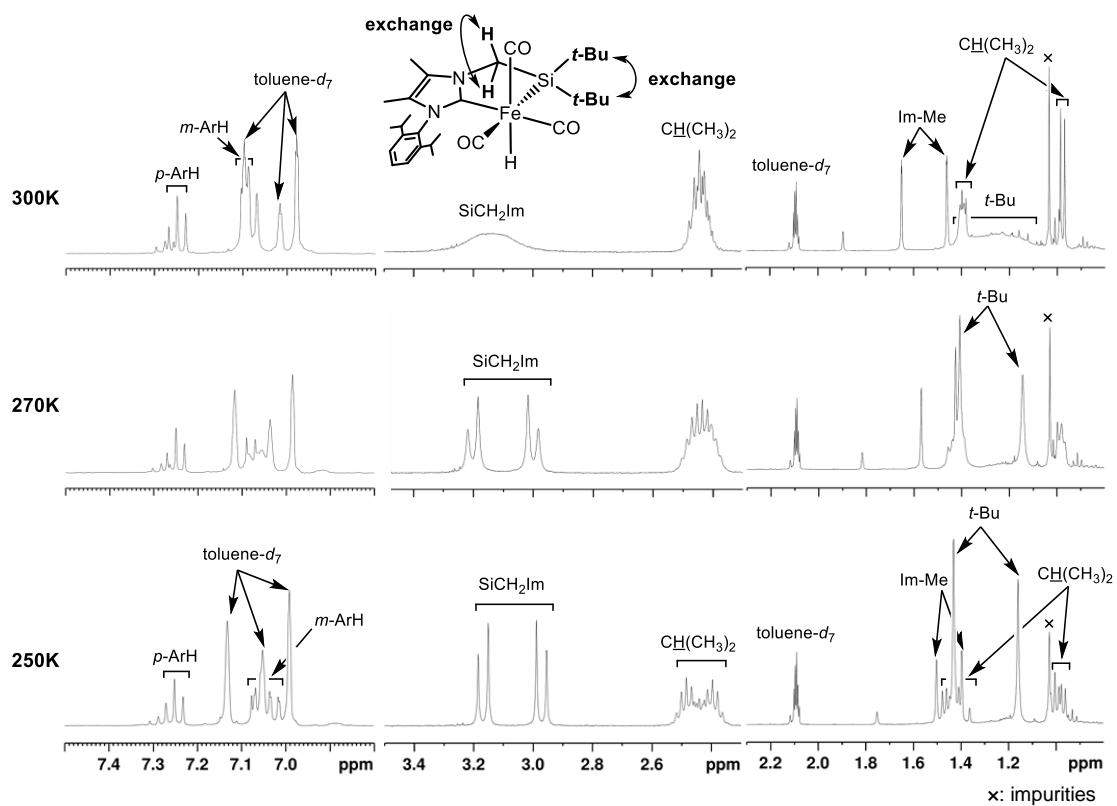


Fig. S25 VT ^1H NMR spectra of **1** (400 MHz, toluene- d_8).

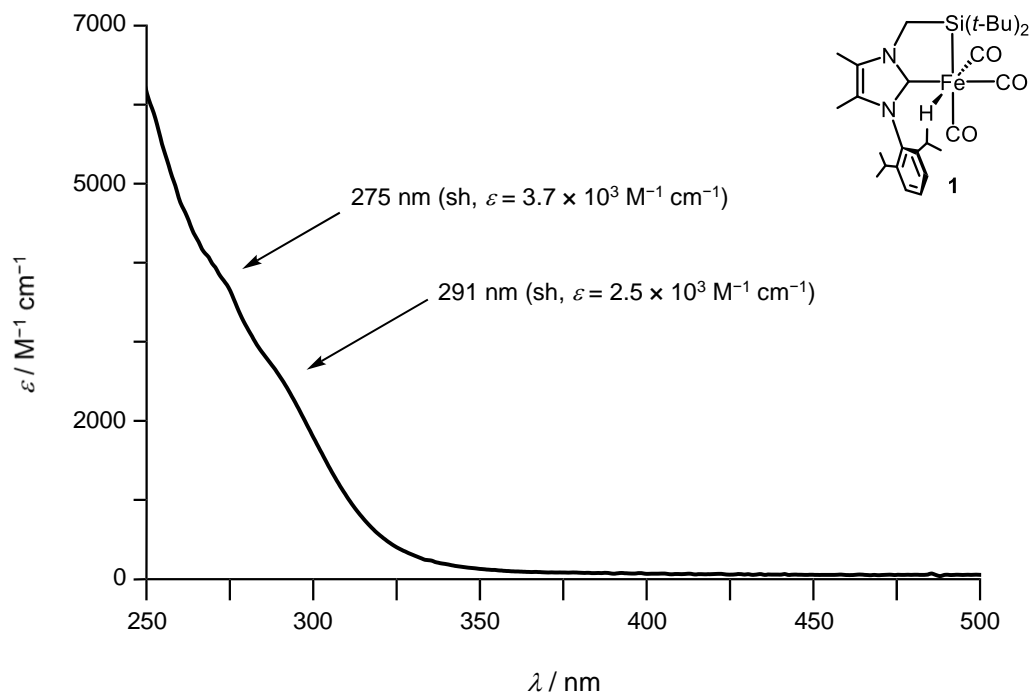


Fig. S26 UV-Vis absorption spectrum of **1** in THF.

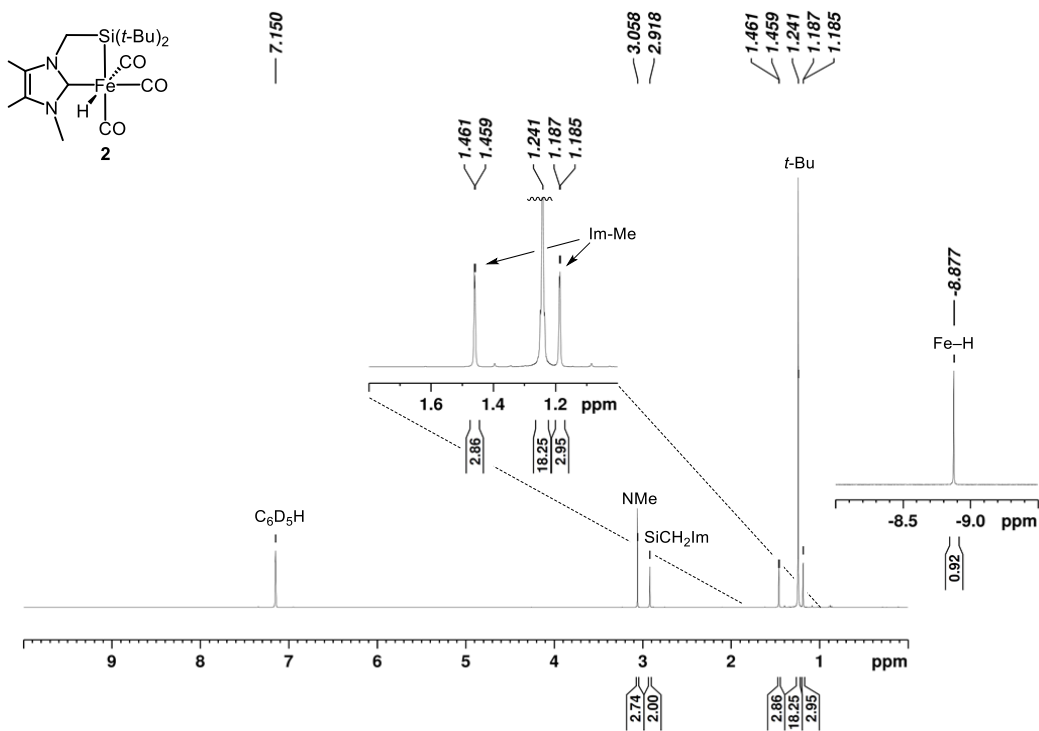


Fig. S27 ^1H NMR spectrum of $\text{Fe}(\text{L}^2)(\text{H})(\text{CO})_3$ (**2**) (400 MHz, r.t., C_6D_6).

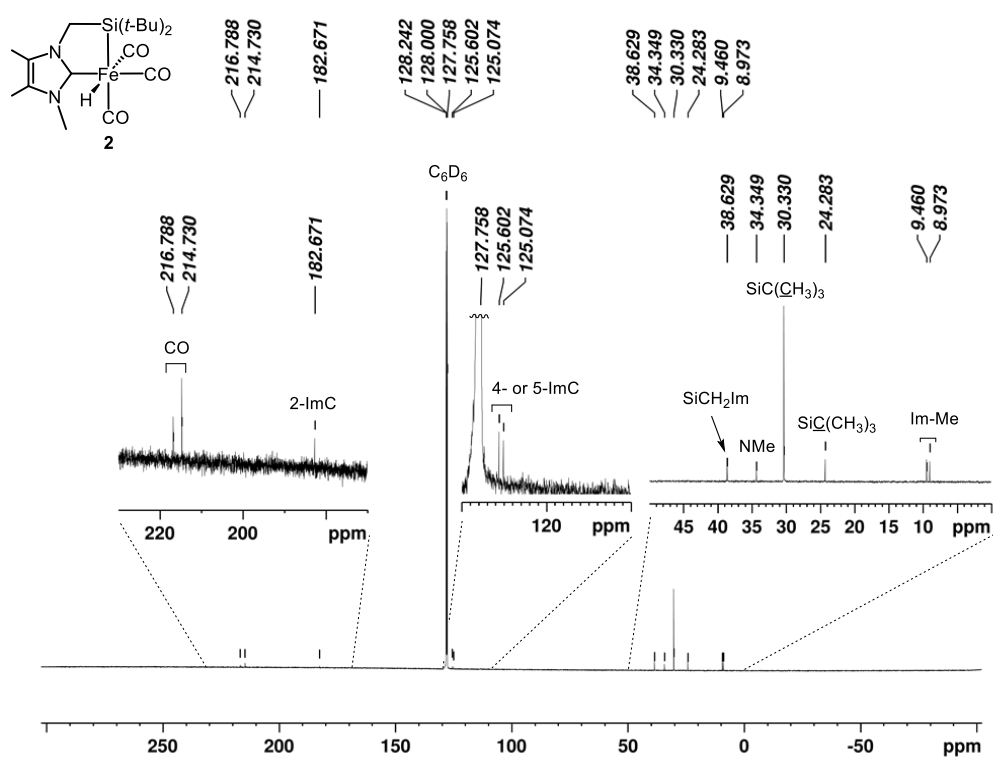


Fig. S28 $^{13}\text{C}\{^1\text{H}\}$ NMR spectrum of **2** (101 MHz, r.t., C_6D_6).

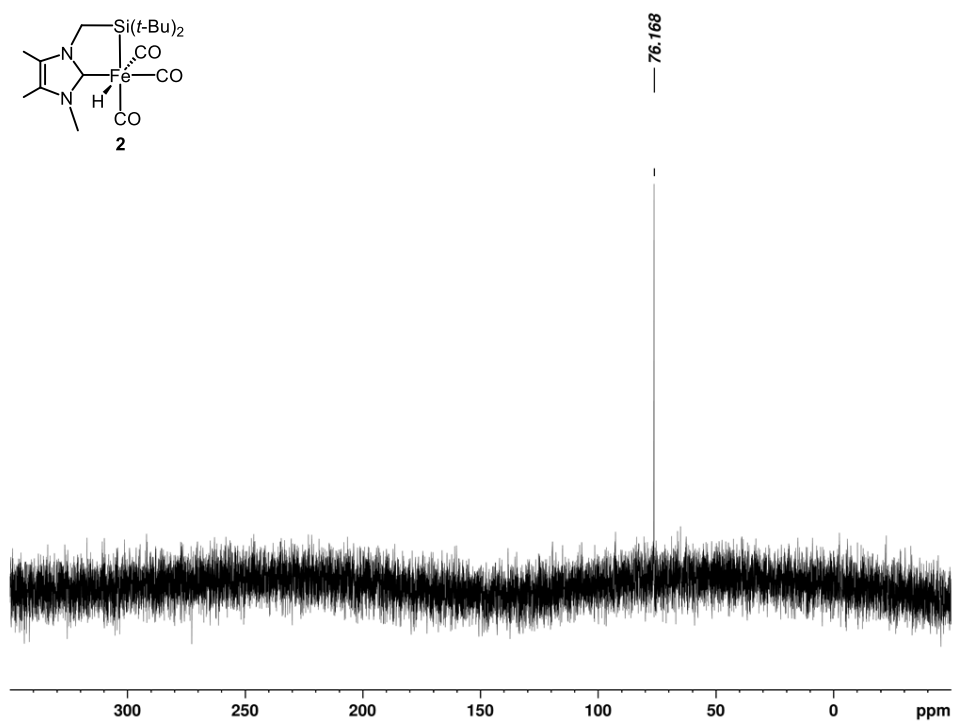


Fig. S29 $^{29}\text{Si}\{^1\text{H}\}$ NMR spectrum of **2** (79.5 MHz, IG, r.t., C_6D_6).

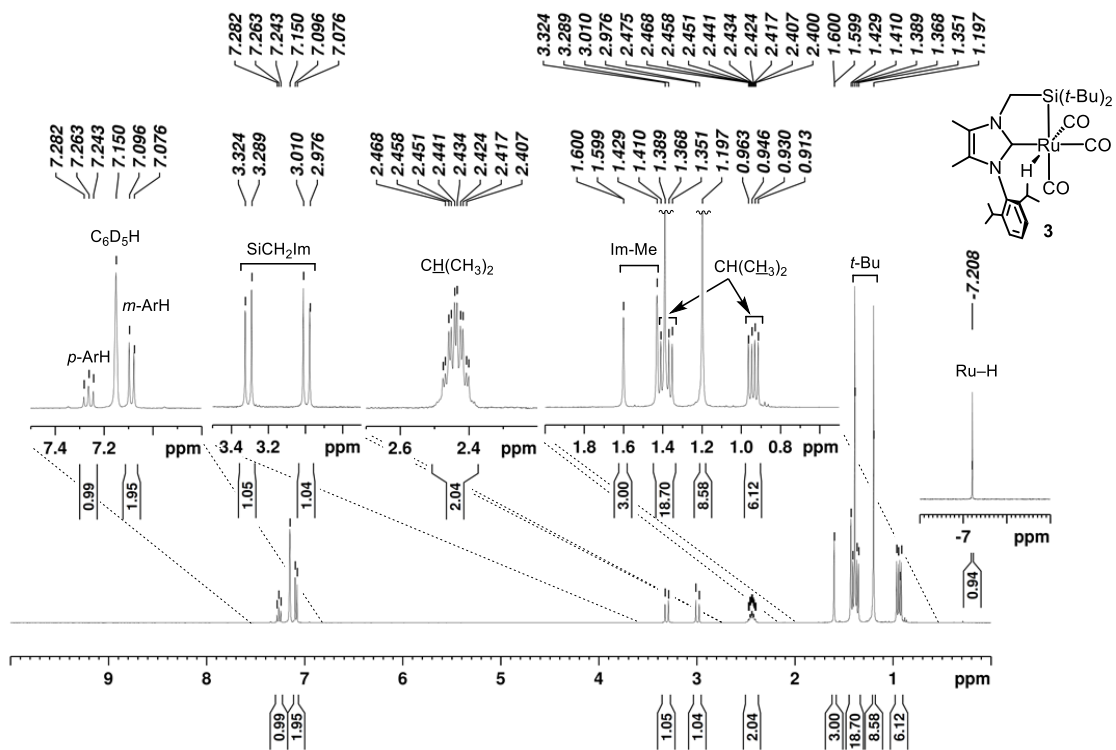


Fig. S30 ^1H NMR spectrum of $\text{Ru}(\text{L}^1)(\text{H})(\text{CO})_3$ (**3**) (400 MHz, r.t., C_6D_6).

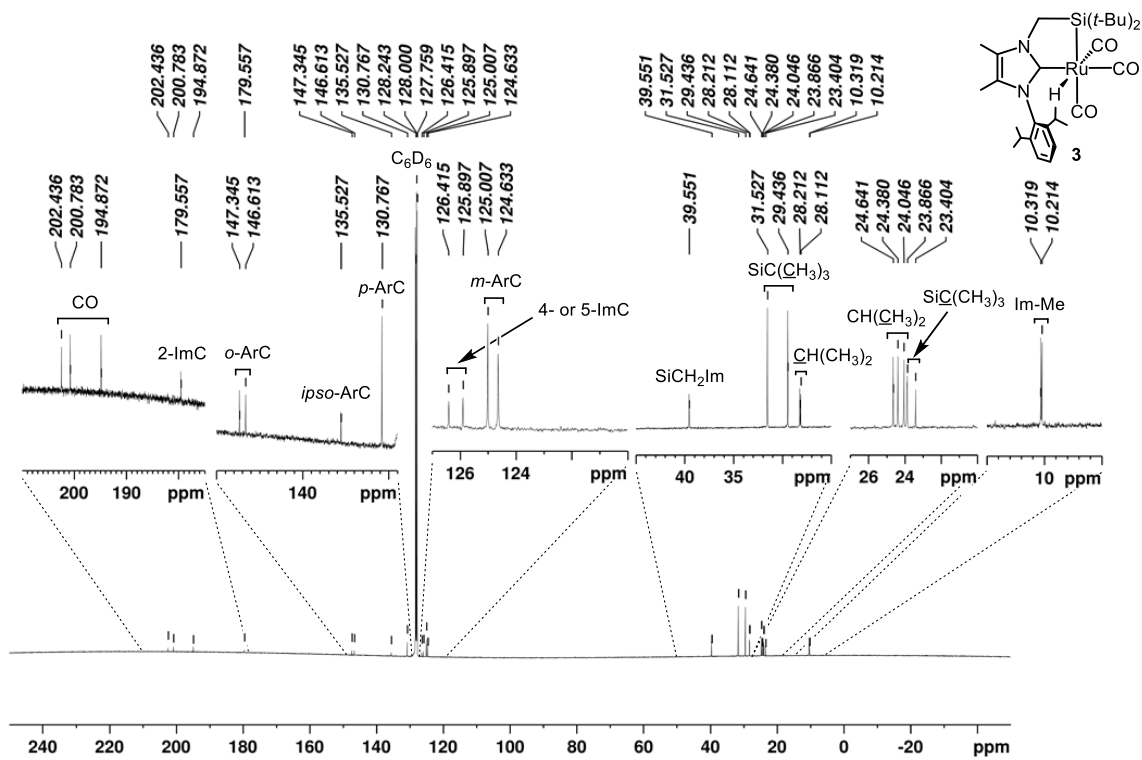


Fig. S31 $^{13}\text{C}\{^1\text{H}\}$ NMR spectrum of **3** (101 MHz, r.t., C_6D_6).

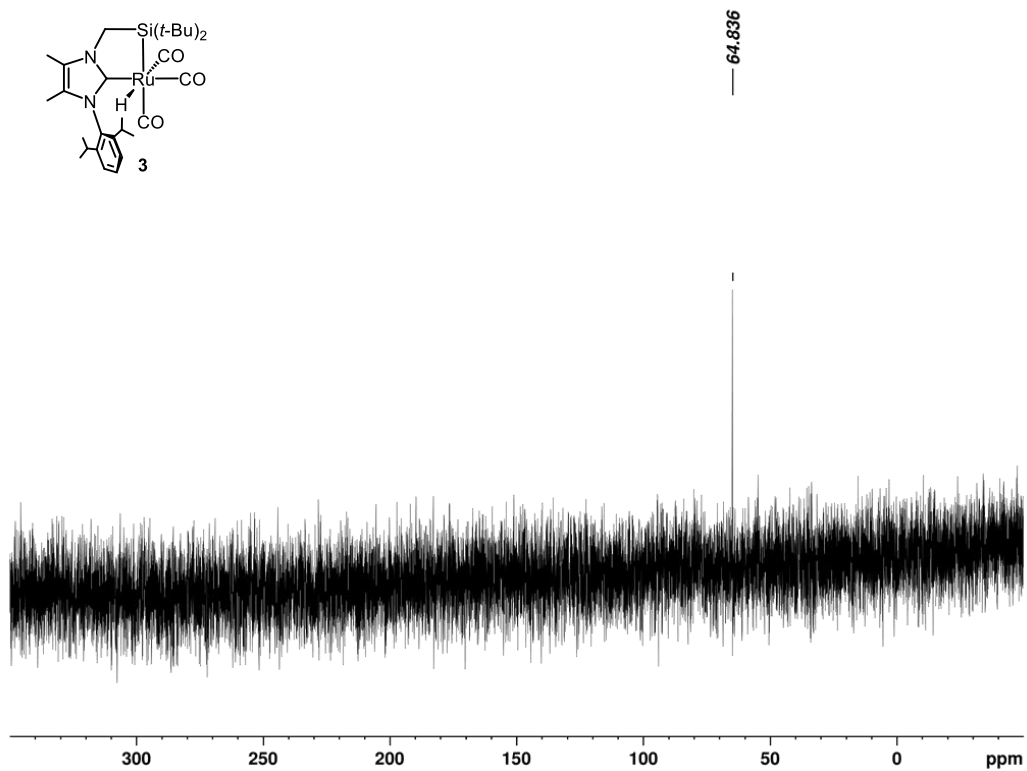


Fig. S32 $^{29}\text{Si}\{^1\text{H}\}$ NMR spectrum of **3** (79.5 MHz, IG, r.t., C_6D_6).

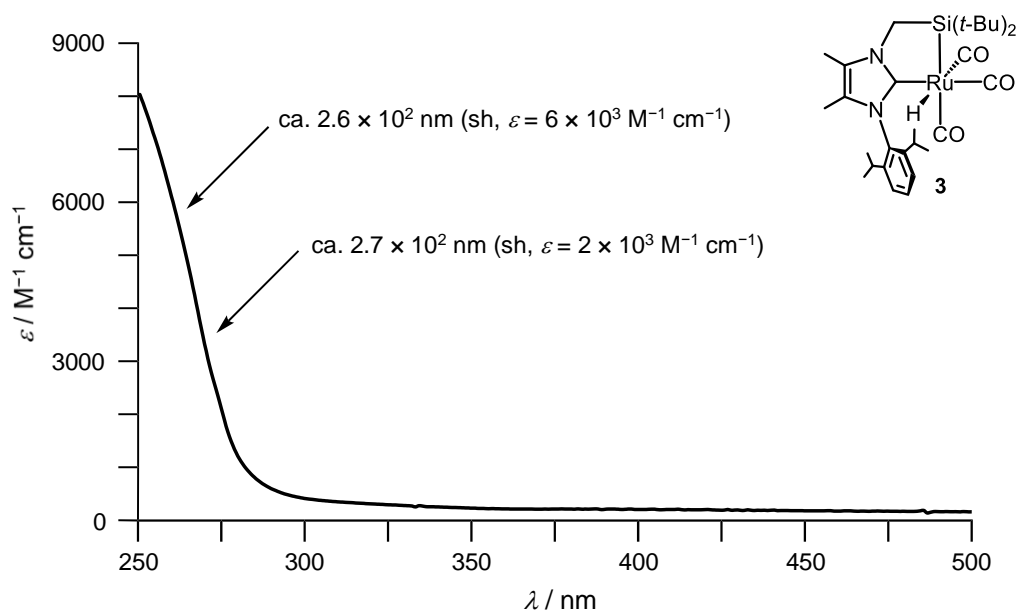


Fig. S33 UV-Vis absorption spectrum of **3** in THF.

6. NMR spectra of *N,N*-bis(boryl)amines in reaction mixtures of catalytic double hydroboration of nitriles

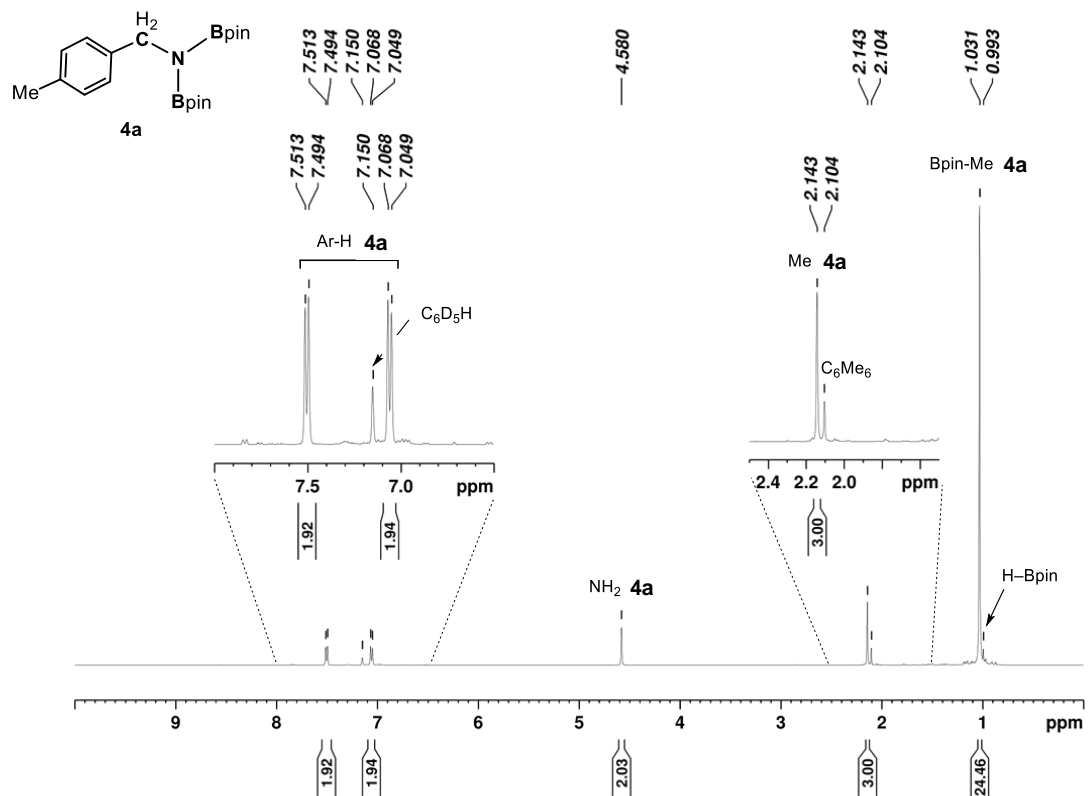


Fig. S34 ¹H NMR spectrum of bis(boryl)amine **4a** in a reaction mixture of catalytic hydroboration of *p*-tolunitrile with HBpin using **1** (400 MHz, r.t., C₆D₆).

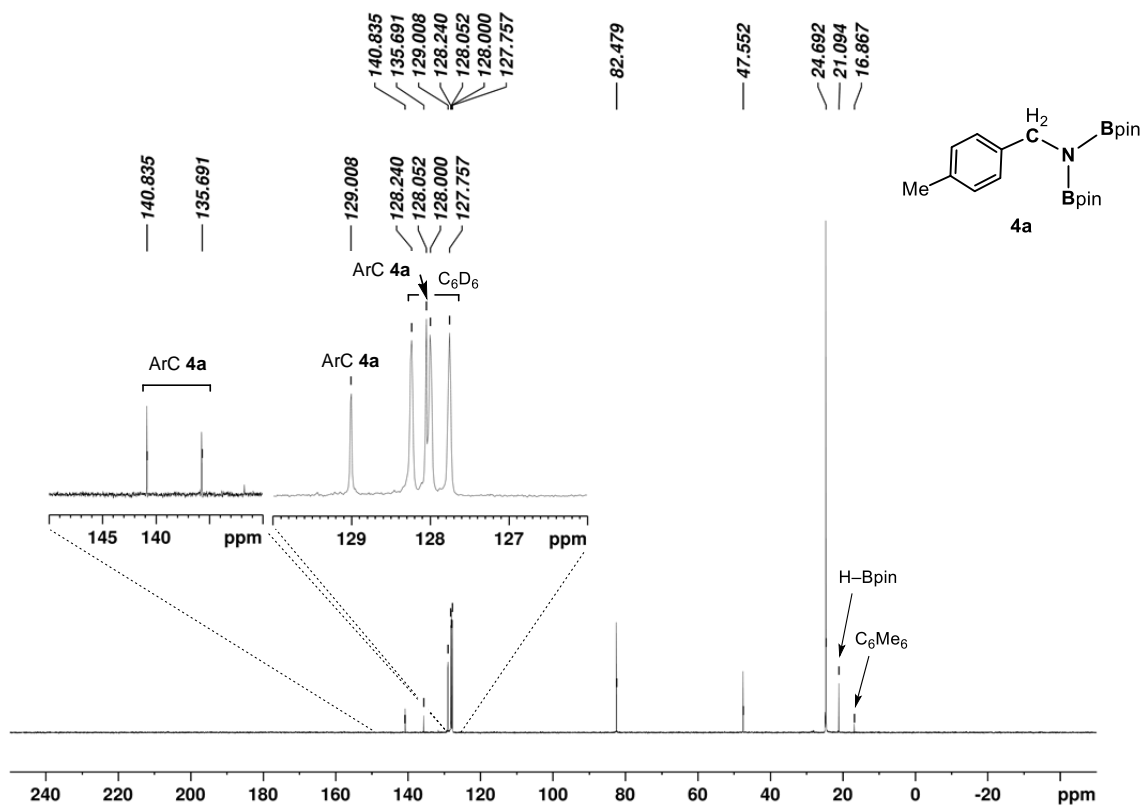


Fig. S35 $^{13}\text{C}\{^1\text{H}\}$ NMR spectrum of bis(boryl)amine **4a** in a reaction mixture of catalytic hydroboration of *p*-tolunitrile with HBpin using **1** (101 MHz, r.t., C₆D₆).

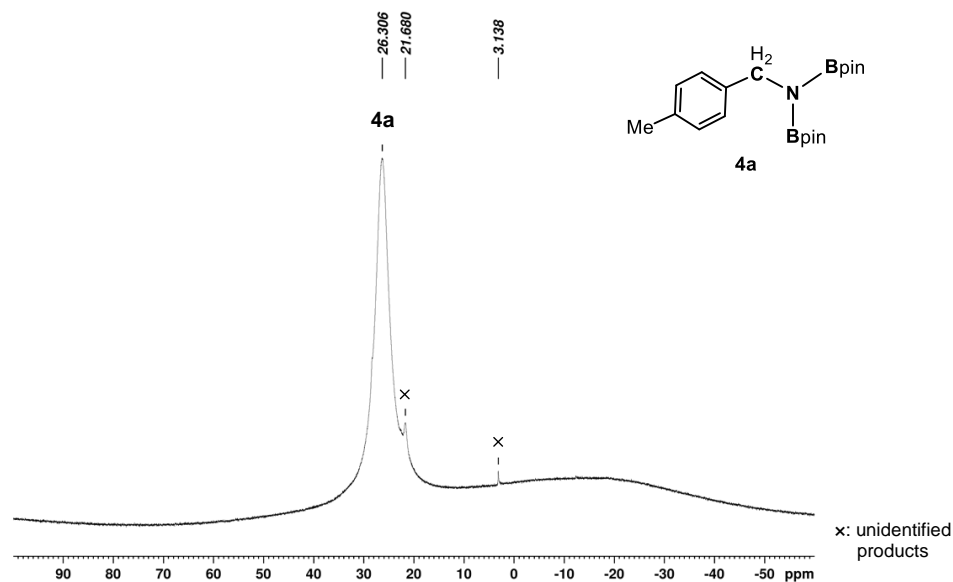


Fig. S36 $^{11}\text{B}\{^1\text{H}\}$ NMR spectrum of bis(boryl)amine **4a** in a reaction mixture of catalytic hydroboration of *p*-tolunitrile with HBpin using **1** (128 MHz, r.t., C₆D₆).

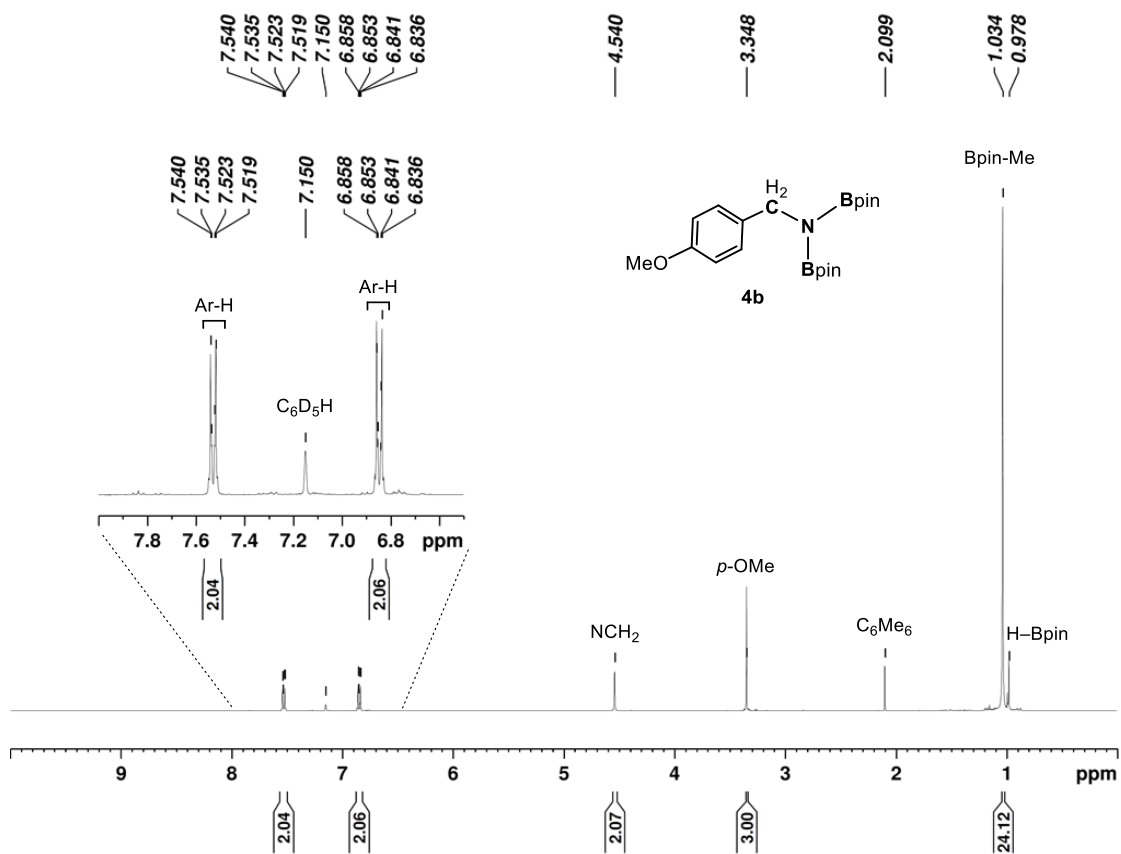


Fig. S37 ¹H NMR spectrum of bis(boryl)amine **4b** in a reaction mixture of catalytic hydroboration of 4-methoxybenzotrile with HBpin using **1** (400 MHz, r.t., C₆D₆).

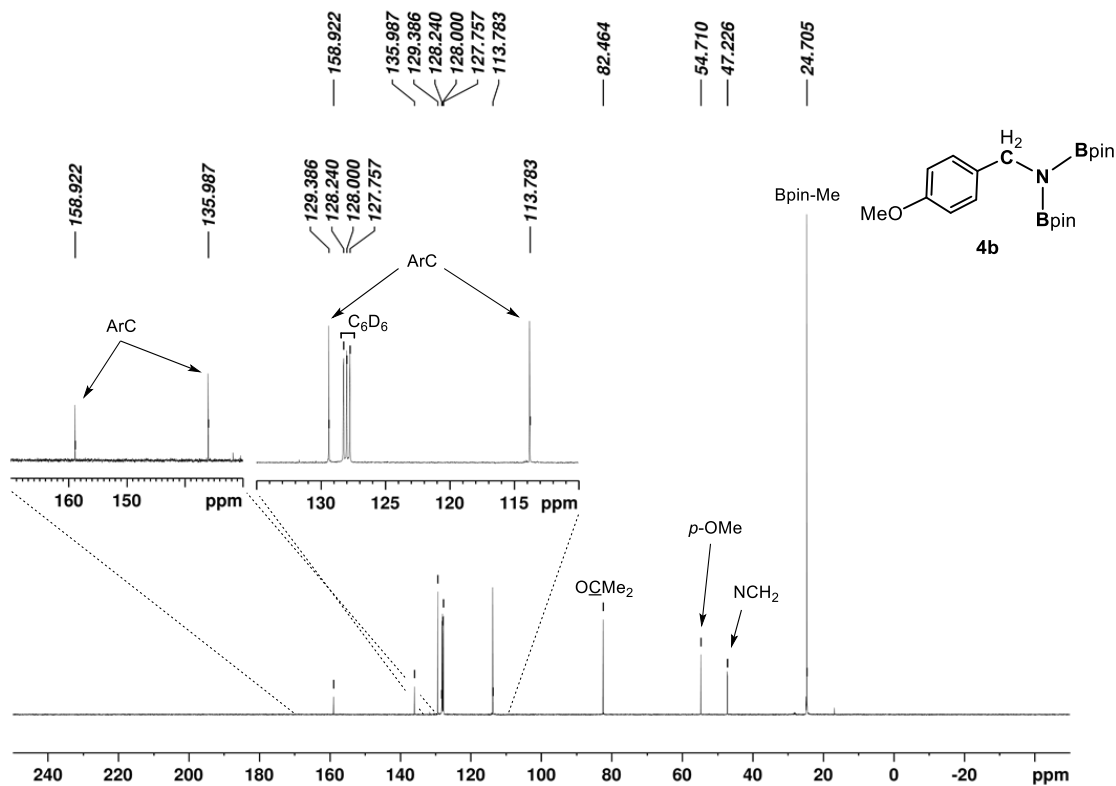


Fig. S38 $^{13}\text{C}\{^1\text{H}\}$ NMR spectrum of bis(boryl)amine **4b** in a reaction mixture of catalytic hydroboration of 4-methoxybenzotrile and HBpin with **1** (101 MHz, C_6D_6).

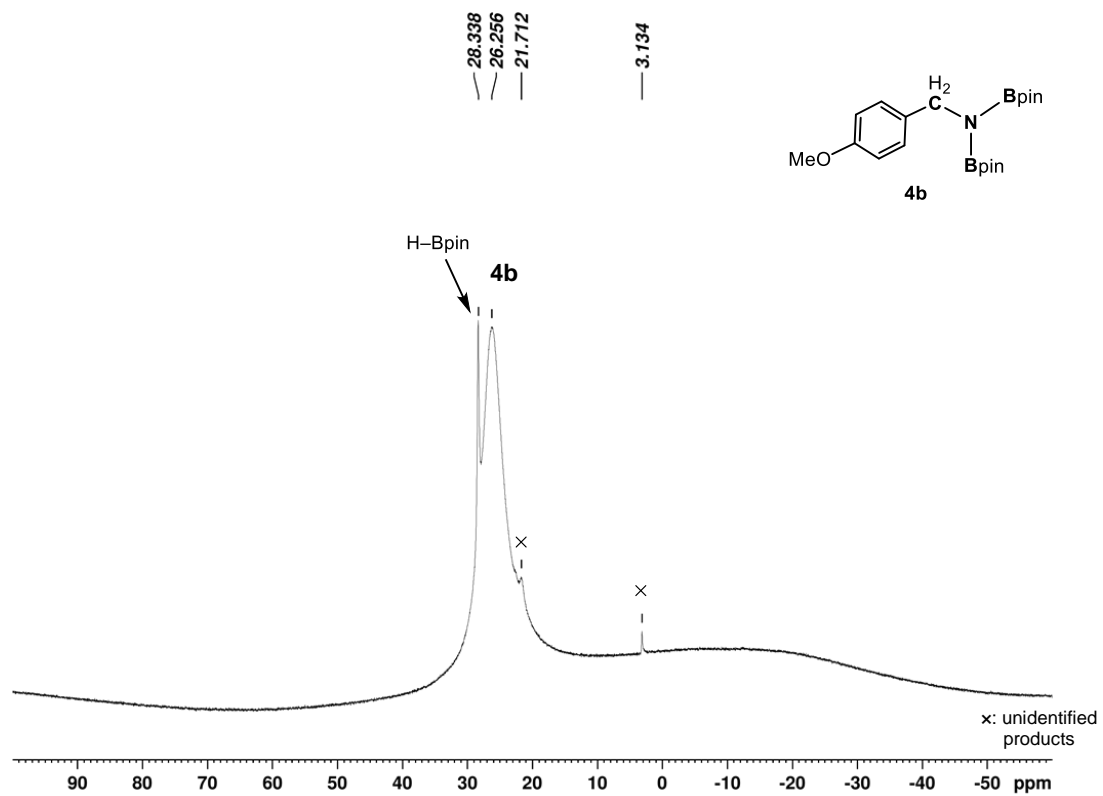


Fig. S39 $^{11}\text{B}\{^1\text{H}\}$ NMR spectrum of bis(boryl)amine **4b** in a reaction mixture of catalytic hydroboration of 4-methoxybenzotrile with HBpin using **1** (128 MHz, C_6D_6).

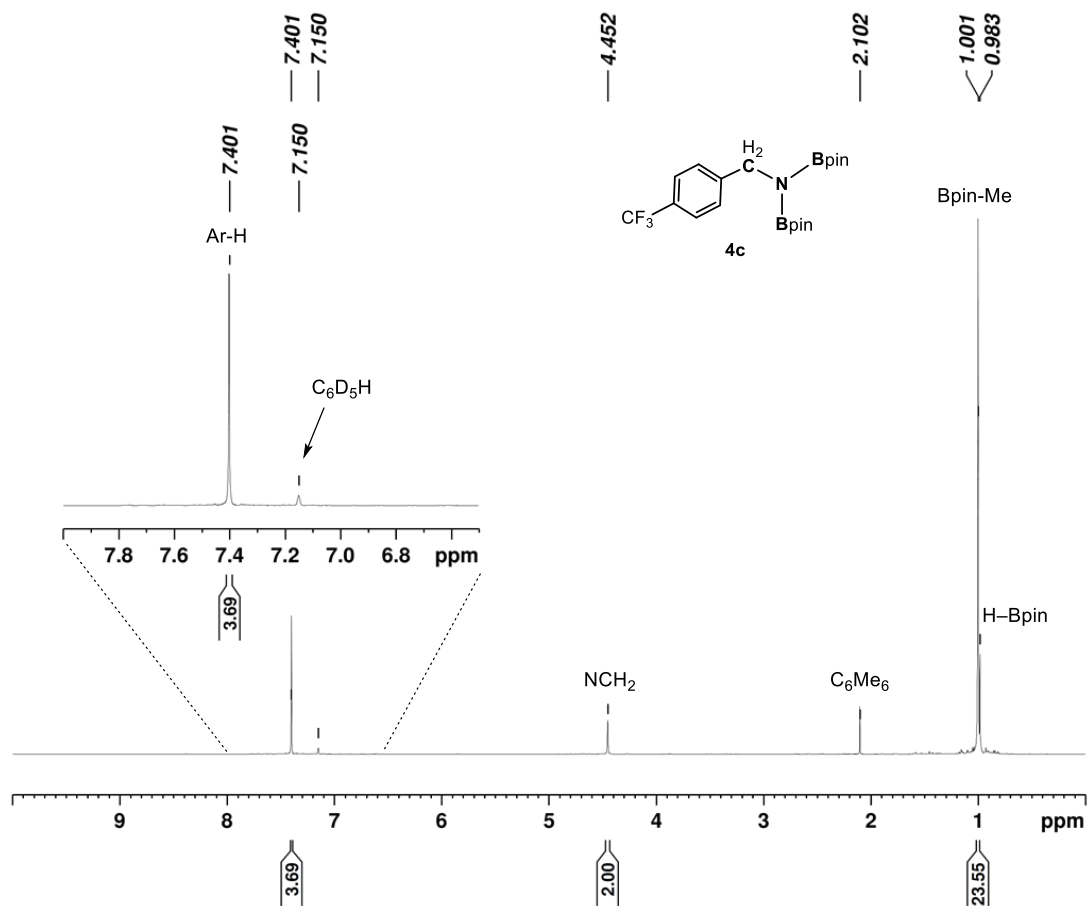


Fig. S40 ¹H NMR spectrum of bis(boryl)amine **4c** in a reaction mixture of catalytic hydroboration of 4-trifluoromethylbenzotrile with HBpin using **1** (400 MHz, r.t., C₆D₆).

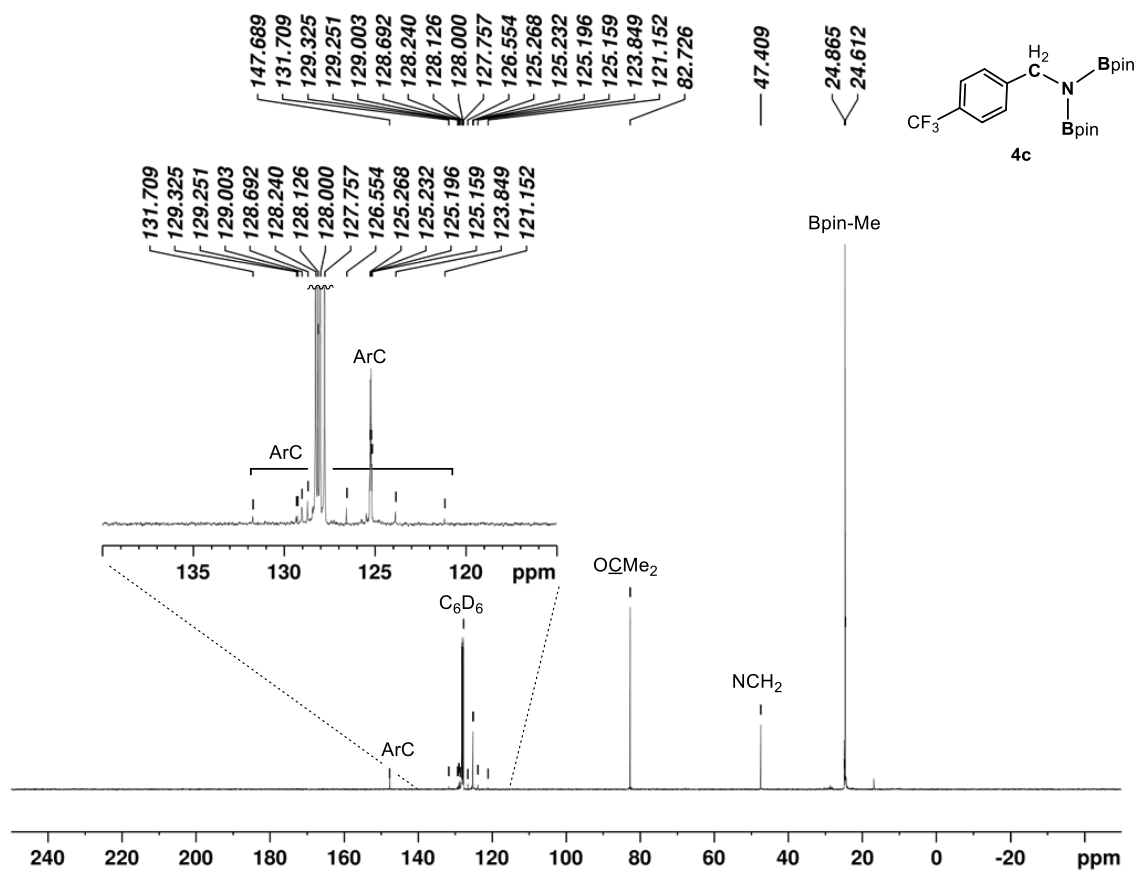


Fig. S41 $^{13}\text{C}\{^1\text{H}\}$ NMR spectrum of bis(boryl)amine **4c** in a reaction mixture of catalytic hydroboration of 4-trifluoromethylbenzotrile with HBpin using **1** (101 MHz, r.t., C_6D_6).

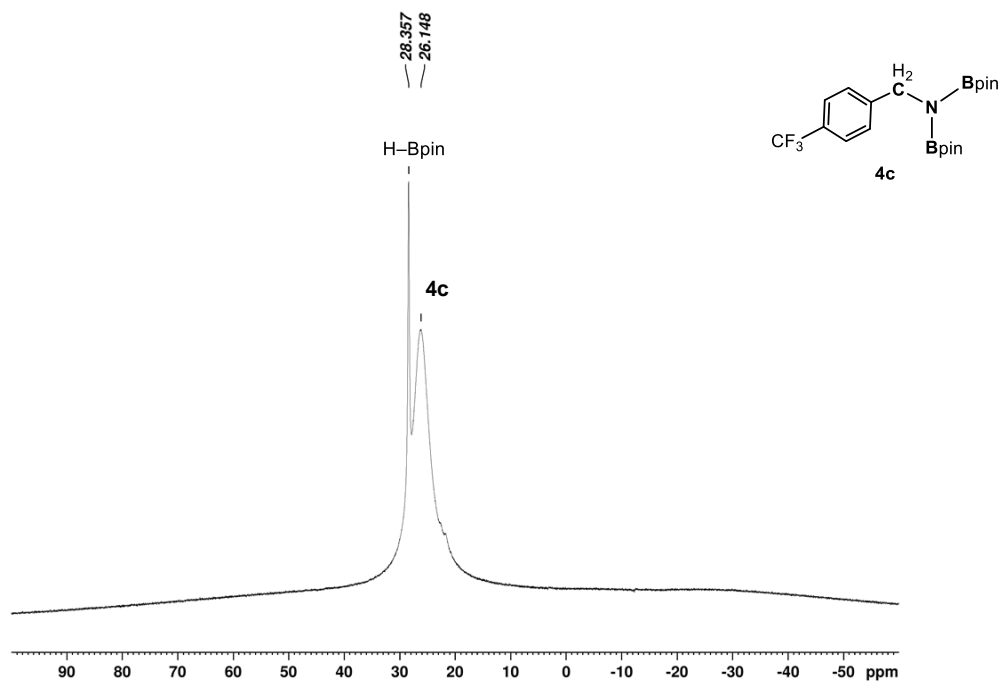


Fig. S42 $^1\text{H}\{^1\text{H}\}$ NMR spectrum of bis(boryl)amine **4c** in a reaction mixture of catalytic hydroboration of 4-trifluoromethylbenzotrile with HBpin using **1** (128 MHz, r.t., C_6D_6).

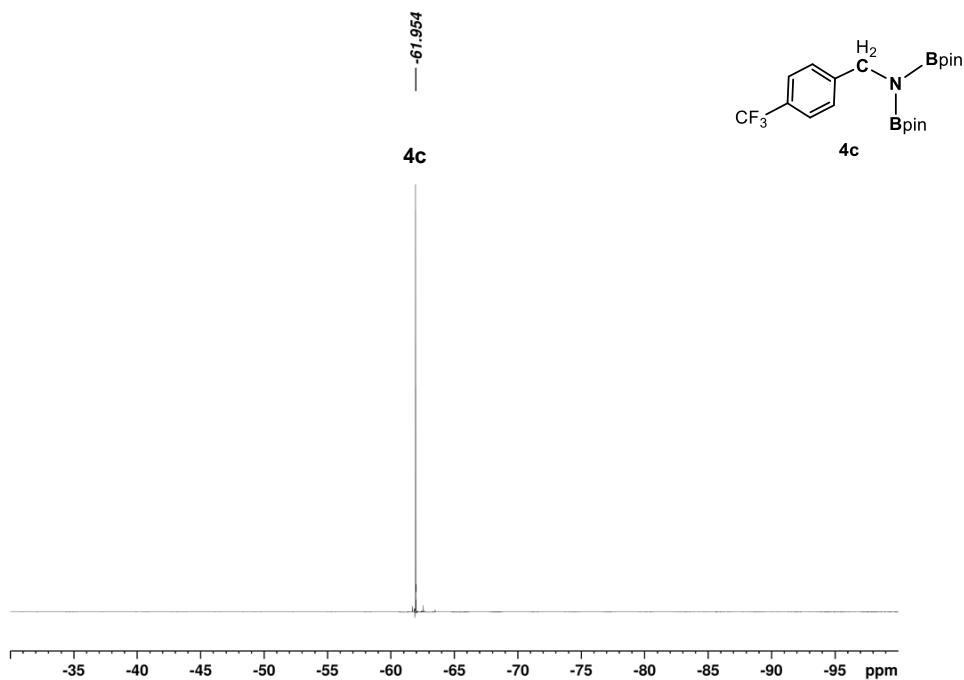


Fig. S43 $^{19}\text{F}\{^1\text{H}\}$ NMR spectrum of bis(boryl)amine **4c** in a reaction mixture of catalytic hydroboration of 4-trifluoromethylbenzotrile with HBpin using **1** (376 MHz, r.t., C_6D_6).

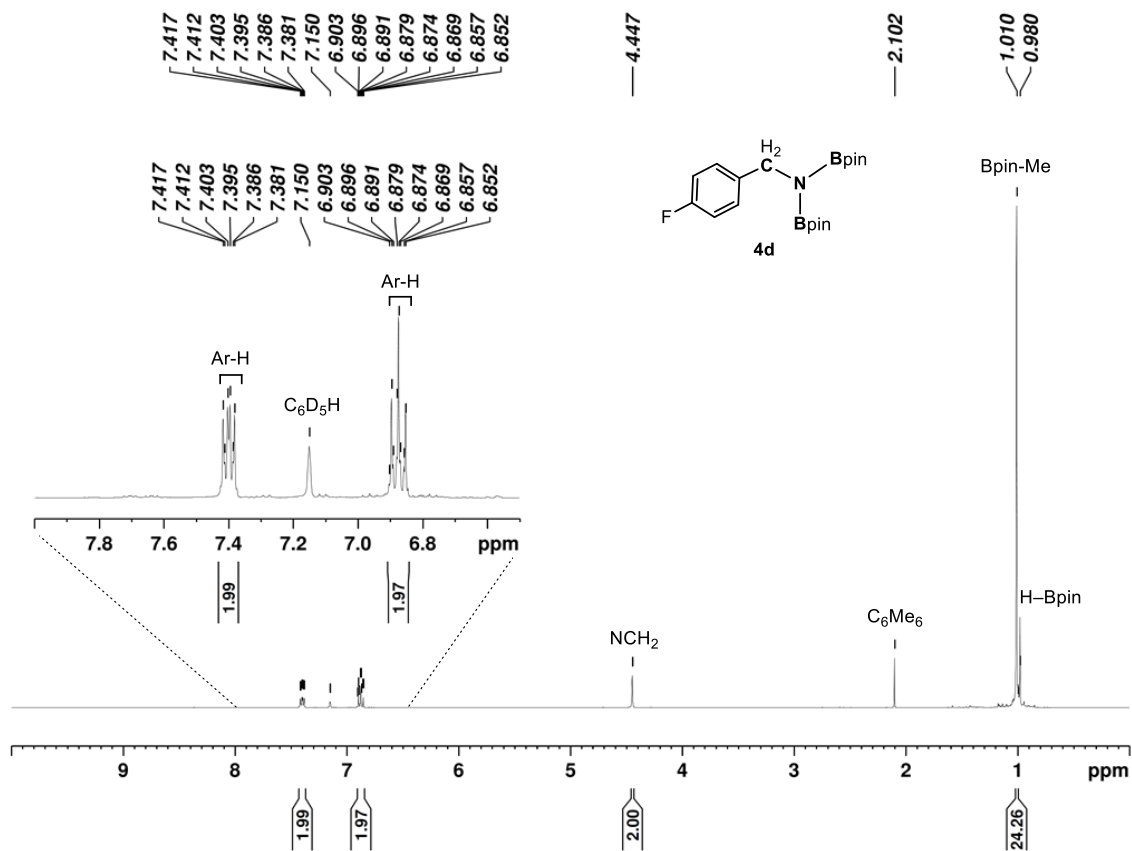


Fig. S44 ¹H NMR spectrum of bis(boryl)amine **4d** in a reaction mixture of catalytic hydroboration of 4-fluorobenzonitrile with HBpin using **1** (400 MHz, r.t., C₆D₆).

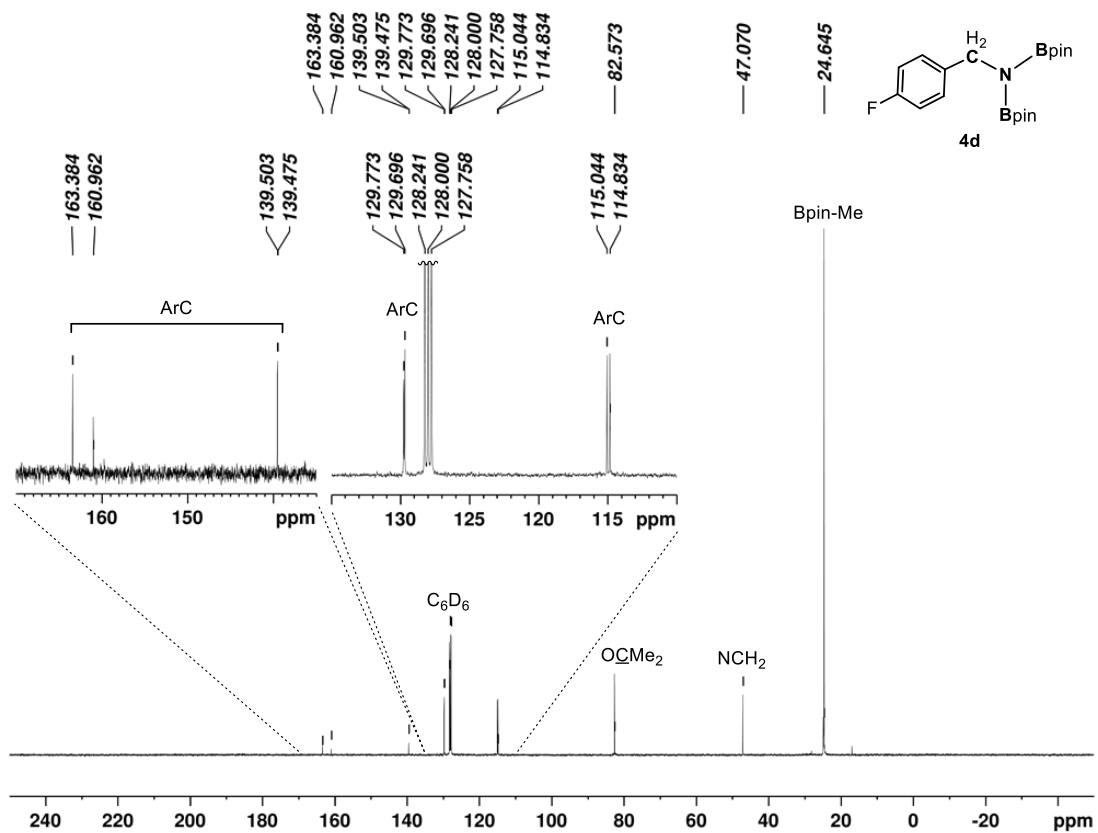


Fig. S45 $^{13}\text{C}\{^1\text{H}\}$ NMR spectrum of bis(boryl)amine **4d** in a reaction mixture of catalytic hydroboration of 4-fluorobenzonitrile with HBpin using **1** (101 MHz, r.t., C_6D_6).

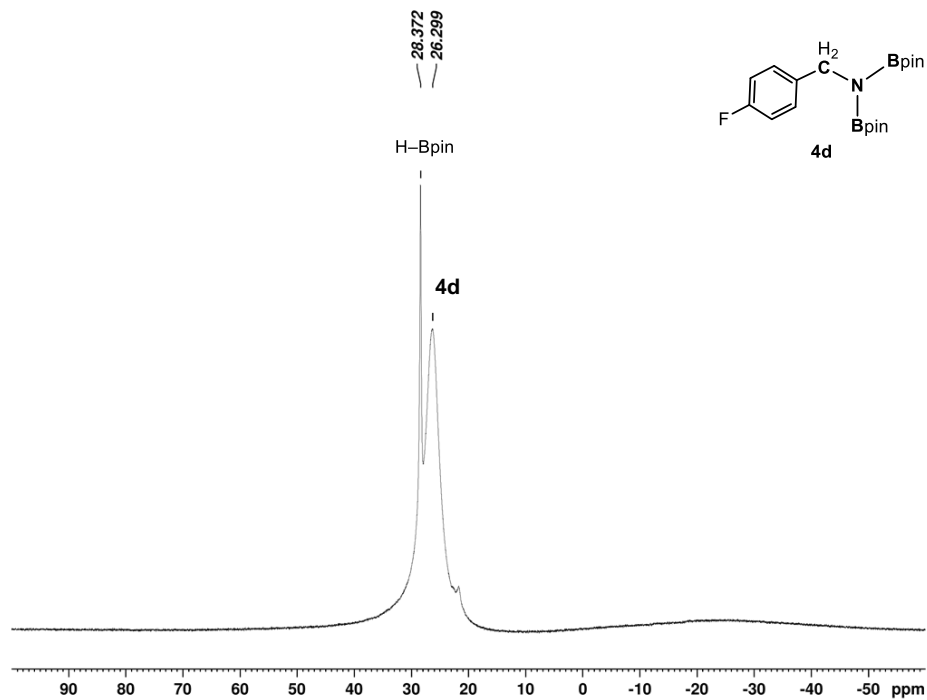


Fig. S46 $^{11}\text{B}\{^1\text{H}\}$ NMR spectrum of bis(boryl)amine **4d** in a reaction mixture of catalytic hydroboration of 4-fluorobenzonitrile with HBpin using **1** (128 MHz, r.t., C_6D_6).

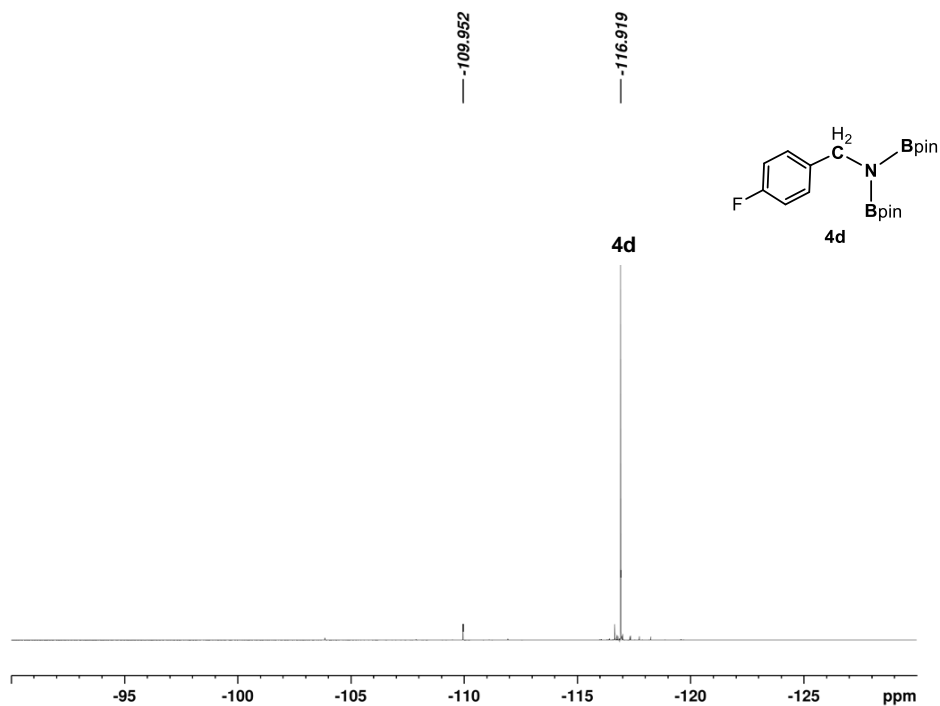


Fig. S47 $^{19}\text{F}\{^1\text{H}\}$ NMR spectrum of bis(boryl)amine **4d** in a reaction mixture of catalytic hydroboration of 4-fluorobenzonitrile with HBpin using **1** (376 MHz, r.t., C_6D_6).

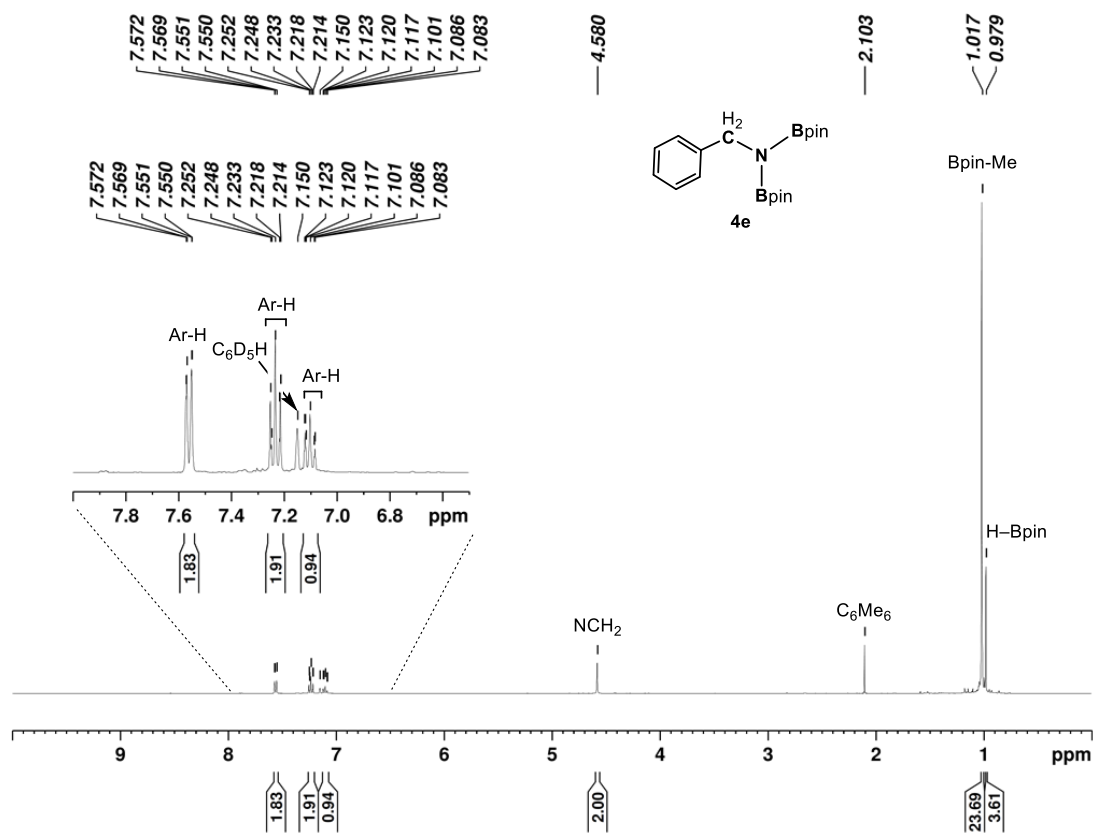


Fig. S48 ^1H NMR spectrum of bis(boryl)amine **4e** in a reaction mixture of catalytic hydroboration of benzonitrile with HBpin using **1** (400 MHz, r.t., C_6D_6).

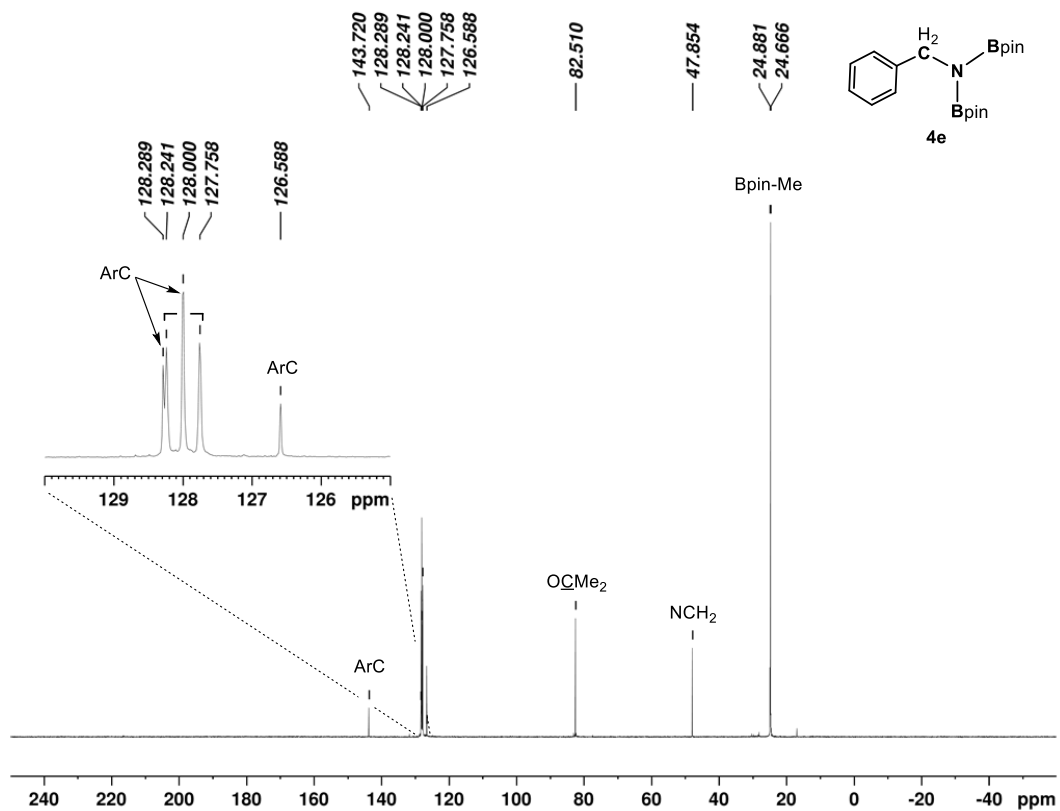


Fig. S49 $^{13}\text{C}\{^1\text{H}\}$ NMR spectrum of bis(boryl)amine **4e** in a reaction mixture of catalytic hydroboration of benzonitrile with HBpin using **1** (101 MHz, r.t., C_6D_6).

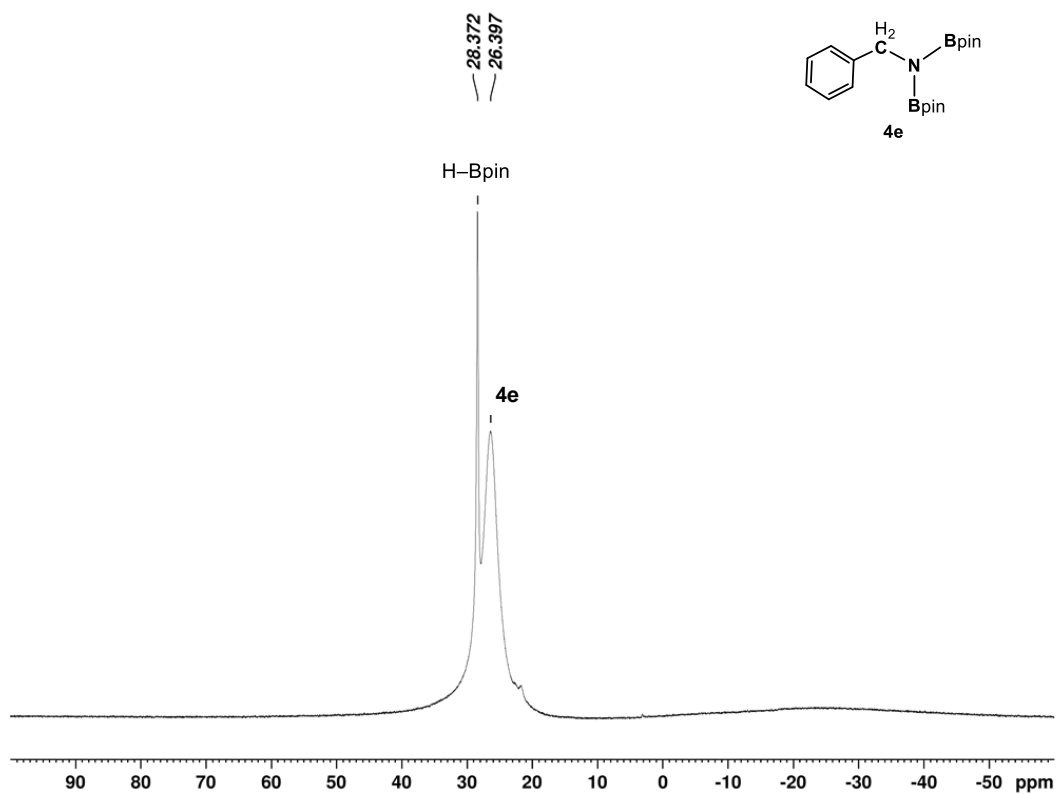


Fig. S50 $^{11}\text{B}\{^1\text{H}\}$ NMR spectrum of bis(boryl)amine **4e** in a reaction mixture of catalytic hydroboration of benzonitrile with HBpin using **1** (128 MHz, r.t., C_6D_6).

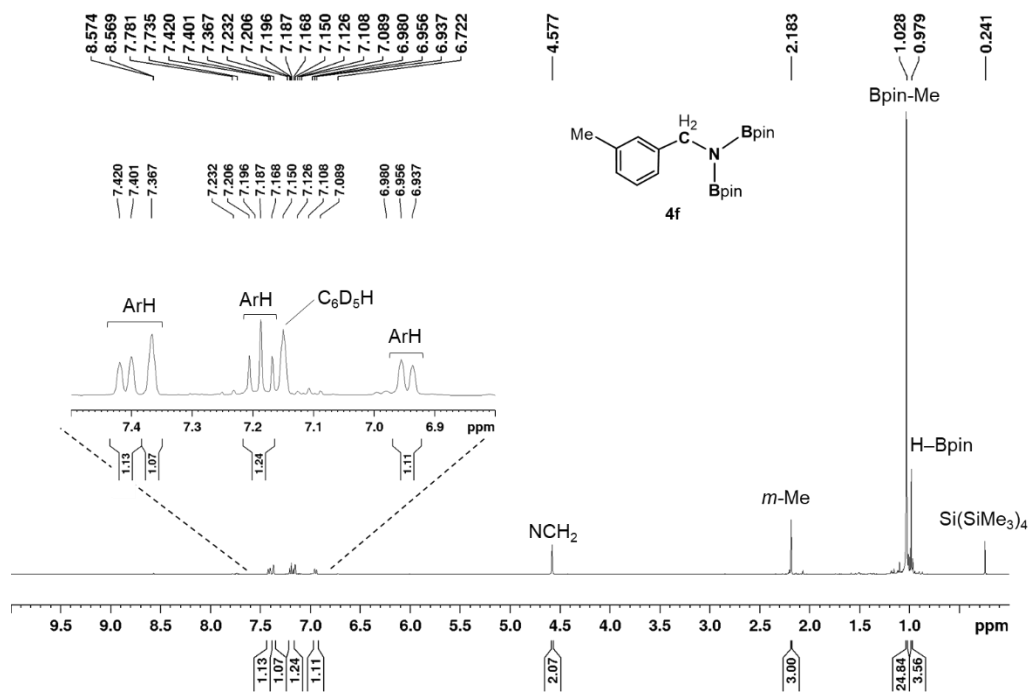


Fig. S51 ¹H NMR spectrum of bis(boryl)amine **4f** in a reaction mixture of catalytic hydroboration of *m*-tolunitrile with HBpin using **1** (400 MHz, r.t., C₆D₆).

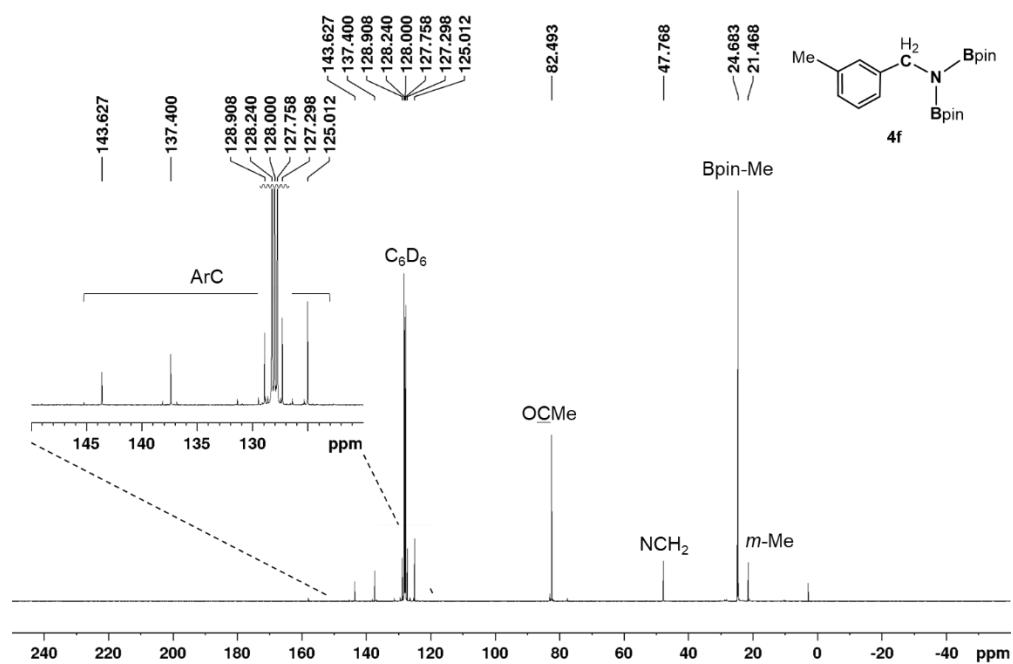


Fig. S52 ¹³C{¹H} NMR spectrum of bis(boryl)amine **4f** in a reaction mixture of catalytic hydroboration of *m*-tolunitrile with HBpin using **1** (101 MHz, r.t., C₆D₆).

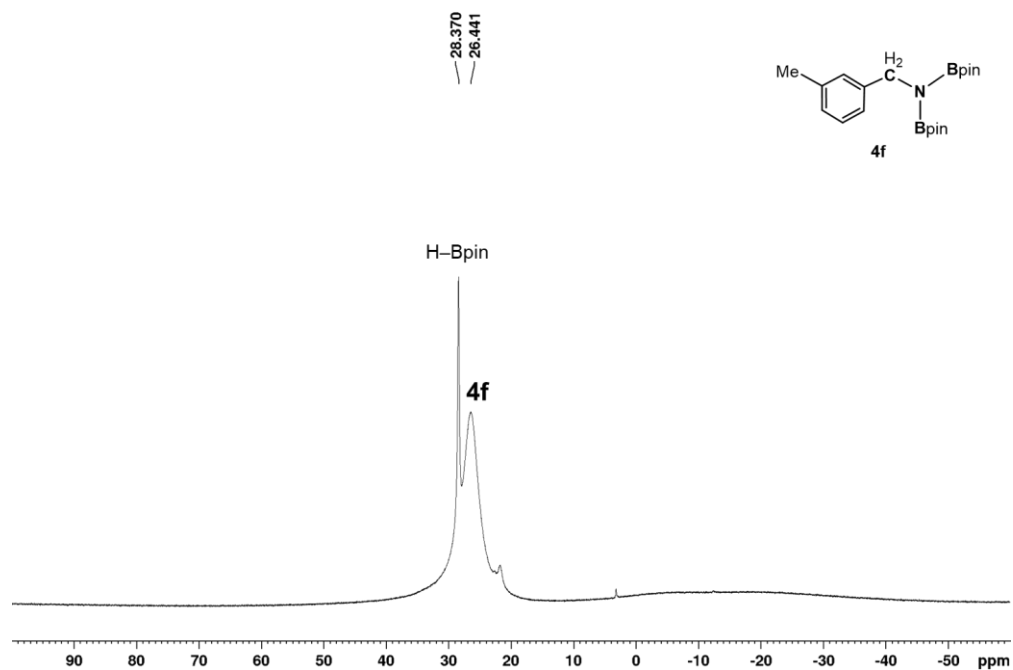


Fig. S53 $^{11}\text{B}\{^1\text{H}\}$ NMR spectrum of bis(boryl)amine **4f** in a reaction mixture of catalytic hydroboration of *m*-tolunitrile with HBpin using **1** (128 MHz, r.t., C_6D_6).

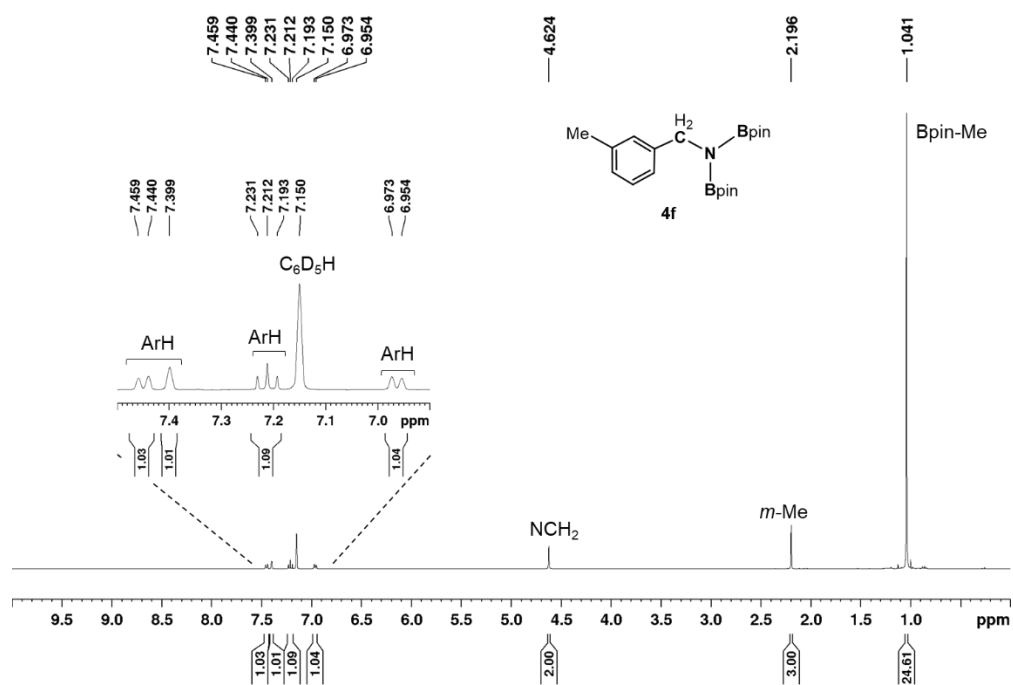


Fig. S54 ^1H NMR spectrum of isolated bis(boryl)amine **4f** (400 MHz, r.t., C_6D_6).

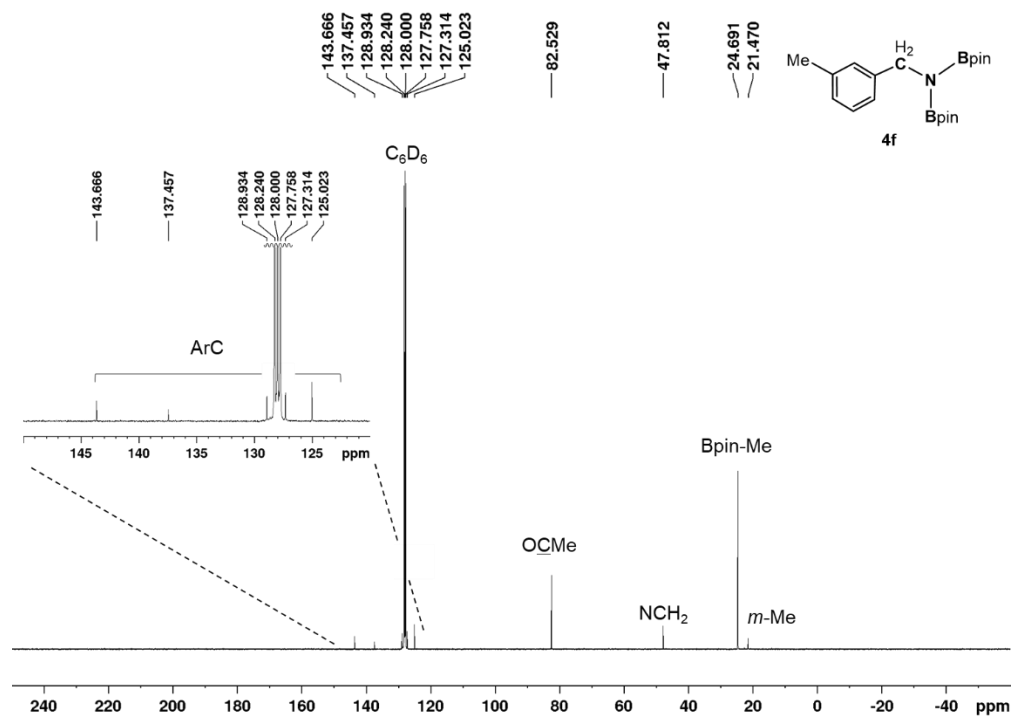


Fig. S55 $^{13}\text{C}\{^1\text{H}\}$ NMR spectrum of isolated bis(boryl)amine **4f** (101 MHz, r.t., C₆D₆).

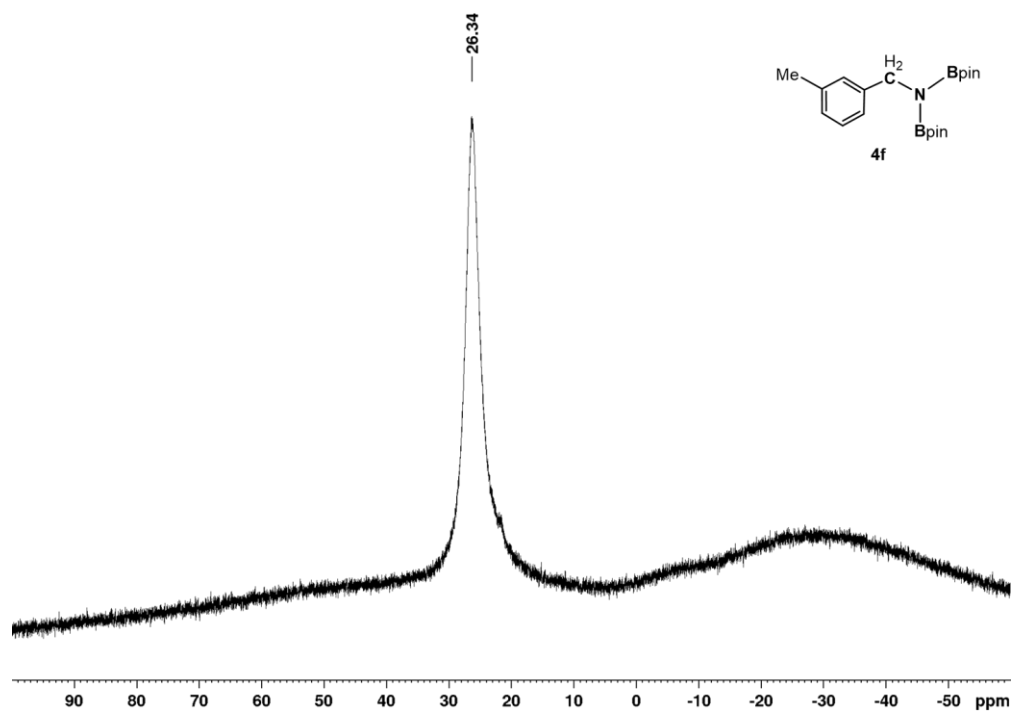


Fig. S56 $^{11}\text{B}\{^1\text{H}\}$ NMR spectrum of isolated bis(boryl)amine **4f** (128 MHz, r.t., C₆D₆).

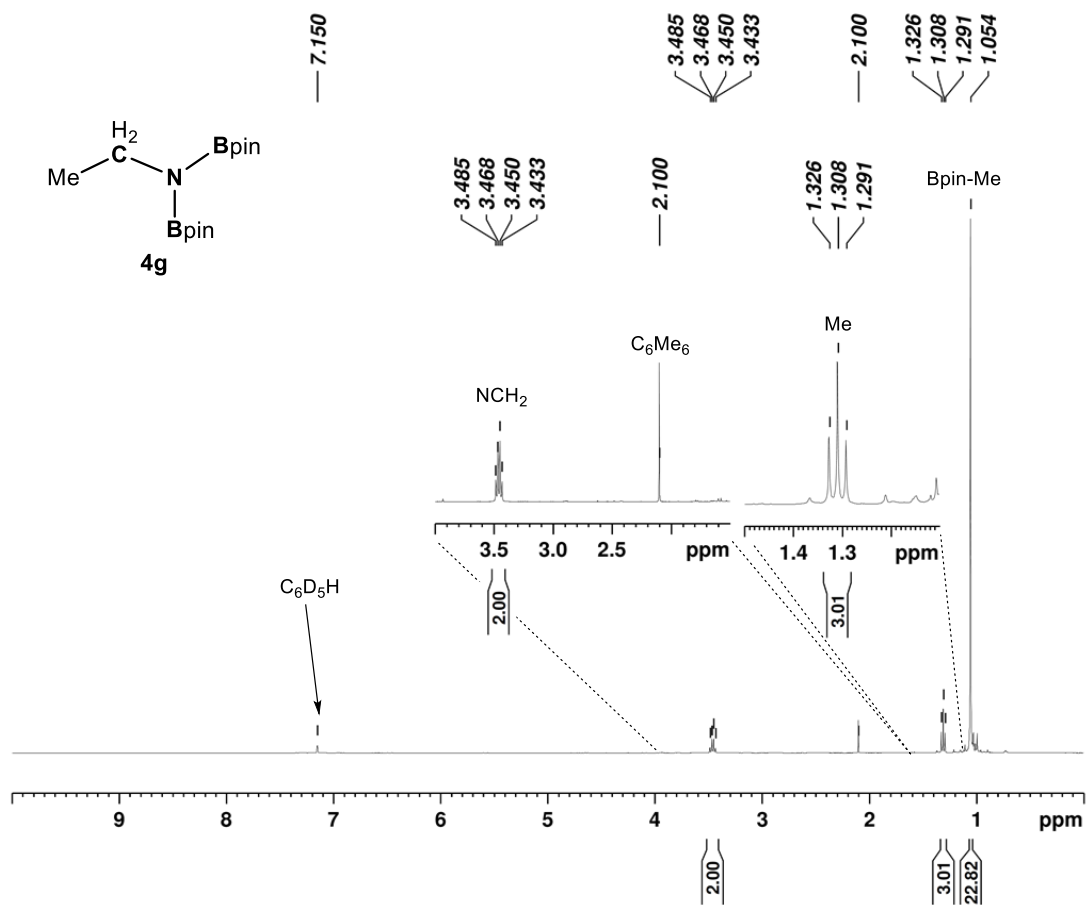


Fig. S57 ¹H NMR spectrum of bis(boryl)amine **4g** in a reaction mixture of catalytic hydroboration of acetonitrile with HBpin using **1** (400 MHz, r.t., C₆D₆).

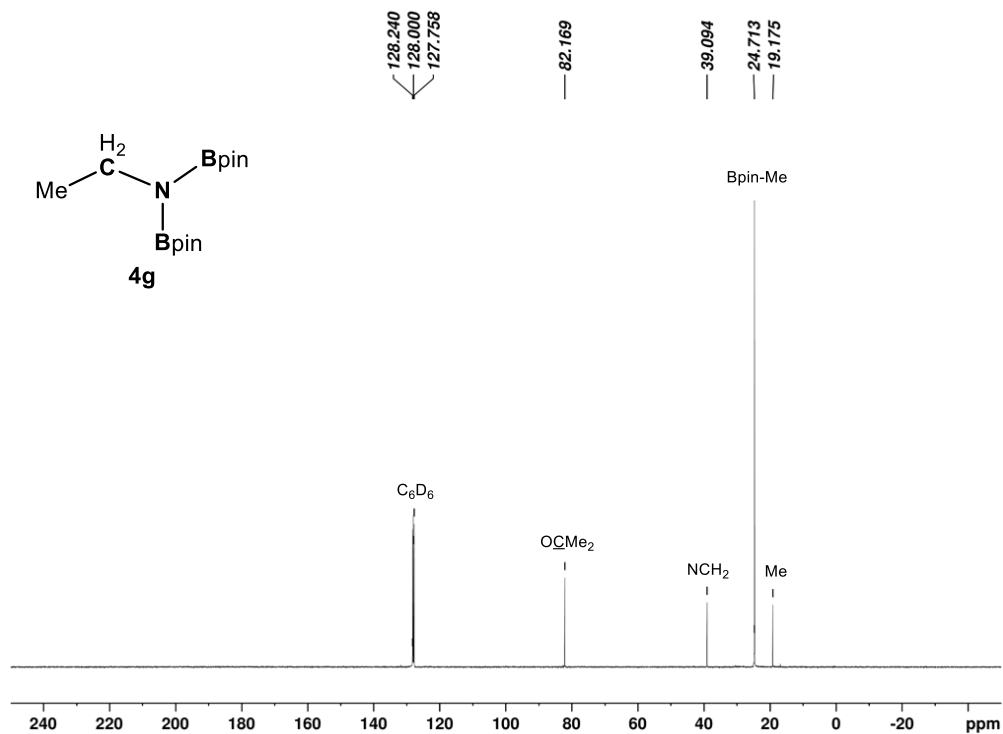


Fig. S58 $^{13}\text{C}\{^1\text{H}\}$ NMR spectrum of bis(boryl)amine **4g** in a reaction mixture of catalytic hydroboration of acetonitrile with HBpin using **1** (101 MHz, r.t., C_6D_6).

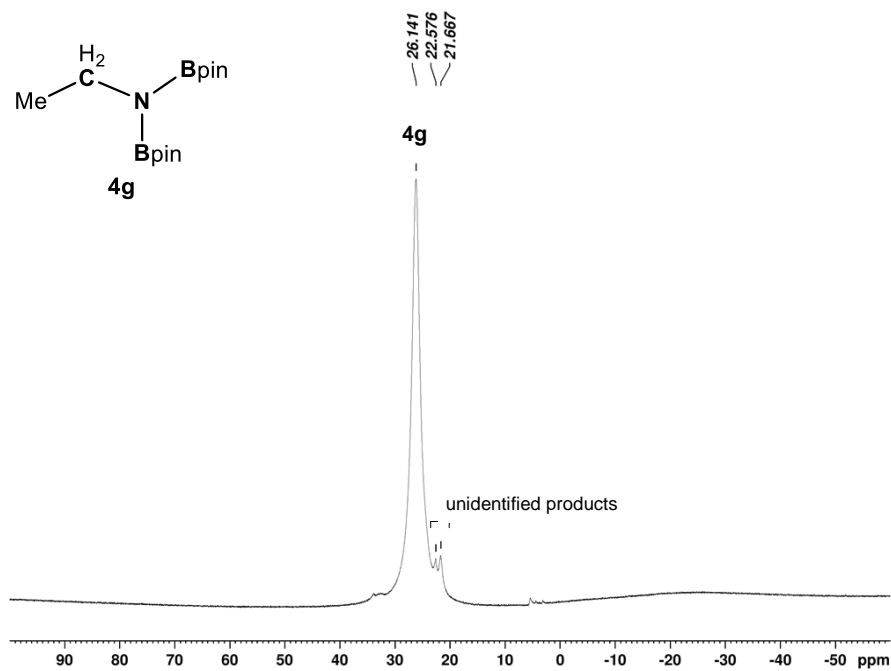


Fig. S59 $^{11}\text{B}\{^1\text{H}\}$ NMR spectrum of bis(boryl)amine **4g** in a reaction mixture of catalytic hydroboration of acetonitrile with HBpin using **1** (128 MHz, r.t., C_6D_6).

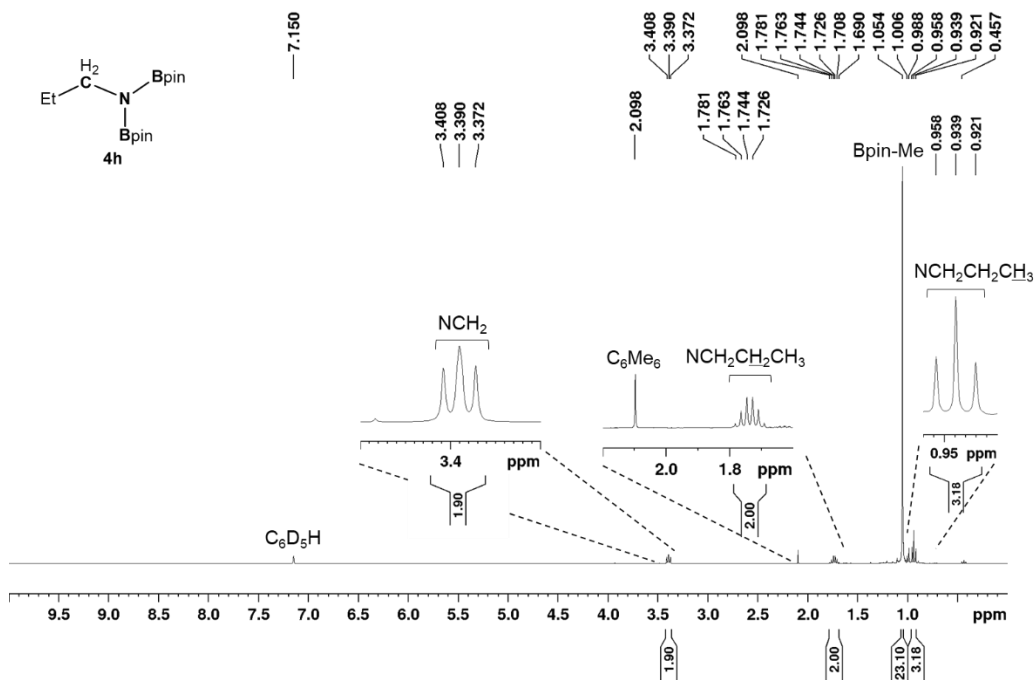


Fig. S60 ^1H NMR spectrum of bis(boryl)amine **4h** in a reaction mixture of catalytic hydroboration of propionitrile with HBpin using **1** (400 MHz, r.t., C_6D_6).

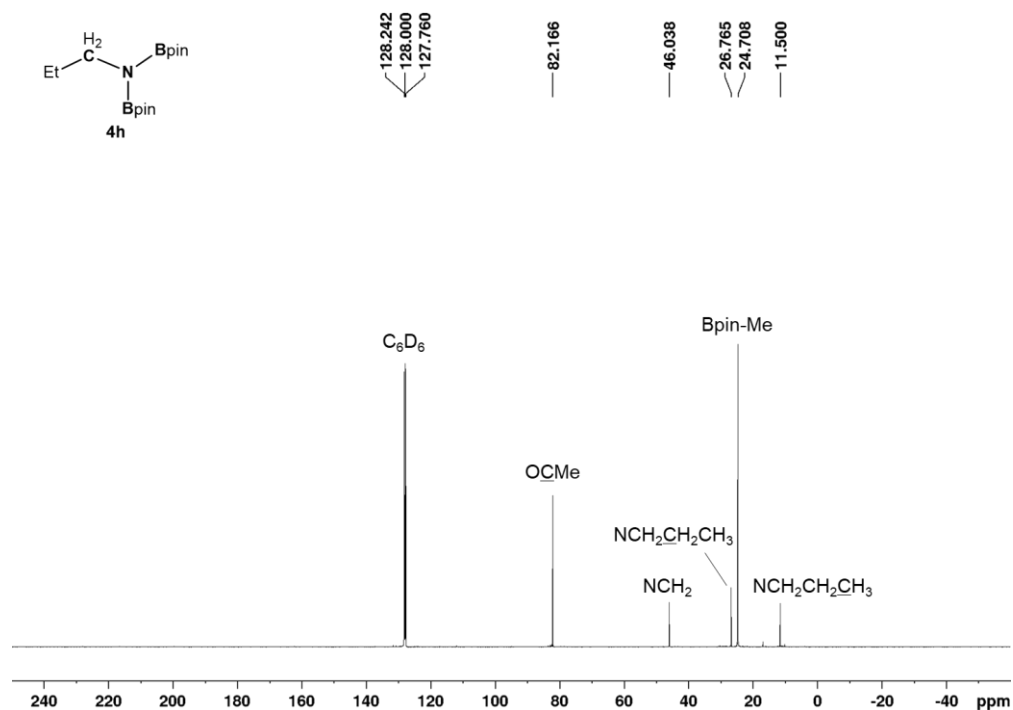


Fig. S61 $^{13}\text{C}\{^1\text{H}\}$ NMR spectrum of bis(boryl)amine **4h** in a reaction mixture of catalytic hydroboration of propionitrile with HBpin using **1** (101 MHz, r.t., C_6D_6).

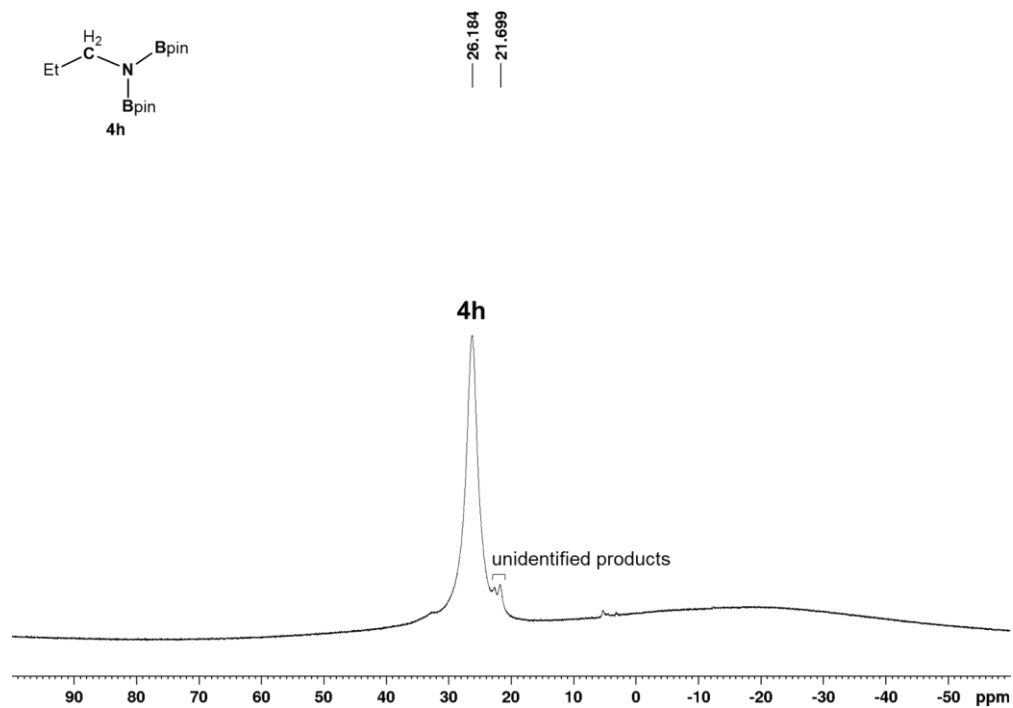


Fig. S62 $^{11}\text{B}\{^1\text{H}\}$ NMR spectrum of bis(boryl)amine **4h** in a reaction mixture of catalytic hydroboration of propionitrile with HBpin using **1** (128 MHz, r.t., C_6D_6).

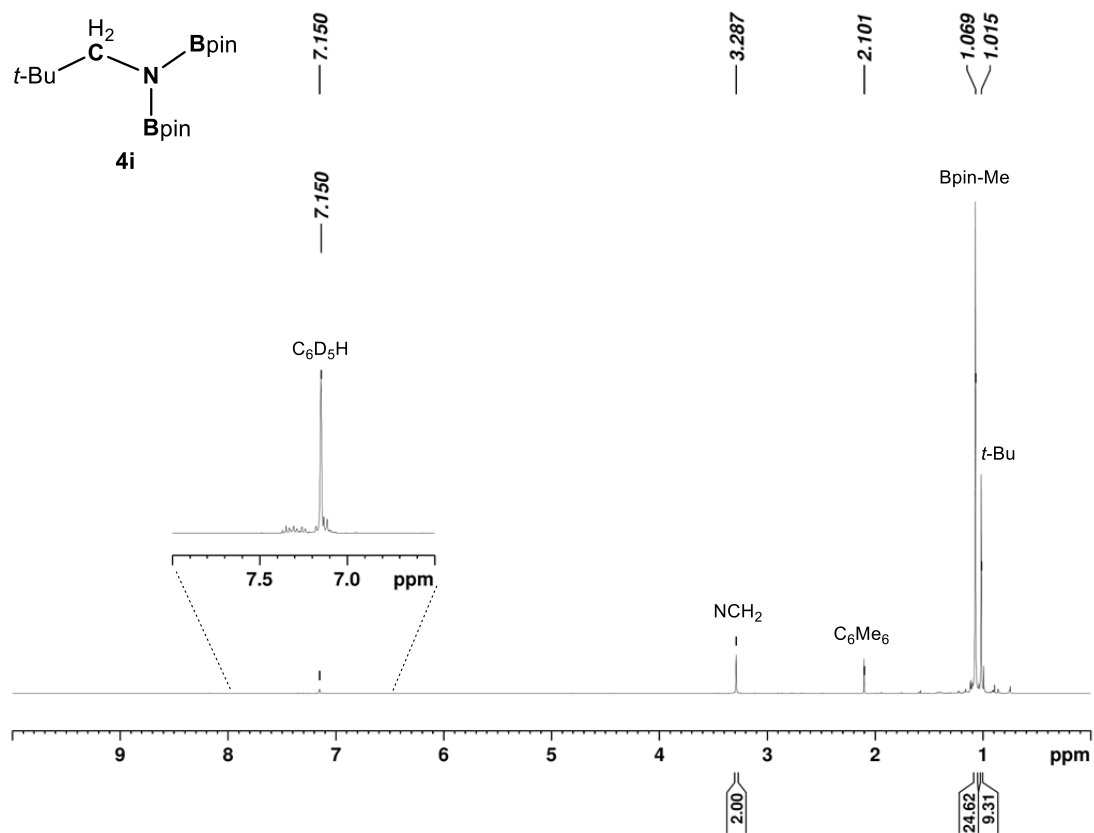


Fig. S63 ¹H NMR spectrum of bis(boryl)amine **4i** in a reaction mixture of catalytic hydroboration of pivalonitrile with HBpin using **1** (400 MHz, r.t., C₆D₆).

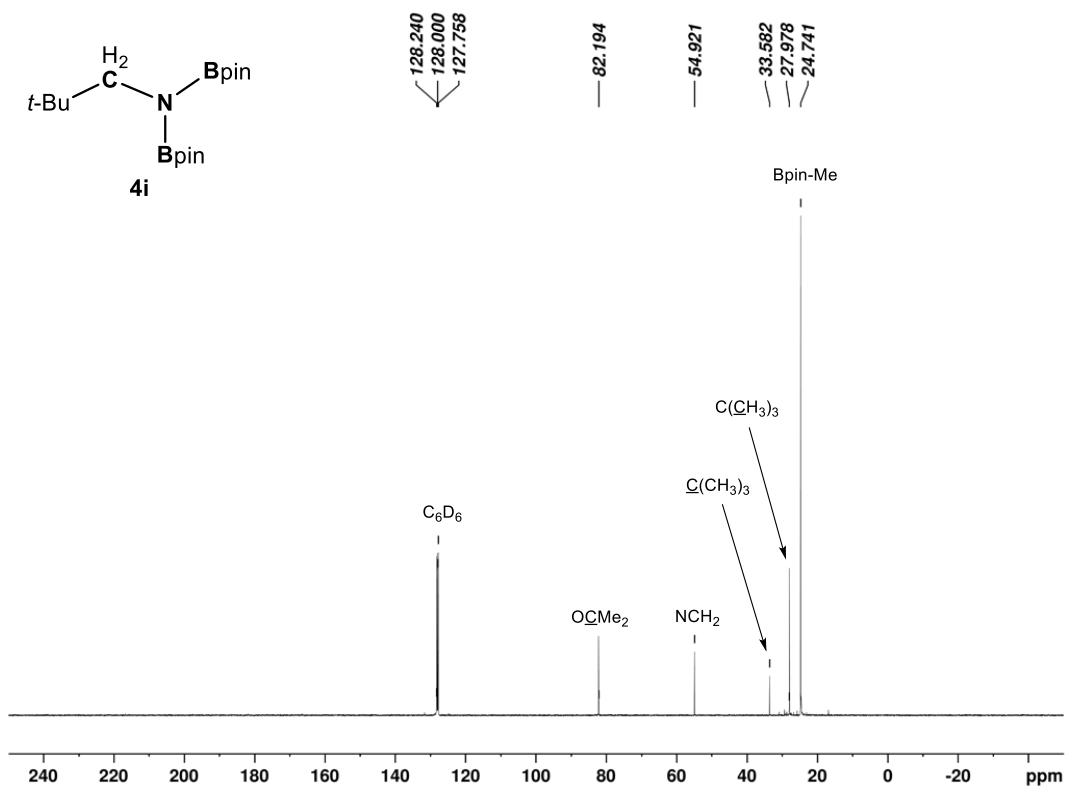


Fig. S64 $^{13}\text{C}\{^1\text{H}\}$ NMR spectrum of bis(boryl)amine **4i** in a reaction mixture of catalytic hydroboration of pivalonitrile with HBpin using **1** (101 MHz, r.t., C_6D_6).

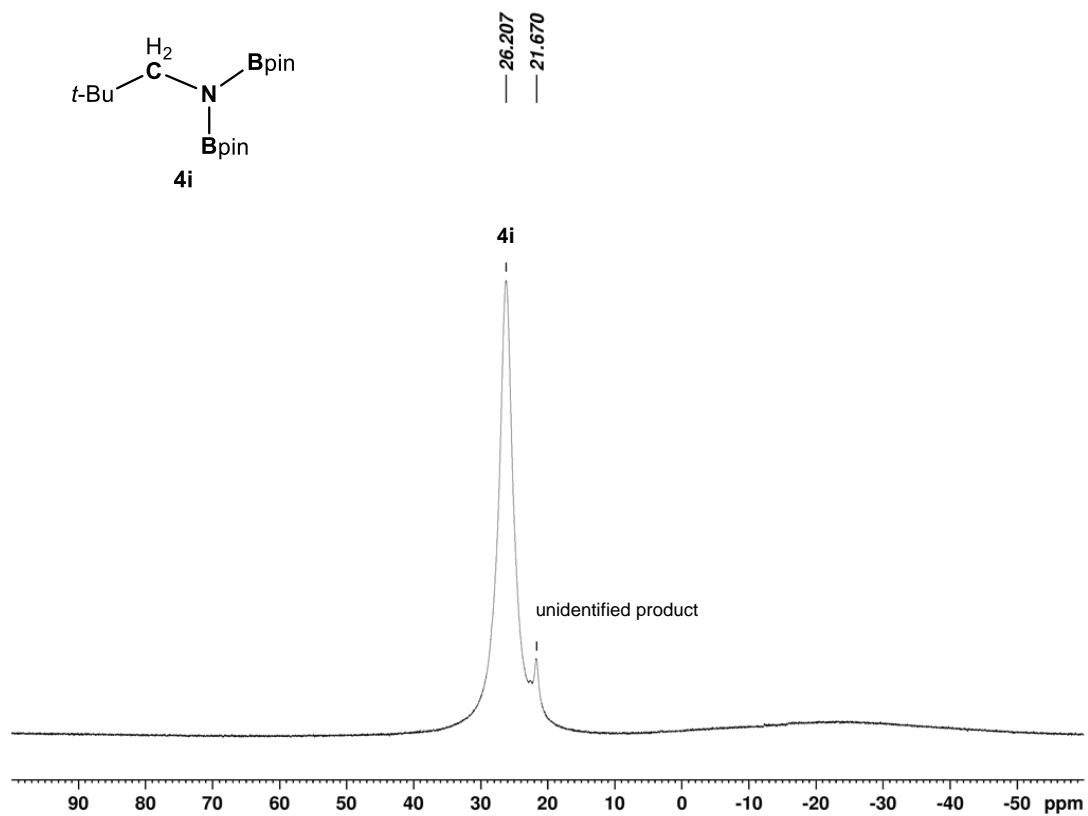


Fig. S65 $^{11}\text{B}\{^1\text{H}\}$ NMR spectrum of bis(boryl)amine **4i** in a reaction mixture of catalytic hydroboration of pivalonitrile with HBpin using **1** (128 MHz, r.t., C_6D_6).

7. NMR and IR spectra of *N*-silylimine complexes 5 and 6

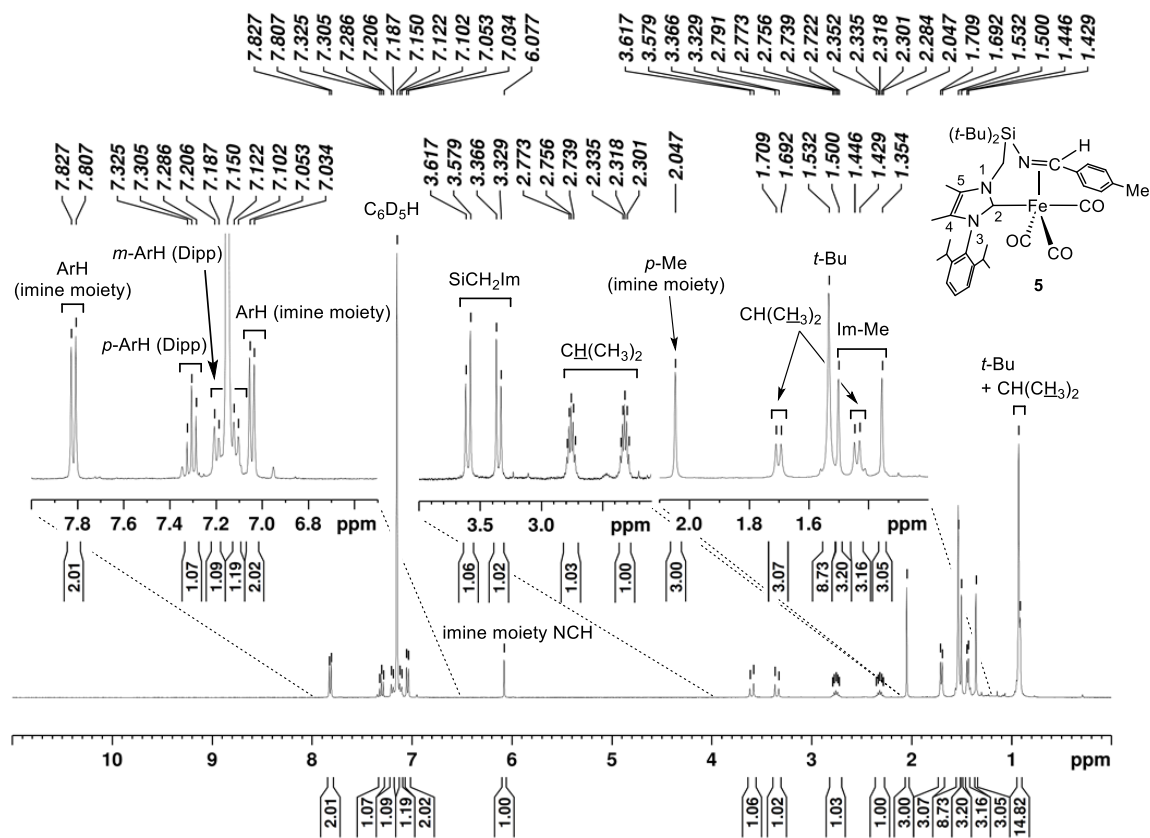


Fig. S66 ^1H NMR spectrum of *N*-silylimine complex 5 (400 MHz, r.t., C_6D_6).

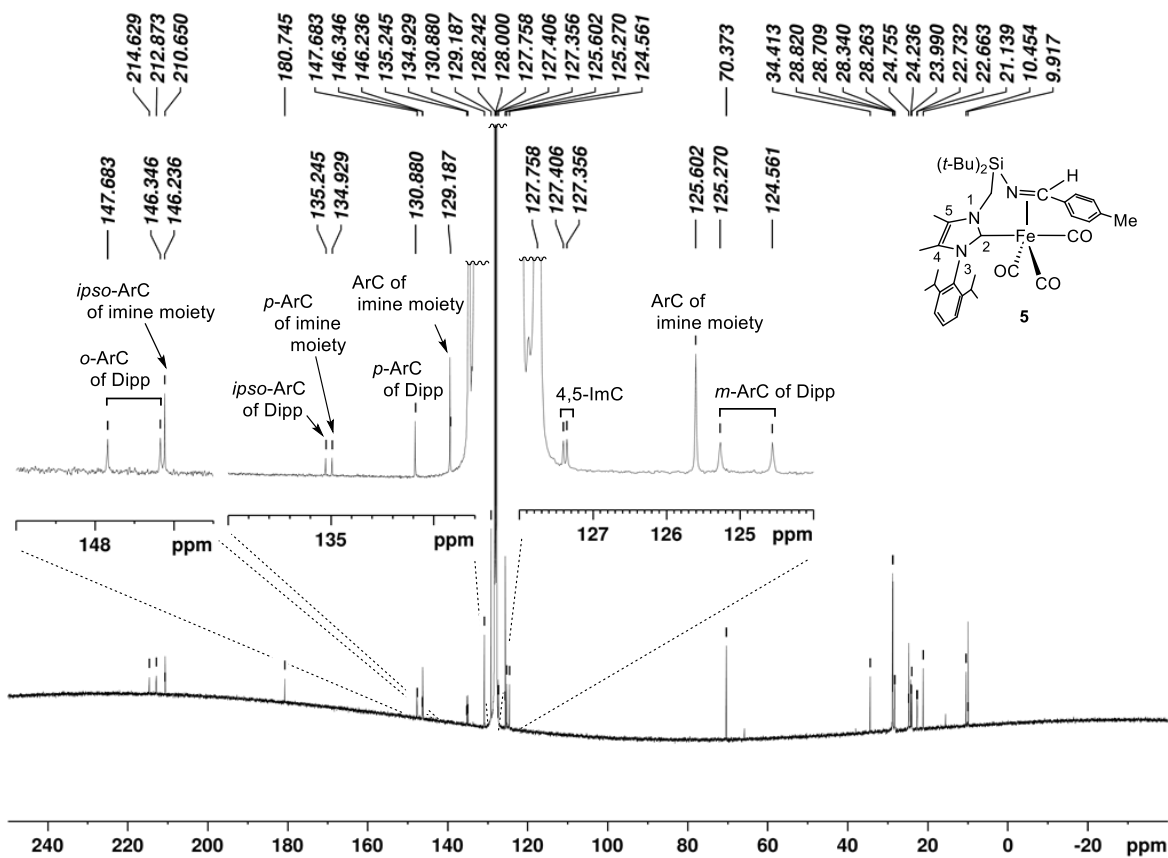


Fig. S67 $^{13}\text{C}\{^1\text{H}\}$ NMR spectrum of *N*-silylimine complex **5** (101 MHz, C_6D_6).

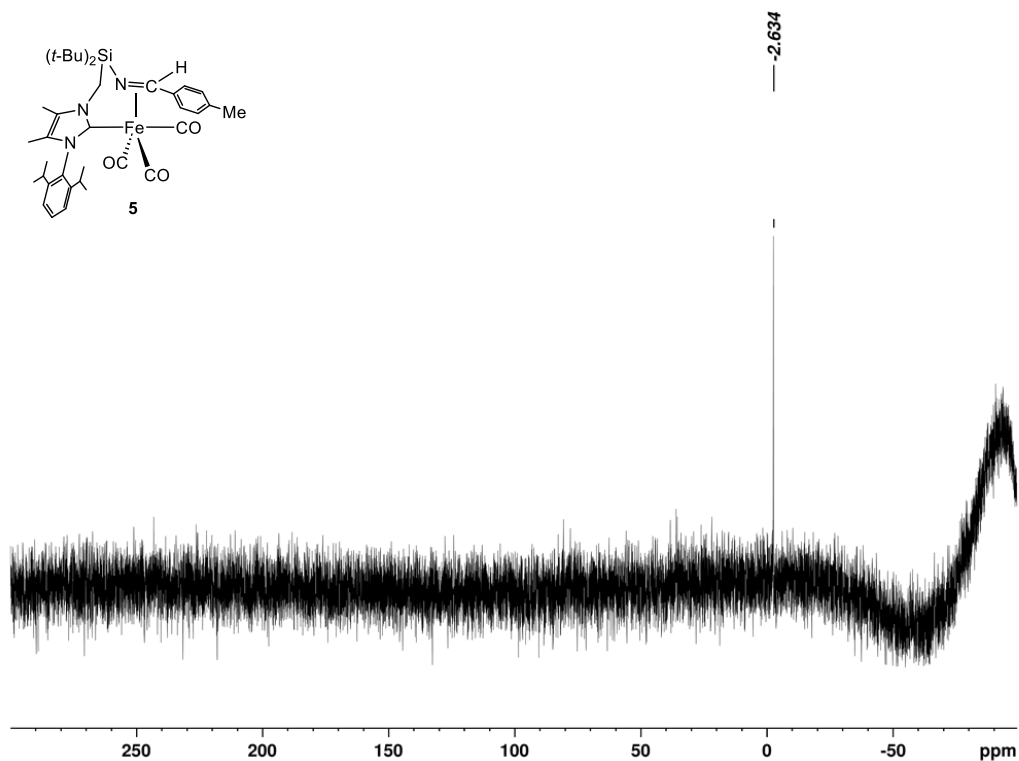


Fig. S68 $^{29}\text{Si}\{^1\text{H}\}$ NMR spectrum of *N*-silylimine complex **5** (79.5 MHz, IG, C_6D_6).

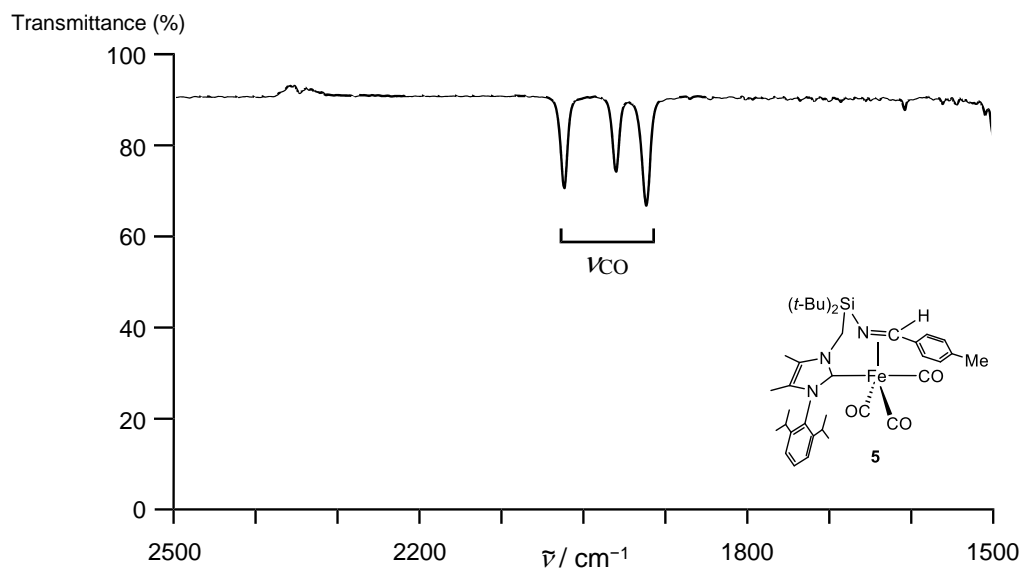


Fig. S69 IR spectrum of *N*-silylimine complex **5** (a toluene solution).

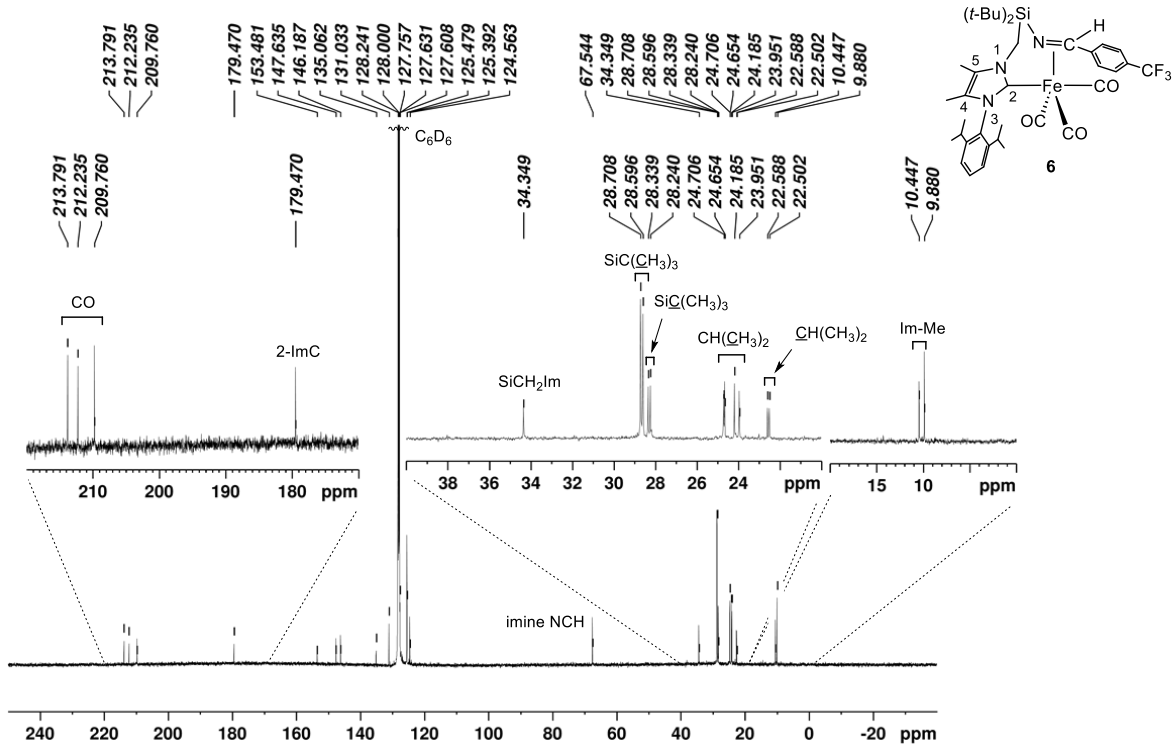


Fig. S71 $^{13}\text{C}\{^1\text{H}\}$ NMR spectrum of *N*-silylimine complex **6** (101 MHz, C_6D_6).

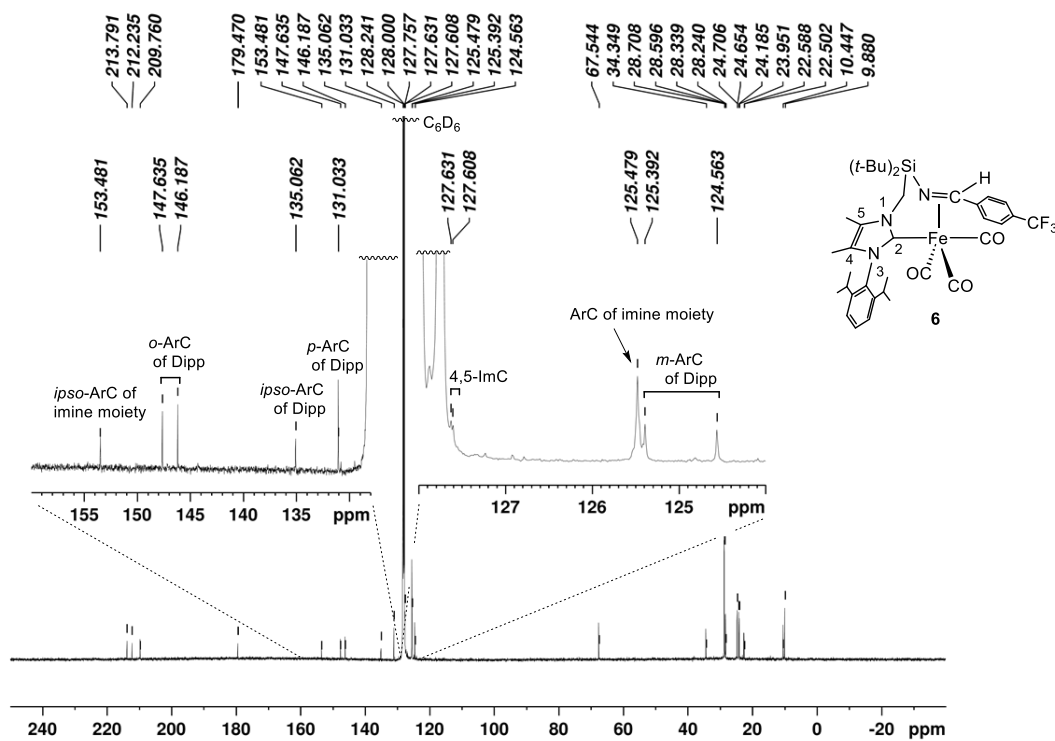


Fig. S72 $^{13}\text{C}\{^1\text{H}\}$ NMR spectrum of *N*-silylimine complex **6** with assignments of aromatic carbons (101 MHz, C_6D_6).

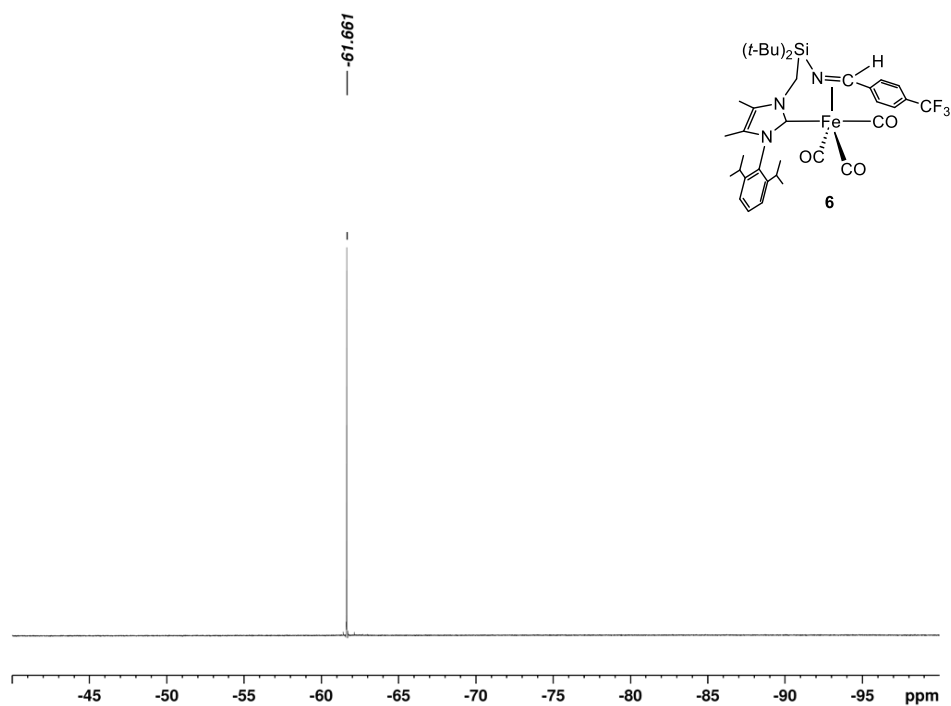


Fig. S73 $^{19}\text{F}\{^1\text{H}\}$ NMR spectrum of *N*-silylimine complex **6** (376 MHz, C_6D_6).

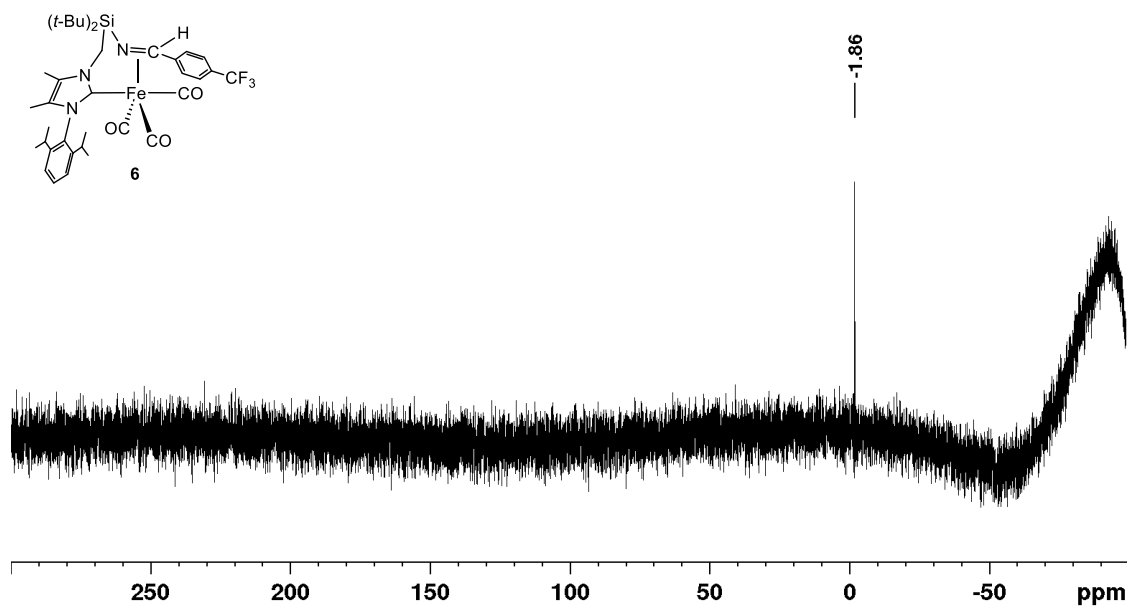


Fig. S74 $^{29}\text{Si}\{^1\text{H}\}$ NMR spectrum of *N*-silylimine complex **6** (79.5 MHz, IG, C_6D_6).

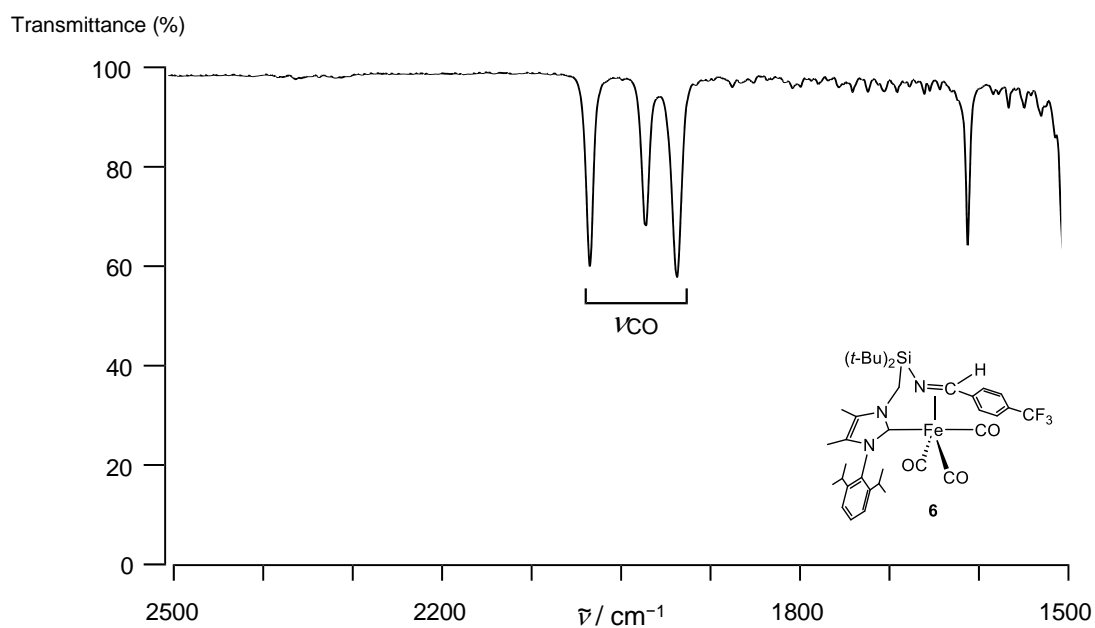


Fig. S75 IR spectrum of *N*-silylimine complex **6** (a toluene solution).